

Public-data File 86-52

THE IGNEOUS PETROLOGY AND GEOCHEMISTRY OF NORTHERN AKUTAN ISLAND, ALASKA

By

J.D. Romick¹

Alaska Division of
Geological and Geophysical Surveys

June 1986

THIS REPORT HAS NOT BEEN REVIEWED FOR
TECHNICAL CONTENT (EXCEPT AS NOTED IN
TEXT) OR FOR CONFORMITY TO THE
EDITORIAL STANDARDS OF DGGS.

794 University Avenue, Basement
Fairbanks, Alaska 99709

¹Department of Geology, Cornell University, Ithaca, New York 14853

CONTENTS

	<u>Page</u>
Abstract.....	1
Acknowledgements.....	1
Introduction.....	1
Purpose and scope.....	1
Geographic setting.....	2
Previous work.....	2
General geology.....	3
Petrology.....	4
Distribution.....	4
Western Akutan Island.....	4
Lava peak flows.....	4
Associated dikes.....	5
Other flows.....	6
Recent lavas.....	6
Central and Eastern Akutan Island.....	7
Open Bight.....	7
Hot Springs Bay valley flows.....	7
Pickup Valley.....	7
Cow Point.....	7
Flows.....	8
Hot Springs Bay valley dikes.....	8
Dikes.....	9
Akutan harbor flows.....	9
Intrusions.....	10
Summary.....	10
Mineralogy.....	11
Clinopyroxene.....	11
Orthopyroxene.....	12
Olivine.....	12
Plagioclase.....	13
Accessory and alteration minerals.....	14
Opaque minerals.....	14
Hornblende.....	14
Apatite.....	14
Carbonate.....	15
Chlorite.....	15
Quartz.....	15
Serpentine minerals.....	15
Crystallization sequence.....	15
Summary.....	16
Geochemistry.....	16
Major oxides.....	16
Statistical analyses.....	17
Normative mineralogy.....	18
Minor element analyses.....	19
Rb and Sr analyses.....	19
Potassium-argon dates.....	19

	<u>Page</u>
Summary.....	19
Geothermometry and geobarometry.....	20
Magma generation models.....	22
Summary.....	23
Evolution of igneous rocks on northern Akutan Island.....	24
References cited.....	26
Appendix I -	30
Appendix II - Major oxides and normative minerals.....	31
Appendix III - Microprobe data for Akutan lavas.....	34
Appendix IV - Rb and Sr analyses.....	41
Appendix V - Petrographic descriptions of Akutan Lavas.....	42
Appendix VI - Application of discriminant functions.....	48

FIGURES

Figure 1. Position of Akutan Island within the Aleutian Arc.....	49
2. Generalized geology of Akutan Island adapted from Byers and Barth.....	50
3. Sketch of Lava Peak showing the relationship between the upper and lower flow series.....	51
4. Change in percentage of olivine and clinopyroxene in the lower flow series exposed on Lava Peak.....	52
5. Mineral banding in a Cow Point dike.....	53
6. Intrusive rocks.....	54
7. Porphyritic intrusive from Sandy Cove.....	55
8. Microprobe analyses for Akutan clinopyroxenes and orthopyroxenes.....	56
9. Clinopyroxene zoning types.....	57
10. Common clinopyroxene twinning types.....	58
11. Microprobe analyses of olivine phenocrysts.....	59
12. Microprobe analyses of plagioclase phenocrysts.....	60
13. Inclusions in plagioclase phenocrysts.....	61
14. Harker variation diagram.....	62
15. MgO-CaO and K ₂ O-CaO plots of Akutan samples.....	63
16. MgO-FeO and Al ₂ O ₃ -FeO plots of Akutan samples.....	64
17. Na ₂ O-MnO plots of Akutan samples.....	65
18. TiO ₂ -K ₂ O plots of Akutan samples.....	65
19. AFM diagram for Akutan samples.....	66
20. Total alkalis vs. silica diagram from Kuno.....	67
21. FeO/MgO vs. SiO ₂ diagram for Akutan samples.....	68
22. CaO/Al ₂ O ₃ vs. FeO/MgO diagram showing CaO and MgO fractionation in Akutan lavas.....	69
23. Dendrograph plot of Akutan lava flows and dikes.....	70
24. Canonical plot of groups, group means, and samples.....	71
25. Normative hypersthene vs. wt percent SiO ₂	72
26. Sr vs. Rb diagram.....	73
27. Rb vs. Rb/Sr diagram.....	74
28. Sr vs. Rb/Sr diagram.....	75
29. Cartoon for Akutan Island showing the central vent, Lava Peak, and the zoned magma chamber.....	76

TABLES

Table	1. Volcanic activity on Akutan Island since 1790.....	77
	2. Modal analyses for western Akutan lavas.....	78
	3. Modal analyses for eastern and central Akutan lavas.....	79
	4. Crystallization sequence for Akutan lavas.....	80
	5. Posterior probabilities for the four groups of lavas distinguished by the cluster analysis.....	81
	6. Neodymium and strontium data for Akutan Island.....	82
	7. Whole rock K-Ar dates for Akutan lavas.....	83
	8. Geothermometry for Akutan mineral pairs.....	84

THE IGNEOUS PETROLOGY AND GEOCHEMISTRY OF NORTHERN AKUTAN ISLAND, ALASKA

By
J.D. Romick¹

ABSTRACT

Volcanism on Akutan Island, in the eastern Aleutian Arc, is characterized by tholeiitic lavas ranging between 46 and 63 wt percent SiO_2 , with FeO^*/MgO ratios between 1.3 and 4.2. Olivine-augite-plagioclase basalts were found at Lava Peak, while the remaining flows and dikes on the island consist of hypersthene-augite-plagioclase basalts and andesites. The Lava Peak basalts had <23 ppm Rb and >400 ppm Sr, while the other lavas sampled had higher concentrations of Rb and lower concentrations of Sr. K-Ar whole-rock dates of lava flows and dikes indicate that they erupted between 1.5 and 1.1 m.y. ago. Clinopyroxene, orthopyroxene, and olivine compositions are uniform across the island, and average $\text{Ca}_{45}\text{Mg}_{42}\text{Fe}_{17}\text{Si}_{206}$, $\text{Mg}_{66}\text{Fe}_{34}\text{SiO}_3$, and $\text{Mg}_{72}\text{Fe}_{28}\text{Si}_{204}$, respectively. Plagioclase compositions vary between An_{93} and An_{51} with the more calcic plagioclase being restricted to the Lava Peak basalts. The chemical trends seen in Akutan lavas are consistent with the shallow-level fractionation of olivine, plagioclase, and clinopyroxene from a parental liquid, and the subsequent eruption of magmas from different levels of a zoned magma chamber.

ACKNOWLEDGMENTS

I would like to thank the Geothermal program of the Alaska Division of Geological and Geophysical Surveys (DGGs) for funding this study. Roman Motyka (DGGs) conducted the microprobe analyses on samples collected, and without his generous support this thesis would not have been possible. I would also like to thank M.W. Wiltse, at the DGGs lab, for analyzing the samples I collected during my field season. Michael Perfit was very gracious in allowing me to use some of his unpublished data on Akutan lavas. My thanks go to my committee for their helpful comments and criticisms on various drafts, which greatly improved the text, to my fellow graduate students for their comments on my ideas, and last (but not least) to my wife, Jan, whose drafting skill and patience made this thesis a great deal easier to complete.

Finally, I take credit for whatever insights the reader may glean from this study, and the blame for whatever errors which appear.

INTRODUCTION

Purpose and Scope

The purpose of this study is to characterize the mineralogy, petrology, and geochemistry of the volcanic rocks exposed on northern Akutan Island. Little is known about the petrology of volcanoes in the eastern Aleutian arc, and this study will help fill the gap in our knowledge of this region.

¹Department of Geology, Cornell University, Ithaca, New York 14853.

Geographic Setting

Akutan Island is located in the eastern Aleutian chain at 54° 05' latitude and 165° 55' longitude, about 45 km northeast of Unalaska Island (fig. 1). Commercial access to Akutan Island is limited to air service by Grumman Goose and boat charter, out of Dutch Harbor on Unalaska Island to Akutan Village.

The island is 29 km long, 21 km wide, and oriented roughly east-west (fig. 2). It is dominated by Akutan Volcano, a 1,304 m high composite volcano. Central and eastern Akutan Island consist of steep ridges separating glacially scoured valleys which radiate away from presently active Akutan Volcano. Western Akutan has a gentle topography dissected by streams flowing off the west flanks of the volcano.

The summit of Akutan Volcano contains a 2 km wide caldera, which may have been formed within the last 500 yr (Byers and Barth, 1953). Within the caldera is a cinder cone, which existed prior to 1931 (Finch, 1935), and a small lake. The caldera is breached on the north side. Northwest of the volcano are two small eruptive centers: an old eroded volcanic center consisting primarily of lava flows, and a cinder cone with two lava flows which erupted sometime before 1870 (Byers and Barth, 1953).

Previous Work

R.H. Finch conducted the first scientific exploration of the island in 1931. He was a member of the U.S. Geological Survey's (USGS) Volcanology section conducting studies of the Aleutian volcanoes in preparation for the establishment of a volcano observation post. Akutan Island was examined because its frequent eruptive activity and relative accessibility made it a convenient place for observation. The result of Finch's (1935) study was a brief description of the geology and a topographic sketch of the island. Finch noted that Dr. T.A. Jaggar had visited the island in 1907 and 1927 and had made some correlations between the sedimentary units on Akutan and those on the Alaska Peninsula, but nothing was published regarding that correlation.

Byers and Barth (USGS) conducted field work on Akutan Island in 1948 as part of the USGS study of the Aleutian Islands after World War II, but no official report was issued. Their geologic map of Akutan Island, (unpublished) was obtained from the USGS archives, in Menlo Park, by R. Motyka of the Alaska Division of Geological and Geophysical Surveys (DGGs). Byers and Barth (1953) discussed the recent 1947 and 1948 eruptions on Akutan Island, but not past volcanic activity, or geology, of the island.

Perfit and Kay did some reconnaissance mapping and sampling of the island in 1974 and the initial results were presented by Perfit (1978). Motyka and others (1981) provided a brief description of Akutan geology, but emphasized the geothermal resources of the island. Perfit and Gust (1981) published some isotope and microprobe analyses of samples from Akutan Island, and discussed how their results related to those of other Aleutian Islands. McCulloch and Perfit (1981) published isotope and rare earth element (REE)

data for Akutan lavas and used the data to develop constraints for magma genesis in the Aleutian Islands.

General Geology

Figure 2 is a copy of the general geology of Akutan Island adapted from Byers and Barth (unpublished map) and slightly modified by Romick and Swanson (in preparation). Akutan Island consists of interbedded lava flows and volcanoclastic deposits overlain in places by younger volcanic deposits associated with Akutan Volcano. The interbedded flows and volcanoclastic material represent older deposits principally exposed on central and eastern Akutan Island. Some of the older rocks are slightly to moderately altered and contain secondary chlorite and carbonate, while the younger volcanics are largely unaltered.

The older rocks can be divided into two units: the lower unit consists of at least 700 m of volcanoclastic deposits with interbedded flows and sills, while the upper unit is dominated by basaltic to andesitic flows with lesser amounts of interbedded volcanoclastic deposits (Motyka and others, 1981).

The older lavas are exposed in glacial valleys whose bottoms are filled with alluvium, stream sediments, and in at least one case, volcanic debris flow deposits. Exposures along the coast indicate that sea level was considerably lower when the valleys formed than at the present time. Valley walls can be traced down below present sea level. Black (1974) indicated that deglaciation occurred at 8400 years ago for Umnak Island. Akutan Island is about 160 kilometers from Umnak Island. Considering the proximity of Akutan Island to Umnak, it seems reasonable to assume that deglaciation occurred on Akutan at roughly the same time. Landsat images of Akutan show that the radial glacial valleys on the island were carved prior to the formation of present Akutan Volcano.

Associated with the older rocks, are numerous dikes, concentrated in Hot Springs Bay, which decrease in abundance eastward. Dikes located around Hot Springs Bay Valley strike north-west. Those located to the west of Hot Springs Bay Valley are generally oriented northeast, but dike orientations span 180 degrees. Gabbroic intrusions are associated with the older volcanic complex. A large sill in Sandy Cove is exposed over approximately 150 m while a smaller intrusion is exposed in the cliff on the west side of Hot Springs Bay. The orientation and arrangement of several linear intrusions, exposed south of Open Bight, (fig. 2) suggests that they may be ring dikes associated with an older caldera system. Dip measurements on the map prepared by Byers and Barth (unpublished) also suggest an older center of volcanic activity near Open Bight (fig. 2).

On northwestern Akutan Island is a 594 m high ridge, here called Lava Peak, where at least 19 flows and 7 dikes are exposed. The flows are separated into two groups by an unconformity (fig. 3). Eleven almost flat-lying flows are overlain by at least 8 flows which have a 24° apparent dip to the west.

Samples were collected from a section about 690 m thick. East of the peak is a highly baked, oxidized, autobrecciated zone which is characteristic of volcanic vents and has been interpreted to be the core of an eroded volcanic center.

The dikes which intrude these rocks are only exposed on the north side of the ridge, and strike in a northwesterly direction. A large dike, exposed east of the flows, intrudes the lower 11 lava flows but is truncated by the upper sequence of flows. The dike is the backbone of the ridge to the east of the flows and may have been a feeder dike from Akutan Volcano during an older period of volcanism.

South of Lava Peak are several flows which are stratigraphically lower than the Lava Peak rocks, and are mantled by recent tephra deposits from Akutan Volcano.

North of Lava Peak is a cinder cone and two lava flows which probably formed before 1870 (Byers and Barth, 1953). Byers and Barth noted that the Russians made no mention of the cone or associated flows during their visit to the island in the 1870's, and suggested that the eruptive activity occurred prior to their visit. Simkin and others (1981) list an eruption on the northwest flank of the volcano in 1855 which may mark the eruption of the Lava Point cone and flows. The cone is approximately 250 m high and 600 m across. The flow is about 4 km² in area, and forms Lava Point (fig. 2).

Recent deposits include flows from 1947 and 1948 eruptions, which did not leave the summit, and the 1978 lava flow which almost reached the north coast. The lava flow followed two stream drainages down the north flank of the volcano and came to within 1 km of the coast. Ash eruptions interspersed with these flows mantle some of the deposits on western Akutan Island, and reached Akutan Village on the east side of the island (Finch, 1935; Byers and Barth, 1953). Volcanic activity, documented on Akutan Island since 1790, is listed in table 1.

PETROLOGY

Distribution

Igneous rocks on Akutan Island consist of older rocks exposed at Lava Peak and on the central and eastern part of the island, and younger rocks associated with Akutan Volcano, exposed on the western side of the island. Figure 2 shows the locations of samples collected from Akutan. The following discussion will describe the petrology of the flows and dikes from which these samples were collected.

Western Akutan Island

Lava Peak Flows

The lower section consists of 11 flows ranging from 1.7 to 12 m thick. The basal flow is the thickest flow exposed. Going up the section the flows thin and then thicken again. Several flows have baked brecciated

upper zones, which grade downward into vesicular rock. All 11 flows contain plagioclase, olivine, and clinopyroxene phenocrysts in a fine-grained holocrystalline groundmass consisting of plagioclase, titanomagnetite, augite, and occasionally olivine (table 2). The rocks are fresh and generally unaltered, although some of the mafic minerals have oxidation stains.

Figure 4 shows the mineralogic changes that occur going up the section. Both olivine and clinopyroxene decrease in abundance going up the section. The ratio of mafic phenocrysts to total phenocrysts decreases going up the section. There is a general decrease in the number of very large (3 to 7 mm) clinopyroxene phenocrysts up the section, as well as a decrease in the overall grain size of the clinopyroxene. Olivine phenocrysts remain about the same size and skeletal olivine crystals are present in all 11 flows. The abundance and size of plagioclase phenocrysts except for the top flow stay, remains constant. In addition to the decrease of both olivine and clinopyroxene, there is a sympathetic relationship between the relative abundances of the two minerals. Figure 4 shows that when olivine abundance is at a maximum, clinopyroxene is at a minimum, and visa versa. There are no soil horizons, or weathering zones, separating one flow from another, indicating that they erupted over a fairly short time period.

Three flows were sampled from the upper part of the section. The exposure is very irregular, making it impossible to measure the thickness of the flows sampled. Individual thicknesses are estimated at between 2 and 5 m. The mineralogy of the three flows is identical to the lower flows. The rocks are porphyritic, with large clinopyroxene, plagioclase, olivine, and opaque minerals fine grained holocrystalline groundmass. The percentage of olivine in the three flows is highly variable and ranges between 8.6 percent for the top flow and 1.6 percent for the bottom flow. The olivine in all three flows has partially oxidized rims.

Associated Dikes

Of the seven dikes that intrude Lava Peak the largest is exposed to the east of Lava Peak and is 10 to 15 m wide (Ak-81-1; fig. 3). In thin section, the dike contains the same mineral assemblage as the Lava Peak flows; randomly oriented phenocrysts of olivine, clinopyroxene, opaque minerals, and plagioclase in a groundmass of opaque minerals, clinopyroxene, and plagioclase laths. A 1.5 m wide zone of red rock near the dike may represent the baked contact between the dike and the country rock. The dike is truncated by the upper sequence of lava flows.

The six other dikes sampled stand out as resistant spines on the north side of Lava Peak. The dikes range in thickness from 0.5 m to 4 m and are oriented N. 70° W. Except for the westernmost dike, the dikes are aphanitic in hand specimen. They contain bands of vesicles aligned parallel to the walls of the dike with individual vesicles elongate in the same direction. This is probably due to cooling from the outside inward, forcing exsolving volatiles toward the center of the dike. Movement of the cooling magma stretched the vesicles in the direction of flow.

The dikes intrude a series of interbedded lava and debris flows located at 100 m elevation. The baked contact of these dikes is one to two centimeters thick. Columnar jointing is moderately well developed and is oriented perpendicular to the walls of the dike.

In thin section, the dikes vary from equigranular fine-grained to porphyritic. Plagioclase is the dominant phenocryst. In several dikes olivine and clinopyroxene are as abundant as plagioclase. The smaller dikes (Ak-81-32, Ak-81-33, Ak-81-34, Ak-81-103A, and Ak-81-103B) show a strong alignment of plagioclase laths in the groundmass. Several of the dikes contain interstitial brown glass.

Other Flows

These flows are located stratigraphically below the Lava Peak flows, and are similar to lavas exposed on the central and eastern side of the island.

The three flows sampled were interbedded with debris flows consisting of a clay-rich matrix with blocks ranging up to several meters in size. Sample Ak-81-16 is from a 7 m thick flow exposed in a canyon wall. It has a scoriaeous top and flow banding. The lava contains about 17 percent plagioclase phenocrysts and very little clinopyroxene and olivine. The groundmass is very fine-grained and makes up about 80 percent of the rock. The two other flows are located stratigraphically above and below Ak-81-16, and contain plagioclase along with varying amounts of hypersthene and clinopyroxene, with trace amounts of olivine and opaque minerals. The groundmass in these rocks is very fine-grained and makes up to 75 percent of the rock.

Recent Lavas

The most recent volcanism on Akutan Island resulted in tephra deposits, the eruption of two lava flows, and a cinder cone on the north and northwest flank of Akutan Volcano. Sometime before 1870 a cinder cone developed just northeast of Lava Peak (fig. 2). A lava flow erupted from the base of the cone, covering about 4 square km, and makes up what is called Lava Point (Byers and Barth, 1953). The lava flow is very blocky, and has two lobes which entered the sea. Erosion has exposed numerous lava tubes on the northern border of the flow which have developed into spectacular bridges and caves. The rock is very vesicular and contains plagioclase phenocrysts, with minor clinopyroxene, olivine, and opaque minerals in a glassy groundmass. The groundmass contains oriented plagioclase laths, some opaque minerals, and a great deal of brown glass.

In 1978 a lava flow erupted in the summit caldera, flowed down the north flank of Akutan Volcano in two lobes, and came within 1 km of the coast (fig. 2). The flow consists of very blocky lava ranging from vesicular to glassy in texture. Plagioclase makes up about 32 percent of the rock, while clinopyroxene, olivine, and opaque minerals make up less than 7 percent. The groundmass consists of oriented plagioclase laths and brown glass.

Central and Eastern Akutan Island

Open Bight

Open Bight is the next valley east of the 1978 lava flow. Samples were collected from two flows (?) exposed at the mouth of the valley. Contacts were concealed so it is unclear whether the rocks are flows or sills. About 31 meters of the upper flow (?) is exposed. Its lower section has large columnar joints, while the upper section is massive. The other sample was collected from a 2 to 5 m thick flow (?) exposed further down on the cliff. Both rocks contain about 32 percent plagioclase, 5 to 8 percent clinopyroxene, trace amounts of orthopyroxene, and 1 to 2 percent opaque minerals, in a trachytic groundmass. Crystal clots of plagioclase, clinopyroxene, and opaque minerals are present. Plagioclase phenocrysts commonly contain glass inclusions.

Hot Springs Bay Valley Flows

Three valleys empty into Hot Springs Bay, the largest being Hot Springs Bay Valley. Samples were collected along the coast and within the valleys. The small central valley was not explored. The westernmost valley is here called Pickup Valley (fig. 2).

Pickup Valley

Samples were collected from the head and walls of Pickup Valley (table 3, fig. 2). Two samples, Ak-81-20 and Ak-81-21, were collected from outcrops described by Byers and Barth (unpublished map, 1948) as possible ring dikes. The samples are porphyritic, and contain randomly oriented plagioclase, clinopyroxene, and opaque phenocrysts in a trachytic groundmass. The groundmass is slightly altered to chlorite and carbonate. Quartz/carbonate veinlets crosscut the groundmass and phenocrysts.

A lava flow exposed west of these samples has a baked lower contact and crudely developed columnar joints. The rock contains a few plagioclase phenocrysts in a very fine-grained trachytic groundmass and is partially altered to chlorite, carbonate, and iron oxide.

Two samples were collected part way down the valley. Ak-81-23 contains plagioclase, clinopyroxene, and orthopyroxene, while Ak-81-24 contains partially altered olivine, plagioclase, and clinopyroxene. Both rocks contain chlorite and carbonate alteration in a holocrystalline trachytic groundmass.

Cow Point

Cow Point is a high bluff separating Pickup Valley from the unnamed valley to the southeast. Twenty-five dikes are exposed in this bluff and have a dominant trend to the northeast, but there is a very wide variability in strike. The dip for the dikes is quite variable, and may range from 0° to 180° for a single dike. They also occur in nested groups of 3 or more.

Mineral banding is fairly common in these dikes. The banding consists of vertical layers with mafic minerals concentrated toward the interior and felsic minerals concentrated toward the exterior (fig. 5). This phenomenon has been studied by several workers (Bhattacharji and Smith, 1964; Gibb, 1968; Komar, 1972A; Komar, 1972b). The mineral segregation seems to be the result of mechanical interactions between phenocrysts during intrusion forcing early-forming minerals towards the center of the dike.

The dikes intrude pyroclastic deposits of poorly sorted volcanic breccia. Some of the dike have fine-grained chilled margins where they contact the pyroclastic debris. Higher on the bluff are several oxidized layers which may represent the eruption of lava flows which baked the underlying debris flows.

In hand specimen, the dikes range from porphyritic, containing plagioclase phenocrysts, to aphanitic. Olivine and clinopyroxene are rare phenocrysts. This lack of mafic minerals is probably due to their alteration to the chlorite present in these rocks. Pseudomorphs of chlorite after clinopyroxene are occasionally seen. The most common groundmass consists of a trachytic mass of plagioclase laths and chlorite. Occasionally the groundmass is composed of an equigranular mixture of plagioclase, clinopyroxene, and opaque minerals.

Flows

The five flows were sampled from the northeast side of Hot Springs Bay Valley range from 3.5 to 10 m thick where exposed. They contain plagioclase, clinopyroxene, and rarely olivine, phenocrysts. The groundmass ranges from fine-grained to medium grained holocrystalline in texture, and shows no preferred orientation. Mafic minerals in the groundmass are partially altered to chlorite and carbonate. Sample Ak-81-65 is the only flow sampled where olivine made up a significant percentage of the phenocrysts. Most of the rocks have some chlorite alteration, and in sample Ak-81-65 the olivine is partially altered to iddingsite.

Five lava flows, exposed farther up the valley differ from those farther down valley in that they are almost completely unaltered, except for rare carbonate grains. They are very fine-grained rocks and consist of phenocrysts of plagioclase, clinopyroxene, orthopyroxene, and opaque minerals in a holocrystalline groundmass. Opaque minerals are unusually abundant, composing 1.4 to 1.6 percent of the rocks.

Hot Springs Bay Valley Dikes

Nine variably altered dikes were sampled at the mouth of Hot Springs Bay Valley. The dikes sampled ranged in width from 1.5 to 3 m. The dominant orientation of these dikes is N 42° W, but orientations varied as much as 40 degrees.

The rocks are porphyritic, with plagioclase being the most abundant phenocryst. Hornblende was present as a phenocryst in Ak-81-43. Sample Ak-81-46 contains 29 percent phenocrysts, but the dikes usually contained

less than 15 percent phenocrysts. The groundmass is fine-grained, trachytic, and composed of plagioclase laths and opaque minerals. Xenoliths, present in some samples were similar in composition and texture to the host dikes, but were usually more altered than the enclosing rocks.

The dikes contain chlorite and carbonate as alteration products replacing mafic phenocrysts, microphenocrysts, and glass.

Dikes

Hot Springs Bay Valley dikes are oriented roughly N. 68° W. with a variation in attitude of about 40°. The dikes range in width from 0.5 to 5 m and also occur as dike swarms up to 13 m wide. They have well developed baked contacts, ranging in thickness from 1 to 4 cm. Vesicles are concentrated toward the center of the dikes and are partially filled with carbonate.

Alteration is quite variable between these dikes and also varies within a particular dike. Five samples were taken across a dike which was dipping at an angle of about 70 degrees. The country rock (Ak-81-106-1.5) intruded by the dike was partially altered to chlorite and carbonate. Alteration in the dike increased toward the center until all of the mafic minerals and part of the groundmass were altered.

The dikes are generally very fine-grained, with trachytic textures. Crystal clots are occasionally present, and usually consist of plagioclase, clinopyroxene, and opaque minerals. Plagioclase is the only individual phenocryst. The groundmass is usually composed of plagioclase laths, opaque minerals, chlorite, and carbonate. One dike, Ak-81-71, contained hornblende and was collected from a dike on the east side of Hot Springs Bay Valley. It was very coarse-grained, consisting of plagioclase, hornblende, and orthopyroxene with no groundmass. Carbonate is present as an interstitial filling, while chlorite is partially replaces plagioclase.

Akutan Harbor Flows

The outcrop between Hot Springs Bay Valley and Akutan Harbor consist of a thick sequence of volcanoclastic deposits, with very few flows or dikes.

Two dikes and a thick lava flow are exposed on the north side of Akutan Harbor (Ak-81-26, Ak-81-102A, 102B). The flow is about 8 m thick with a lower section consisting of well developed columnar joints. It is a very fine-grained equigranular rock with rare plagioclase phenocrysts and a holocrystalline groundmass consisting of clinopyroxene, plagioclase, and titanomagnetite. The plagioclase laths have a strongly preferred orientation. Except for a small amount of chlorite in the groundmass the rock is unaltered.

The two dikes that intrude the flow are different in mineralogy and texture. Dike Ak-81-102A is 1.5 m wide and is flow banded and contains only plagioclase phenocrysts. The groundmass is holocrystalline and partially altered to chlorite. Dike Ak-81-102B is 5 m wide and contains chloritized

olivine phenocrysts, and large clinopyroxene and plagioclase phenocrysts in a holocrystalline groundmass composed of clinopyroxene, plagioclase, and titanomagnetite.

Intrusions

Three phaneritic intrusive rocks were sampled on Akutan Island. One sample (Ak-81-100) was a piece of float found on Lava Peak, another (Ak-81-102) was collected from a large plug located in Sandy Cove, while the third (Ak-81-73) was exposed in the cliff west of Pickup Valley. These three intrusives exhibit different textures.

Ak-81-100 is a coarsely crystalline equigranular rock consisting of plagioclase and clinopyroxene. In thin section, the plagioclase and clinopyroxene grains range from 1 to 2 mm in size (fig. 6a). The subhedral to euhedral shape of the plagioclase and clinopyroxene suggest that the two minerals did not grow in place, but were concentrated after most of their growth was completed, possibly by crystal settling in a magma chamber.

In contrast, Ak-81-73 (fig. 6b) has an ophitic to subophitic texture that one would expect for a magma crystallizing under static conditions, with clinopyroxene crystallized around plagioclase.

In contrast to the previous intrusives, Ak-81-102 is a porphyritic rock containing clinopyroxene and plagioclase phenocrysts in a holocrystalline groundmass (fig. 7). The plagioclase contains inclusions of opaque minerals and clinopyroxene and appears to have crystallized after these two mafics nucleated. The clinopyroxene does not contain any inclusions. The groundmass contains plagioclase, clinopyroxene, and an opaque phase.

Summary

Akutan lavas fall into two petrographic groups: the flows and dikes in which clinopyroxene and orthopyroxene are the major mafic minerals, and the flows and dikes in which olivine and clinopyroxene are the major mafic minerals. A rare lava type is represented by the hornblende-bearing andesite dikes exposed in Hot Springs Bay Valley. The only flow sampled which was not porphyritic was Ak-81-26, from Akutan Harbor. The lack of phenocrysts indicates that this flow was very fluid, and may have erupted at a higher temperature, or more quickly, than other flows on the island. The other flows contain individual phenocrysts and crystal clots. The crystal clots are probably the result of crystals clumping together during growth in a magma chamber, or they may be xenocrysts from earlier lavas. There has been some suggestion that crystal clots represent the reequilibration of an amphibolite mantle to lower pressures (Stewart, 1975), but the variety in composition of the crystal clots, and the lack of any relic amphibole suggests that this is not the case on Akutan.

The dikes exposed on Akutan Island range from porphyritic to aphanitic, and alteration in these rocks is quite variable. While some of the alteration seen is due to fluids associated with emplacement of the dikes, some of the alteration seen may be due to sea water alteration (D. Hawkins, personal

commun., Motl and Holland, 1978). This is especially true of those dikes exposed along the coast.

The dikes were examined to determine if they might be related to formation of an older caldera. Significant differences in K-Ar ages of dikes from the same localities suggests that they are not (Romick and others, in preparation).

MINERALOGY

Akutan lavas are characterized by phenocrysts of plagioclase, clinopyroxene, olivine, orthopyroxene, opaque minerals, and alteration products in a finer-grained groundmass. Plagioclase is the only mineral present in all of the samples.

Clinopyroxene

Calcium-rich augite is the one type of clinopyroxene present as phenocrysts. Figure 8 shows the results of microprobe analyses of Akutan clinopyroxenes and orthopyroxenes. The clinopyroxene compositions vary about 13 percent Fs, 8 percent Wo, and 2 percent En. The augite from Lava Peak Flows is the most Fs poor, while lavas from Hot Springs Bay contain the highest percent Fs. Perfit and Gust's (1981) microprobe analyses of phenocrysts in basalts and andesites are very similar to the analyses in this study.

There are two texturally distinct populations of clinopyroxene. The first is a group of large anhedral to subhedral phenocrysts up to 7 mm long. These large grains are commonly zoned, but rarely twinned. In contrast, the second population of clinopyroxene consists of smaller subhedral grains which average 0.75 to 1.5 mm in size, and are commonly twinned as well as zoned. Both populations occur as individual phenocrysts and as glomerocrysts. The glomerocrysts are up to 8 mm long and are usually composed of anhedral grains 0.5 to 2 mm long.

It would be convenient to be able to divide these two dissimilar groups into two generations of growth, the larger grains growing earlier in a relatively undisturbed environment, while the smaller phenocrysts growing in a fairly active environment, possibly which the magma was erupting. However, there are no compositional differences between the two groups of phenocrysts, which one might expect if they crystallized at different times.

The clinopyroxenes are biaxial positive with a 2V ranging from 35 to 60°. The large phenocrysts have low birefringence while the small phenocrysts are moderately birefringent. In plain light the clinopyroxenes are pale green and nonpleochroic.

The groundmass pyroxenes are also pale green in plain light, biaxial positive, and have low birefringence. The grains are, in general, too small for 2V determination.

Figure 9 shows the variety of zoning found in Akutan pyroxenes. Figure 11a shows well developed "hourglass" zoning. Most authors ascribe the zoning to different growth rates in different crystallographic directions (Strong, 1969; Gray, 1971; Hollister and Gancarz, 1971; Wass, 1973). The resulting skeletal form is later filled by clinopyroxene richer in FeO, TiO₂, Na₂O, and Al₂O₃. Another type of zoning, not illustrated, appears as an anhedral core surrounded by a euhedral rim. Deer and others (1978) suggest that this type of zoning results from melting the grain during movement of the magma prior to eruption. Thereafter the temperature drops and a euhedral rim forms around the partially melted crystal (Deer and others, 1978). The zoning indicates that the clinopyroxene was not always in equilibrium with the surrounding liquid. Diffusion of cations within the crystal lattice is not fast enough to allow the crystal composition to readjust in response to the change in liquid composition. The system's response to disequilibrium is to mantle the crystal with a rim that can coexist with the liquid. As the composition of the liquid changes so does the composition of the rim until crystallization halts the process, or the crystal is resorbed.

Several types of twins occur in the clinopyroxenes (fig. 10). They range from simple growth twins to polysynthetic twins with (010) as the composition plane.

Orthopyroxene

The orthopyroxene present in Akutan rocks is hypersthene. The mineral appears in two forms: 1) as euhedral to anhedral phenocrysts rimmed by clinopyroxene, and 2) as subhedral to anhedral phenocrysts without reaction rims. The two textural types can occur in the same rock, and microprobe analyses indicate that there is little compositional difference between the two orthopyroxenes (see Appendix III). Nor are there any differences in the composition of angite rimming the hypersthene and angite as independent phenocrysts. This suggests that whatever causes the rimming of orthopyroxene by clinopyroxene, it is not due to compositional differences between the two orthopyroxenes (fig. 8).

The hypersthene phenocrysts are 0.5 to 0.75 mm long, biaxial negative with a 2V between 55 and 70°, and have low birefringence. The phenocrysts have pale pink, to yellow, to green pleochroism. Extinction is parallel to cleavage, and the hypersthene is untwinned.

Olivine

Olivine never makes up more than 8 percent of the rock when it is present, and usually makes up only 2 to 4 percent. It is generally subhedral and anhedral in form, commonly occurring as fragments of grains. Occasionally euhedral olivine is present, and skeletal varieties are common in some of the western flows. The phenocrysts are rarely greater than 1 mm in diam. The olivine commonly has an oxidized outer rim, or is partially altered to iddingsite. Biaxial positive and negative varieties of olivine occur in Akutan lavas. The skeletal variety analyzed by microprobe in figure 11 are biaxial negative and have a compositional range between FO₇₅ and FO₆₉. No biaxial positive olivine was analyzed. Figure 16 also shows the microprobe results

from Perfit and Gust (1981). For rocks containing only olivine and clinopyroxene, Perfit and Gust's (1981) data closely compares with this study's although some of their analyses have values up to Fo_{90} .

The olivine has high relief, moderate to high birefringence and is clear in plain light. Zoning is either very weak or nonexistent.

Plagioclase

Plagioclase is the most abundant mineral in Akutan lavas. It is present as phenocrysts and in the groundmass of all of the flows and dikes examined. Plagioclase makes up 8 to 44 percent of lavas and may make up to 100 percent of the phenocrysts present in a particular rock. Plagioclase phenocrysts range from 0.5 to 7 millimeters in length. Inclusions of glass, clinopyroxene, and opaque minerals are occasionally present.

Plagioclase phenocrysts are generally subhedral to euhedral in form, although there are anhedral fragments present. Normal, oscillatory, and reversed zoning are present in Akutan plagioclase. Twinning is ubiquitous, and albite and carlsbad twins are the most common types. Cruciform penetration twins are seen occasionally.

Figure 12 shows the type of compositional zoning present in samples from Akutan Island. Microprobe data for the Lava Peak Flows shows the plagioclase to be very calcic (An_{90} to An_{80} core values) and zoned between core and rim about 10 percent anorthite. The zoning in these rocks appears as normal zoning, where anorthite content decreases from core to rim, and as oscillatory zoning where rim and core are approximately equal in anorthite content, and the intermediate interior more sodic.

Plagioclase from Hot Springs Bay lavas are more albitic and show less zoning. One sample is zoned between An_{45} and An_{50} , while another is zoned 1 percent between An_{50} and An_{51} .

Sample Ak-81-73 is from a gabbroic intrusive on the west side of Hot Springs Bay. The plagioclase from this sample shows extreme zoning. One phenocryst is zoned between An_{93} and An_{60} , while another is zoned from An_{87} to An_1 midway to the rim, with an outer rim of alkali feldspar.

The division between the Lava Peak flows and the other lavas seen in the microprobe data may, or may not, be a real phenomenon. More analyses are needed to confirm the apparent separation of values.

Figure 13 shows the variety of glass inclusions present in plagioclase phenocrysts. They occur as a fine dusting in the core, at some intermediate point between core and rim, in the rim, or some combination of the three. The zone of inclusions is usually parallel to the crystal boundaries. In some cases the inclusions are not oriented with respect to the crystal faces and appear as irregularly shaped blebs in the interior of the phenocryst. The textures shown in figure 13 indicate a change in the conditions of crystal growth. This change may correspond to conditions of higher undercooling,

possibly caused by changes in temperature or pressure. Undercooling is the difference between the liquidus temperature of the crystal and the temperature of the liquid the crystal is growing in. As the degree of undercooling increases, crystal growth changes from planar to skeletal. (Lofgren, 1980) High growth rate, combined with the skeletal crystal form, may make it possible for the crystal to trap liquid as it grows. The trapped liquid is quenched to a glass. A change to lower undercoolings would result in a return to planar crystal boundary growth, and the euhedral outline seen on Akutan plagioclase.

Other types of inclusions include large amounts of brown glass trapped in the interior of plagioclase grains, and clinopyroxene and opaque grains which appear to have been trapped in the plagioclase as it crystallized.

The plagioclase in samples Ak-81-73 and Ak-81-100, both coarse grained intrusives, are essentially inclusion-free. Emplacement at depth would cause gradual cooling, resulting in crystallization at low undercooling. This would cause planar crystal boundary growth. The slow cooling rate would also result in low growth rates which would not allow glass to be trapped within plagioclase phenocrysts.

Accessory and Alteration Minerals

Opaque Minerals

Opaque phenocrysts, generally, make up less than 1 percent of Akutan lavas, and are usually restricted to the groundmass. Those phenocrysts that are present are subhedral to anhedral and less than 0.75 mm in diam. Skeletal varieties were observed in some samples and probably crystallized late in the history of the magma. The opaque minerals were occasionally seen as inclusions in angite and hypersthene phenocrysts, and rarely in olivine and plagioclase. Some euhedral forms are present and usually appear as cubes or octahedrons, suggesting they are some type of magnetite. Opaque minerals, when present in the groundmass, are usually euhedral to subhedral and approximately the same size (0.1 to 0.2 mm) as the other groundmass minerals present.

Hornblende

Hornblende is present in two samples, both dikes from Hot Springs Bay Valley. The amphibole has olive green to light green pleochroism (X=yellow-green, Y=brownish-green, and Z=green) and moderate birefringence. It is anhedral and 0.25 to 1.5 mm in diam. Hornblende never makes up more than 1 percent of the rock.

Apatite

Apatite occurs as euhedral rods in plagioclase. It is approximately 0.1 mm long and was present in trace amounts in most of the rocks examined.

Carbonate

Carbonate is a common alteration mineral in the older lavas on Akutan. It is a common vesicle filling and alteration product of mafic minerals and groundmass, and occasionally replaces plagioclase. The carbonate is uniaxial negative, has variable relief, is clear in plain light, and has very high birefringence. The grain size is quite variable, ranging from microcrystalline to 4 mm in diam.

Chlorite

Chlorite is the most common alteration product of Akutan lavas. It has moderate birefringence and occurs as microcrystalline grains with light to dark green, and light to medium yellow, pleochroism. Chlorite may make up to 10 percent of the rock and commonly occurs as pseudomorphs of olivine and clinopyroxene. It sometimes occurs as a lining in amygdules where carbonate fills the interior of the amygdule.

Quartz

Quartz is occasionally present as an alteration mineral, and usually occurs in veinlets associated with carbonate. It occurs in trace amounts and is less than 0.25 mm in size.

Serpentine Minerals

Olivine is rarely altered to a nonpleochroic serpentine mineral. It is fibrous, has low birefringence low relief and occurs as pseudomorphs after olivine.

Crystallization Sequence

Table 4 show the crystallization sequence for Akutan lavas. In general, plagioclase is the first mineral to crystallize. Opaque minerals occasionally crystallize before plagioclase (Marsh, 1976), as in samples Ak-81-20, Ak-81-34, Ak-81-38, and Ak-81-62, but usually crystallize after nucleation of plagioclase and are seen enclosed by olivine and clinopyroxene. Olivine is the next phenocryst to crystallize. In those samples where both olivine and orthopyroxene are present, olivine appears to have crystallized before orthopyroxene. In those samples where orthopyroxene is present and olivine is not, orthopyroxene is the next phenocryst to form after the opaque minerals. Clinopyroxene is the last phenocryst to form, unless skeletal olivine, or hornblende are present, then they are last phenocrysts to begin crystallizing. A generalized crystallization sequence for Akutan lavas is plagioclase-opaque minerals-olivine/orthopyroxene-clinopyroxene-skeletal olivine/hornblende-groundmass. While there is no experimental data on the crystallization of Akutan lavas, work done on Atka basalts by Baker and Egger (1983) at various pressures reproduces the crystallization sequence described above for magmas which crystallized at less than 8 Kb pressure. The early or late appearance of opaque minerals depended upon the oxygen fugacity of the system. Thus, the sequence based upon textural relationships appears in Akutan basalts and andesites appears to be consistent with experimental work on rocks of similar composition.

Summary

Mafic mineral compositions on Akutan are remarkably uniform suggesting that whatever changes have occurred in the magmas which formed Akutan lavas, the factors influencing mineral composition (pressure, temperature, PH_2O , liquid composition, etc.) remained fairly constant. Unalaska Island, Frosty Peak Volcano, and Adak Island pyroxenes and plagioclase are very similar in composition to Akutan minerals (Byers, 1959; Drewes and others, 1961; Marsh, 1976; Perfit and Gust, 1981) suggesting that the lavas for many Aleutian volcanoes are similar in composition, and form minerals of similar composition.

What is variable on Akutan is the relative abundance of particular minerals. Olivine is abundant in Lava Peak rocks, while orthopyroxene is more abundant in some of the Hot Springs Bay lavas. Plagioclase and clinopyroxene are the only ubiquitous minerals in Akutan lavas.

GEOCHEMISTRY

Major Oxides

Appendix 1 lists the results of major oxide analyses. Oxide totals ranged from 98.52 percent to 100.71 percent. Harker variation diagrams are shown in figure 14. MgO , FeO , and CaO decrease with increasing SiO_2 , while Na_2O and K_2O generally increase with increasing SiO_2 . Curves for TiO_2 and Al_2O_3 are flat with respect to SiO_2 , and Fe_2O_3 data are too dispersed to draw any conclusions regarding a particular trend. The relative merits of these plots versus plots of more complex ratios are discussed by Cox and others (1979) and Maaloe and Peterson (1981). Samples from Lava Peak and from the other parts of the island do not plot as separate groups on the Harker diagrams.

These diagrams are supposed to represent the "liquid line of descent" of a fractionating magma. As certain elements are incorporated into early-forming minerals, their concentration in the remaining liquid decreases, while those elements not used in the minerals increase in abundance. These trends, whether increasing or decreasing, indicate changes in the liquid composition as it fractionates. Ideally, one should use analyses from glasses (quenched liquid) to obtain accurate measurements of composition, however this is rarely possible. Most volcanics are crystallized to some degree, and many are porphyritic. The local addition or subtraction of phenocrysts in these rocks may significantly affect where samples plot on the trends, although porphyritic rocks may still represent liquid compositions. If, for instance, olivine crystals settle towards the bottom of a cooling flow that portion will be enriched in olivine. If a sample is taken from that part of the flow and analyzed it will plot above the trends for FeO and MgO , because it has been enriched in those components by the addition of olivine. Likewise, samples taken from the part of the flow depleted in olivine will plot below the trends because they are depleted in the two oxides due to the removal of olivine. If many of the samples analyzed are porphyritic, considerable scatter in the trends can occur due to the above effect. This may be

the case for Akutan samples. Partial alteration of some of the samples may also affect the analyses by preferentially adding or subtracting certain elements.

Oxide-oxide plots were constructed to see if any distinction could be drawn between the Lava Peak rocks and the other lavas on the island. The results are shown in figures 15 through 18. Again, no clear distinction can be made between the Lava Peak volcanics and other volcanics on Akutan Island. The fact that the two groups of lavas do not plot as separate trends suggests that they were not derived from different parental magmas or significantly different sources.

An AFM diagram (fig. 19) shows a slight iron enrichment similar to other plots of Aleutian rocks (Marsh, 1976). The FeO/MgO vs SiO₂ diagram (fig. 21) also shows the mild iron enrichment trend typical of Aleutian tholeiites as defined by Kay and others (1982). Marsh (1976) noted that Aleutian trends were higher in iron enrichment than the trend for Cascade rocks, but lower than the trend for Tongan volcanics. Again, the lava Peak rocks and the other lavas intermix on the diagram. In a total alkalis (K₂O+Na₂O) versus SiO₂ diagram (fig. 20), Akutan rocks fall in the high-alumina field as defined by Kuno (1966). Perfit (1978) suggests that it is possible to derive these high-alumina rocks from high magnesium basalts found on Akutan Island.

The effect of fractionation of plagioclase, olivine, and augite can be seen in figure 22. As the magma(s) differentiated, the CaO/Al₂O₃ ratio decreased and the FeO/MgO ratio increased. This is due to the precipitation of early-forming calcic plagioclase and magnesian olivine and augite. This left the remaining liquid enriched in FeO and depleted in CaO and MgO, resulting in the trend observed.

Statistical Analyses

The oxide data were analyzed by two multivariate statistical methods to see if more sophisticated techniques could distinguish the two petrographic groups. The oxide data was analyzed by cluster analysis (McCammon and others, 1970), and then a stepwise multiple discriminant analysis (Jennrich and Sampson, 1981). A dendrograph (McCammon and others, 1970), obtained from the cluster analysis, is shown in figure 23.

Cluster analysis separates samples into groups (or clusters) based upon measured variables. The number of clusters that result from the analysis are not known beforehand, and samples are generally free to enter any cluster that develops. In contrast, discriminant analysis requires the number of groups to be set prior to analysis, with each sample assigned to a particular group (Davis, 1973). By minimizing the within-group variance and maximizing the between-group variance, the discriminant analysis identifies the variable, or variables, which distinguish the groups. Stepwise multiple discriminant analysis constructs a linear equation for each group by going through a series of simple analyses which move from one analysis to the next by adding, or subtracting, a classification variable along the way (Jennrich, 1977).

The cluster analysis distinguished four general groups of lavas (fig. 23). The stepwise discriminant analysis used P_2O_5 and TiO_2 to identify the four groups. The discriminant functions for the four groups are listed below. P_2O_5 and TiO_2 are in weight percent and X is the value of the discriminant. See appendix V for an example of how the discriminant functions are used.

WestF	$X=100.33TiO_2+264.09P_2O_5-83.22$
EastF	$X=93.55TiO_2+245.03P_2O_5-72.26$
WestD	$X=151.90TiO_2+414.89P_2O_5-194.84$
EastD	$X=125.68TiO_2+343.05P_2O_5-133.74$

Based on the multiple discriminant analysis we had difficulty distinguishing the two groups of flows defined by the cluster analysis. Samples classified as EastF by the cluster analysis were classified as WestF by the discriminant analysis and visa versa. Table 5 lists the posterior probabilities for the two groups of flows. The probabilities represent the chance that any particular analysis will be classified in a particular group. A high probability in one group is needed for a clear classification. Most of the flows listed in table 8 could be classified into either group.

A canonical plot of the groups and their means is the best two-dimensional display of the relationship between the four groups and is shown in figure 24. The two groups of flows have only slight differences between their means.

Both groups of dikes plot well away from either group of lava flows. Both partially altered and unaltered dikes plotted together indicating that the difference between the flows and dikes is a real phenomenon and not a result of alteration. Two dikes (Ak-81-50, Ak-81-38) plot with the lava flows.

The statistical analyses also suggest that the lava flows on Akutan Island are chemically similar and are difficult to distinguish on the basis of major element chemistry. The cluster analysis grouped Lava Peak flows with flows from other parts of the island. The discriminate analysis permitted some rearrangement of the groups, but it also could not distinguish the two petrographic groups.

Normative Mineralogy

Appendix 1 lists the normative mineralogy for the 31 samples from Akutan. All of the rocks contain normative hypersthene, which by definition must be present in tholeiitic rocks (Cox and others, 1979). Most of the rocks are quartz normative. Five samples are olivine normative and their geographic distribution does not follow any pattern across the island. Lava Peak flows range from slightly olivine normative at the bottom to quartz normative further up the sequence. They also have greater than 11 percent normative hypersthene, while the other volcanics generally have less than 11 percent hypersthene (fig. 25).

Minor Element Analyses

Rb and Sr Analyses

Figure 26 is a plot of Sr versus Rb igneous rocks from Unalaska (Perfit and others, 1980). Akutan Island samples plot along the same trend as volcanics and intrusives from Unalaska Island, but tend to be lower in Sr.

Figures 27 and 28 are plots of Rb versus Rb/Sr and Sr versus Rb/Sr, respectively. These two diagrams successfully distinguish Lava Peak volcanics (higher Sr and lower Rb and Rb/Sr) from the other volcanics on the island.

McCulloch and Perfit's (1981) data are also plotted on the two diagrams. Two samples, Ak-4-EJ and Ak-4-33, plot in the Lava Peak field, but the third sample does not show a close relationship to either group. Unfortunately, it is not known whether the petrology of his samples is similar to that of the Lava Peak flows.

McCulloch and Perfit (1981) distinguished tholeiitic Akutan rocks from calc-alkaline rocks in the Aleutians by plotting Ba (ppm) versus K_2O and Rb/Sr versus K_2O . Their results suggest that tholeiitic rocks have higher BaO and Rb/Sr values for a given K_2O than the calcalkaline suites. Akutan samples plot in McCulloch and Perfit's tholeiitic region, for the K_2O versus Rb/Sr diagram, but the separation between the tholeiitic and cal-alkaline fields is not very good and the fields overlap at the mafic end.

McCulloch and Perfit's (1981) Sr and Nd isotope data for Akutan are shown in table 6 and are comparable to results reported by other workers (Kay and others, 1978; Kay, 1980; Marsh, 1976) for Aleutian lavas.

Potassium-Argon Dates

Four K-Ar whole rock dates were obtained from R. Armstrong at the University of British Columbia, Vancouver, British Columbia for two samples from eastern Akutan and two from Lava Peak (table 7). Lava flows from Lava Peak, Pickup Valley, and Hot Springs Bay Valley give ages around 1.2 m.y. AK-81-30, a dike from the base of Lava Peak, may be about 0.3 m.y. older than the three flows dated.

Summary

Both oxide-oxide plots and multivariate statistical analyses indicate that the major element chemistry of two petrographic groups of lava follow similar trends. Rb and Sr plots successfully distinguish the two petrographic groups, and suggest that the two groups may be related via some fractionation scheme. This is also indicated by the decrease in CaO/Al_2O_3 with increasing FeO/MgO (shown in fig. 22). Whole rock potassium-argon dates indicate that the Lava Peak satellite vent and the main vent lava suites erupted contemporaneously between 1.1 and 1.5 m.y. B.P. The major element chemistry of these lavas is typical of rocks derived from mantle material

(McCulloch and Perfit, 1981). Neodymium and strontium isotope ratios reported by McCulloch and Perfit (1981) also suggest that the lava were derived from mantle material, and that contamination by continental crust was negligible.

GEOOTHERMOMETRY AND GEOBAROMETRY

Two geothermometers and one geobarometer were used to estimate equilibrium temperatures and pressures for mineral pairs in Akutan lavas. Both geothermometers could not be used on the same samples, because none of the samples analyzed by microprobe contained the three phases needed.

Wood and Banno's (1973) geothermometer used the distribution of FeO and MgO between orthopyroxene and clinopyroxene to determine the equilibrium temperature. This geothermometer was used on a sample collected from Pickup Valley (Ak-81-23). Wells (1977) modified Wood and Banno's geothermometer using additional microprobe data. His geothermometer is used to corroborate the results obtained from Wood and Banno's (1973) geothermometer. Powell and Powell's (1974) geothermometer used the distribution of Mg and Fe between olivine and clinopyroxene to determine equilibrium temperatures. This geothermometer was used on two samples from Lava Peak (Ak-81-1 and Ak-81-13). The results for the geothermometry are shown in table 8. They indicate equilibrium temperatures between 992 and 1,330° C for both sets of mineral pairs.

Wood (1976) noted several problems with the olivine-clinopyroxene geothermometer which would result in temperature estimates that did not reflect the actual crystallization temperature, but seem geologically reasonable. The temperature determining equation for Powell and Powell's (1974) geothermometer is:

$$T = \frac{-2X_{Al}(920000 + 3.6P) - 0.0435(P-1) + 10100}{8 + R \ln D - 714.3(2X_{Al})}$$

$$\text{where } X_{Al} = X_{Al} + X_{Ti} + X_{Cr} + X_{Fe}$$

$$D = (X_{Mg,ol}/X_{Fe,ol}) (X_{Fe,Ml}/X_{Mg,Ml})$$

and $X_{Fe,ol}$ and $X_{Mg,ol}$ equal the mole fractions of Fe and Mg in olivine, respectively.

$$X_{Fe,Ml} = \frac{H1}{1 + (X_{Mg}/X_{Fe})_{Cpx}}$$

$$X_{Mg,Ml} = H1 - X_{Fe,Ml}$$

$$H1 = 1 - X_{Al}$$

$$R = 1.98726 \text{ cal/mole K}$$

P = pressure in bars

Other difficulties involve the pressure dependence of the olivine-clinopyroxene geothermometer and whether the phenocrysts used are in equilibrium. A crystallization pressure must be supplied in the equation to determine the temperature. The values listed in table 8 are for pressures between 1 bar and 15 kb.

The olivine in Akutan lavas commonly occurs as both skeletal and subhedral grains. Both types of phenocrysts are similar in composition. It is not known whether this is due to buffering of the olivine composition by the liquid, or to the two types of grains crystallizing during the same time period. If both types of grains crystallized during the same time interval, then the skeletal olivine indicates crystallization at higher undercoolings. The clinopyroxene is subhedral, suggesting that it crystallized at a lower undercooling than the skeletal olivine. Clinopyroxene crystals are zoned over a compositional range of 5 mole percent, while zoning of both phenocrysts may mean they formed under similar conditions and are in equilibrium with each other.

Wood and Banno's (1973) orthopyroxene-clinopyroxene geothermometer is pressure independent, or at least they feel the pressure effect can be ignored because of some evidence published by Davis and Boyd (1966) which indicated a 30 kb change in pressure only changed the equilibrium temperature 50° C. This is within the error of the technique. They assume that any Al₂O₃ in the pyroxenes does not affect the activity of the Mg in either of the pyroxenes appreciably.

The determining equation is:

$$T = \frac{-10202}{\ln(A_{\text{cpx}}/A_{\text{opx}}) - 7.65 X_{\text{Fe}}^{\text{opx}} + 3.88 (X_{\text{Fe}}^{\text{opx}})^2 - 4.6}$$

$$\text{where } A_{\text{cpx,opx}} = \left(\frac{\text{Mg}^2}{(\text{Fe} + \text{Mg}^2 + \text{Ca}^2 + \text{Mn}^2 + \text{Na}^1)} \right) \left(\frac{\text{Mg}^2}{\text{M}2 (\text{Fe}^2 + \text{Fe}^3 + \text{Mg}^2 + \text{Al}^3 + \text{Cr}^3 + \text{Ti}^4)} \right) \text{M}1$$

and $X_{\text{Fe}}^{\text{opx}}$ = mole percent Fe in orthopyroxene

The amounts are in mole fractions. Wood and Banno (1973) feel that the temperatures are accurate to ± 70 degrees C. They ignore Fe³ in the pyroxenes because if 10 percent of the Fe² as Fe³, the equilibrium temperature goes up 20 to 30°, which is within the error of the technique.

Wells (1977) modified Wood and Banno's (1973) pyroxene geothermometer to fit additional pyroxene equilibrium data. Wells' corrections may result in an increase or decrease in the temperature estimate.

The determining equation is:

$$T = \frac{7341 \text{opx}}{3.355 + 244 X_{\text{Fe}} - \ln K}$$

where $K = \frac{\text{activity of Mg in clinopyroxene}}{\text{activity of Mg in orthopyroxene}}$
(see Wood and Banno, 1973)
 $X_{\text{Fe}}^{\text{OPX}}$ = mole percent Fe in orthopyroxene

The temperatures obtained from this geothermometer are listed in table 8. In this instance the temperatures calculated are too high.

The lack of precision in these temperature estimates results from the insufficient data available regarding the thermodynamics which govern Fe and Mg substitution in cation sites. These temperatures should be considered rough estimates of equilibrium temperature for the mineral pairs concerned, and not accurate measurements.

As yet, no good geobarometers have been developed for mafic igneous rocks. Finnerty (1976) examined the exchange of Mn, Ca, Mg, and Al between garnet, olivine, clinopyroxene, and orthopyroxene in attempt to develop a suitable geothermometer and geobarometer. To use their geobarometer olivine must be in equilibrium with orthopyroxene and clinopyroxene, because the pyroxene pair buffered the system with respect to calcium. Finnerty and Boyd (1977) worked with ultramafic rocks and the two pyroxenes were the only calcium bearing phases present. None of the rocks examined in this study contain all three mafic minerals, but plagioclase is always present and may act as a calcium buffer for the system. If it is valid to use plagioclase as a buffer, Finnerty and Boyd's technique suggest that the olivine crystallized at some pressure less than 10 kb which is consistent with the experimental studies of Baker and Eggler (1983).

From the crystallization sequence of phases in Aleutian lavas, Marsh (1976) estimated their crystallization temperatures to be between 1,150 and 1,101° C, at pressures between 1 and 5 kb. Perfit and Gust's (1981) estimate of crystallization temperatures based upon ortho-clinopyroxene pairs ranges between 990°C and 1,100°C. These values compare well with those discussed above. Marsh (1976) noted that other workers found that plagioclase was the liquidus phase in andesitic magmas with less than 2 percent water (Eggler and Burnham, 1973). For water saturated conditions plagioclase was replaced by orthopyroxene as the liquidus phase above about 500 bars pressure. Marsh concluded that crystallization took place at about 500 bars in andesitic magmas with less than 2 percent water.

The temperatures obtained from the geothermometers are in the range expected for an erupting magma, but do not provide any additional information regarding the origin of Akutan lavas.

MAGMA GENERATION MODELS

Several models have been suggested to account for the chemical composition of Aleutian lavas. Most of these involve partial melting of oceanic crust with some oceanic sediments, depleted mantle, or combinations of all three to account for the minor element and REE abundances.

Coats (1962) used a "megathrust" to carry sediments down to mantle depths where they melted to form a rhyolitic melt. The melt then mixed with basaltic liquids to form andesitic magmas. Marsh (1976) derived Aleutian magmas from partial melts of subducted oceanic crust. He argued that there was not sufficient water in the mantle to form the magmas, and a more likely place would be subducted oceanic crust. Marsh did not use sediment contamination to modify the magma.

McCulloch and Perfit (1981) argued that REE and minor element ratios precluded the formation of Aleutian magmas directly from melted oceanic crust. Rather a multistage mixing/melting model was invoked in which the depleted mantle below the arc is metasomatized by a partial melt of oceanic crust. McCulloch and Perfit suggested that between 2 and 8 percent oceanic sediments are required to generate the variable large-ion lithophile enrichments and Sr and Nd isotope values in these magmas.

Kay and others (1978) also argued for sediment mixing to account for Pb and Sr values differing from those of MORB. Aleutian samples have Pb isotope ratios between those of MORB and Pacific sediments, which can be accounted for by contamination of about 2 percent sediments. Both Kay and others (1978) and McCulloch and Perfit (1981) note that the lack of variability and low values of the Sr isotope ratios indicate that passage through old continental material has not affected the composition of these magmas.

Perfit and Gust (1981) suggested that the high magnesium basalts found on Akutan and Unalaska islands could represent primary magmas. The high-alumina basalts and basaltic andesites seen on the islands could be generated by fractionation of olivine, clinopyroxene, and plagioclase from the magnesium-rich basalts. Kay (1978) also suggested that these high-magnesium lavas were primary melts.

Eichelberger (1978) derived andesites from a mixture of rhyolite and depleted mantle. He suggested that under hydrous conditions, the lower oceanic crust would be amphibolite. Up to a 20 percent melt derived from this composition would be rhyolitic. This rhyolitic component would mix with a basaltic melt derived from mantle material to form andesites.

Kay (1980) modeled magma generation using mass balance calculations, and concluded that one could account for the variety of magma types in the Aleutians by partially melting different amounts of subducted sediments, oceanic crust, and depleted mantle.

Summary

The diversity of opinion regarding the origin of andesitic magma indicates the lack of knowledge of both mantle composition and the role played by the subducted oceanic slab and sediments. It is agreed that magmas are related to regions of subduction, but the role of the subducted slab, mantle, and sediments in the development of andesitic magmas is still under debate.

EVOLUTION OF IGNEOUS ROCKS ON NORTHERN AKUTAN ISLAND

The lack of continuous outcrop makes it difficult to ascribe any detailed petrologic trends to Akutan lavas. The only location on northern Akutan Island where flows are exposed in a section not separated by debris flow deposits is at Lava Peak. There, the lower series of lava flows follows a typical trend for a fractionating magma: the lavas become more silica-rich up section, and the percentage of mafic minerals decreases with increasing silica content. Elsewhere on the island exposures do not allow for similar interpretations. Flows are commonly separated by thick sequences of pyroclastic debris making it impossible to determine whether a sequence of flows is the product of one, or more, magmas.

Two petrographic groups are present on Akutan Island: Lava Peak flows and dikes, and lavas exposed elsewhere on the island. Clinopyroxene and orthopyroxene are the major mafic minerals in the latter lavas, while olivine and clinopyroxene are the mafic minerals in Lava Peak flows. Only rarely is olivine present in other lavas from Akutan Island, and even more rarely is it abundant. This appears to be due to higher silica values, making orthopyroxene the stable mafic phase. The most recent volcanics, the pre-1870 and 1978 lava flows, are petrologically similar to volcanics exposed on the central and eastern part of the island (see table 4).

Many aspects of the major element chemistry of the two petrologic groups are quite similar. Oxide diagrams and multivariate statistical analyses do not suggest any differences in the way the two groups fractionated or their parental magmas. The use of TiO_2 and P_2O_5 as discriminates indicates that the variance of the more abundant oxides is too great to be able to distinguish the four groups identified by the cluster analysis. Even these two oxides can not clearly distinguish between the two groups of lava flows, although they are able to distinguish between flows and dikes.

Both Rb and Sr analyses, and plagioclase microprobe analyses, suggest compositional differences between Lava Peak flows and other lavas on the island. The Lava Peak flows are higher in Sr and lower in Rb and Rb/Sr than lavas from the remainder of the island. Lava Peak flows appear to have a more calcic plagioclase than plagioclase in lavas from other parts of the island.

Whole rock potassium-argon dates of 3 lava flows and one dike indicate volcanic activity began at least 1.5 m.y. ago. The Lava Peak flows and lava flows from the eastern and central part of the island were erupting contemporaneously about 1.1 m.y. ago.

Any model developed to explain the igneous activity on Akutan Island must explain: 1) the different mineral assemblages, 2) the overall chemical similarity between the two petrographic groups, 3) the differences in Rb and Sr contents, 4) the differences in phenocryst abundance, and 5) the identical radiometric ages of the two groups of flows.

One model which accounts for these differences relies on a compositionally zoned magma chamber (fig. 29). According to this model, the lavas exposed over most of the island are from central vent eruptions, which drew

magma from the top of the chamber. Lava Peak flows are from lateral eruptions which tapped magma lower in the chamber. Crystallization and settling of early-forming plagioclase, olivine, and clinopyroxene from the upper part of the magma chamber would create an upper layer deficient in phenocrysts and enriched in silica and incompatible elements. The local concentration of these phenocrysts would create a lower layer enriched in phenocrysts and relatively silica deficient. Lavas erupting from the top of the magma chamber would be relatively phenocryst poor and sufficiently enriched in silica that orthopyroxene would replace olivine as the first mafic phase to crystallize, resulting in fine-grained rocks containing orthopyroxene and clinopyroxene phenocrysts.

The Lava Peak eruptions, tapping a lower layer in the chamber, would be enriched in early formed phenocrysts and relatively silica poor. The result would be phenocryst-rich rocks containing olivine and clinopyroxene. The tholeiitic character of Akutan lavas is the result of iron enrichment in the liquid caused by the suppression of iron oxide precipitation.

Different Rb and Sr abundances in the two petrologic groups result from partitioning of the two cations in the melt. Rb (8-fold coordination) cations have ionic radii of 1.49 Å, while Sr (6 to 8-fold coordination) cations have ionic radii of 1.16 Å (Shannon and Prewitt, 1969). The smaller divalent Sr cation can substitute for Ca (ionic radius= 1.00 Å) in plagioclase, while Rb is excluded from the plagioclase crystal lattice and is concentrated in the residual liquid. The early-forming plagioclase would selectively remove Sr from the upper layer of the magma chamber, leaving a liquid relatively enriched in Rb. The lower layer, enriched in plagioclase phenocrysts, would also be enriched in Sr. Magma drawn from the upper layer would have more Rb and less Sr than magma from lower layers.

The overall chemical similarity between the two petrologic groups is due to their derivation from the same magma body, however some magma mixing may have complicated many of the simple trends seen. Simultaneous eruptions from different regions of the magma chamber resulted in lavas with the same radiometric age, but different characteristics.

Magma composition on Akutan Island has not changed appreciably through time. While Lava Peak flows can be distinguished from the other lava flows on the island, the small range in chemical composition for these lavas making evolutionary interpretation impossible. This compositional monotony is characteristic of Aleutian lavas, and suggests that the magmas erupt so quickly that they do not differentiate significantly, or are replenished by the source material, resulting in lavas of relatively uniform composition.

Dike orientations on Lava Peak, the location of the Lava Peak center, and the location of the recent cinder cone and lava flow suggest a persistent zone of weakness existing on the northwestern side of the island since at least 1.5 million years ago. The character of rocks from this zone has changed such that the most recent lavas are similar to the main vent lavas, and not the Lava Peak flows.

Akutan Island is composed of basaltic and andesitic lavas, ranging from 46 to 63 percent silica; compositions typical of other Aleutian volcanoes (Byers, 1959; Drewes and others, 1961; Marsh, 1976; Kay and others, 1982). Mineral compositions are also similar between various volcanoes (Byers, 1959; Drewes, 1961; Marsh, 1976; Perfit and Gust, 1981). The similarity in oxide analyses, mineralogy, and isotopic ratios suggests that Akutan lavas, and the other Aleutian volcanoes, are derived from a similar, if not the same, source.

Current theories suggest that Aleutian magmas result from partially melting oceanic crust and/or mantle, contaminated by 2 to 8 percent sediments, which rises through the overlying plate and erupts on the surface. Nd and Sr isotope analyses indicate a mantle origin for Akutan lavas (McCulloch and Perfit, 1981; DePaolo, 1981). Ba/La and Pb/La ratios suggest that continental sediments also play a role in the development of Akutan magmas. At present, it is difficult to constrain the relative importance of mantle vs oceanic crust in Aleutian magmas.

Volcano distribution in island arcs may be due to segmentation of the subducting oceanic plate (Stoiber and Carr, 1973; Hughes and others, 1980). Kay and others (1982) developed a segmentation model to explain the distribution of tholeiitic and calc-alkaline volcanoes in the Aleutian arc. Their model restricts tholeiitic volcanoes to segment boundaries, with calc-alkaline; volcanoes found in segment interiors. The segments are defined by zones of great earthquake movement. Akutan Island is in the middle of their Cold Bay segment. According to their model, Akutan lavas should be calc-alkaline; instead they show tholeiitic affinities (Perfit and Gust, 1981). Kay and others' model breaks down because little petrologic information is available for volcanoes in the eastern Aleutian arc. Whether or not tholeiitic and calc-alkaline volcanoes fit into a segmentation model will not be clear until a great deal more information is gathered on the petrology and geochemistry of the region.

This study described the petrology and geochemistry on northern Akutan Island. The southern half of the island should be examined in similar detail. In particular, Flat Tip Peak should be examined to see if it is petrologically similar to Lava Peak. Additional plagioclase microprobe analyses should be conducted to see if the compositional difference between Lava Peak plagioclase and the other lavas is a real phenomenon. Several more potassium-argon dates are needed to constrain the period of igneous activity more closely. It is not known what compositional type (tholeiitic or calc-alkaline) is currently erupting from Akutan Volcano. A detailed study of the geochemistry and petrology of the volcano is needed to identify the current trend and describe its relation to lavas erupted in the past.

REFERENCES CITED

- Baker, D.R., and Eggler, D.H., 1983, Fractionation paths of Atka (Aleutians) high-alumina basalts; constraints from phase relations, *Journal of Volcanology and Geothermal Research*, v, 18, p. 387-404.
- Bhattacharji, S., and Smith, C.H., 1964, Flow differentiation, *Science*, v. 145, p. 150-153.

- Black, R.F., 1974, Geology and ancient Aleuts, Amchitka and Umnak Island, Aleutians, Arctic Anthropology, XI-2, p. 126-140.
- Byers, F.M., 1959, Geology of Umnak and Bogoslof Islands, Aleutian Islands, Alaska, U.S. Geological Survey Bulletin 1028-L, p. 267-352.
- Byers, F., and Barth, T., 1953, Volcanic activity on Akun and Akutan Islands, Pacific Science Conference, 7th, New Zealand, 1949, Proceedings, v. 2, p. 382-397.
- Carmichael, I., Turner, F., and Verhoogen, J., 1974, Igneous Petrology, McGraw-Hill Book Company, New York, 739 p.
- Coats, R., 1962, Magma type and crustal structure in the Aleutian arc: in Crust of the Pacific Basin, Geophysical Monograph No. 6, American Geophysical Union, p. 92-109.
- Cox, K., Bell, J., and Pankhurst, R., 1979, The interpretation of Igneous Rocks, George Allen and Unwin, London, 450 p.
- Davis, B., and Boyd, F., 1966, The join $Mg_2Si_2O_6$ -- $CaMgSi_2O_6$ at 30 kilobars pressure and its application to pyroxenes from kimberlites, Journal of Geophysical Research, 71, p. 3567-3576.
- Davis, J.C., 1973, Statistics and Data Analysis in Geology, John Wiley & Sons, New York, 550 p.
- Deer, W., Howie, R., and Zussman, J., 1978, Rock Forming Minerals: Single Chain Silicates, v. 2A, John Wiley and Sons, New York, 668 p.
- DePaolo, J., 1981, Nd isotope studies: some new perspectives on earth structure and evolution, EQS, 62, No. 14, p. 137-140.
- Drewes, H., Fraser, G.D., Snyder, G.L., and Barnett, H.F., 1961, Geology of Unalaska Island and adjacent insular shelf, Aleutian Island, Alaska, U.S. Geological Survey Bulletin 1028-S, p. 583-676.
- Eggler, D.H., and Burnham, C.W., 1973, Crystallization and fractionation trends in the system andesite- H_2O - CO_2 - O_2 at pressures to 10 kb: Geological Society of America Bulletin, v. 84, p. 2517-2532.
- Eichelberger, J., 1978, Andesitic volcanism and crustal evolution, Nature, v. 275, p. 21-27.
- Finch, R., 1935, Akutan Volcano, Zeitschrift fur Vulkanologie, Band XVI, p. 155-160.
- Finnerty, T., 1976, Exchange of Mn, Ca, Mg, and Al between synthetic garnet, orthopyroxene, and olivine, Carnegie Institution Geophysical Laboratory 1976 Year Book, p. 572-579.
- Finnerty, T., and Boyd, F., 1977, Pressure-dependent solubility of calcium in fosterite coexisting with diopside and enstatite, Carnegie Institution Geophysical Laboratory 1977 Year Book, p. 713-717.
- Gibb, F.G., 1968, Flow differentiation in the xenolithic ultrabasic dykes of the Cuillins and the Strathaird Peninsula, Isle of Skye, Scotland, Journal of Petrology, v. 9, p. 411-443.
- Gray, N.H., 1971, A parabolic hourglass structure in titanaugite, The American Mineralogist, v. 56, p. 952-958.
- Hollister, L.S., and Gancarz, A.J., 1971, Compositional sector-zoning in clinopyroxene from Narce area, Italy, The American Mineralogist, v. 56, p. 959-979.
- Hughes, H.M., Stoiber, R.E., and Carr, M.J., 1980, Segmentation of the Cascade volcanic chain, Geology, v. 8, p. 15-17.
- Jennrich, R.I., 1977, Stepwise Discriminant Analysis, in Statistical Methods for Digital Computers, Edited by K. Enslein, A. Ralston, and H. Wilf, v. III, Wiley-Interscience, New York, p. 76-95.

- Jennrich, R.I., and Sampson, P., 1981, Stepwise Discriminant Analysis, in BMDP Statistical Software, Edited by W.J. Dixon, University of California Press, Berkeley, p. 519-537.
- Kay, R., 1977, Geochemical constraints on the origin of Aleutian magmas: in Island arcs, Deep sea Trenches, and Back Arc Basins, Edited by M. Talwani and W. Pitman III, American Geophysical Union, p. 229-242.
- Kay, W., 1978, Aleutian magnesium andesites: melts from subducted Pacific Ocean Crust, *Journal of Volcanology and Geothermal Research*, No. 4, p. 117-132.
- Kay, W., 1980, Volcanic arc magmas: Implications of a melting-mixing model for element recycling in the crust-upper mantle system, *Journal of Geology*, v. 88, No. 5, p. 497-522.
- Kay, W., Sun, S., and Lee-Ru, C., 1978, Pb and Sr isotopes in volcanic rocks from the Aleutian Islands and Pribilof Islands, Alaska, *Geochimica et Cosmochimica Acta*, v. 42, p. 263-273.
- Kay, S.M., Kay, R.W., and Citron, G.P., 1982, Tectonic controls on tholeiitic and calc-alkaline magmatism in the Aleutian arc, *Journal of Geophysical Research*, v. 87, p. 4051-4072.
- Komar, P.D., 1972a, Mechanical interactions of phenocrysts and flow differentiation of igneous dikes and sills, *Geological Society of America Bulletin*, v. 83, p. 973-987.
- Komar, P.D., 1972b, Flow differentiation of igneous dikes and sills; profiles of velocity and phenocryst concentration, *Geological Society of America Bulletin*, v. 83, p. 3443-3448.
- Kuno, H., 1966, Lateral variation of basalt magma type across continental margins and island arcs, *Bulletin Volcanologique*, v. 29, p. 195-222.
- Lofgren, G., 1980, Experimental studies on the dynamic crystallization of silicate melts, in *Physics of magmatic processes*, R.B. Hargraves (ed.), Princeton University Press, p. 487-551.
- Maaloe, S., and Peterson, T.S., 1981, Petrogenesis of oceanic andesites, *Journal of Geophysical Research*, v. 86, p. 10273-10286.
- Marsh, B., 1976, Some Aleutian andesites: their nature and source, *Journal of Geology*, v. 84, No. 1, p. 27-46.
- Marsh, B., 1979, Island arc development: some observations, experiments, and speculation, *The Journal of Geology*, v. 87, p. 687-713.
- McCulloch, M., and Perfit, M., 1981, $^{143}\text{Nd}/^{144}\text{Nd}$, $^{87}\text{Sr}/^{86}\text{Sr}$ and trace element constraints on the petrogenesis of Aleutian island arc magmas, *Earth and Planetary Science Letters*, 56, p. 167-179.
- McCammon, R.B., and Wenniger, G., 1970, The dendrograph, Computer Contribution 48 State Geological Survey, University of Kansas, Lawrence Kansas.
- Miyashiro, H., 1974, Volcanic rock series in island arcs and active continental margins, *American Journal of Science*, v. 274, p. 321-355.
- Mottl, M.J., and Holland, H.D., 1978, Chemical exchange during hydrothermal alteration of basalt by seawater-I. Experimental results for major and minor components of seawater, *Geochimica et Cosmochimica Acta*, v. 42, p. 1103-1115.
- Motyka, R., Moorman, M., and Liss, S., 1981, Assessment of thermal springs sites Aleutian arc, Atka Island to Becherof Lake--preliminary results and evaluation, Alaska Division of Geological and Geophysical Surveys Open-file Report 144, p. 90-96.
- Nolan, J., 1969, Physical properties of synthetic and natural pyroxenes in the system diopside-hedenbergite-acmite, *Mineralogical Magazine*, v. 37, No. 286, p. 216-229.

- Perfit, M., 1978, The petrochemistry and strontium isotope composition of mafic basalts from the Aleutian Islands, Abst., Annual Meeting of Geological Society of America, p. 470.
- Perfit, M., Brueckner, H., Lawrence, J., and Kay, R., 1980, Trace element and isotopic variation in a zoned pluton and associated rocks, Unalaska Island, Alaska: A model for fractionation in the Aleutian calcalkaline suite, Contributions to Mineralogy and Petrology, No. 73, p. 69-87.
- Perfit, M., and Gust, D., 1981, Petrochemistry and experimental crystallization of basalts from the Aleutian Islands, Alaska, Abstr. IAVCEI Symposium on Arc Volcanism, p. 288-289.
- Powell, M., and Powell, R., 1974, An olivine-clinopyroxene geothermometer, Contributions to Mineralogy and Petrology, No. 48, p. 249-263.
- Romick, J.D., and Swanson, S.E., Geology of Northern Akutan Island, in preparation.
- Rutstein, M., and Yund, R., 1969, Unit cell parameters of synthetic diopside-hedenbergite solid solutions, The American Mineralogist, v. 54, p. 238-245.
- Shairer, J., and Boyd, F., 1957, Pyroxenes, Carnegie Institution Geophysical Laboratory 1957 Year Book, p. 223-225.
- Shannon, R.D., and Prewitt, C.T., 1969, Effective ionic radii in oxides and fluorides, Acta Crystallographica, p. 925-946.
- Simkin, T., Siebert, L., McCelland, L., Bridge, D., Newhall, C., and Latter, J., 1981, Volcanoes of the World, The Smithsonian Institution, Hutchinson Ross Publishing Company, Stroudsburg, Pennsylvania, 232 p.
- Stewart, D., 1975, Crystal clots in calc-alkaline andesites as breakdown products of high-Al amphiboles, Contributions to Mineralogy and Petrology, v. 53, p. 195-204.
- Stoiber, R.E., and Carr, M.J., 1973, Quaternary volcanic and tectonic segmentation of Central America, Bulletin Volcanologique, v. 37, p. 304-325.
- Strong, D.F., 1969, Formation of the hour-glass structure in augite, Mineralogical Magazine, v. 37, N. 288, p. 472-479.
- Wass, S.Y., 1973, The origin and petrogenetic significance of hour-glass zoning in titaniferous clinopyroxenes, Mineralogical Magazine, v. 39, N. 302, p. 133-144.
- Wells, P., 1977, Pyroxene thermometry in simple and complex systems, Contributions to Mineralogy and Petrology, No. 62, p. 129-139.
- Wood, B., and Banno, S., 1973, Garnet-orthopyroxene and orthopyroxene-clinopyroxene relationships in simple and complex systems, Contributions to Mineralogy and Petrology, No. 42, p. 109-124.
- Wood, B., 1976, An olivine-clinopyroxene geothermometer, Contributions to Mineralogy and Petrology, No. 56, p. 297-303.

APPENDIX I

APPENDIX II - Major oxides and normative minerals (in weight percent).

	<u>AK-81-1</u>	<u>AK-81-2</u>	<u>AK-81-3</u>	<u>AK-81-5</u>	<u>AK-81-8</u>	<u>AK-81-14</u>	<u>AK-81-23</u>	<u>AK-81-30</u>	<u>AK-81-38</u>	<u>AK-81-39</u>	<u>AK-81-50</u>	<u>AK-81-51</u>
<u>Oxides</u>												
SiO ₂	49.78	48.99	50.01	51.89	50.63	49.78	56.70	48.89	55.62	55.71	46.04	56.43
TiO ₂	0.96	0.99	0.97	1.03	0.95	0.96	0.86	1.67	1.10	1.05	1.04	0.91
Al ₂ O ₃	17.36	18.78	19.31	18.80	17.41	17.54	17.37	16.90	15.93	16.10	16.95	17.60
Fe ₂ O ₃	5.85	3.43	4.70	3.03	3.58	3.95	3.54	2.96	2.96	2.49	4.00	3.40
FeO	4.55	6.93	5.45	6.53	6.57	6.21	4.00	10.30	5.36	5.00	6.66	4.77
MnO	0.19	0.21	0.20	0.21	0.19	0.19	0.19	0.25	0.20	0.26	0.19	0.17
MgO	6.49	5.81	5.06	4.27	6.80	6.19	2.89	5.01	2.53	1.75	7.98	3.18
CaO	10.26	10.39	10.11	9.31	10.37	10.20	6.68	10.30	5.72	6.16	11.34	7.26
Na ₂ O	2.74	2.87	2.90	3.40	2.65	2.89	4.16	2.98	4.01	4.49	2.10	3.70
K ₂ O	0.86	0.69	0.80	1.06	0.85	0.98	1.35	0.74	2.17	1.89	0.77	1.20
P ₂ O ₅	0.20	0.20	0.22	0.24	0.21	0.22	0.23	0.20	0.33	0.36	0.21	0.21
Total	99.24	99.29	100.73	99.77	100.21	99.11	97.97	100.20	95.93	95.26	97.28	98.83
<u>Normative minerals</u>												
Ap	0.46	0.46	0.51	0.56	0.49	0.51	0.53	0.46	0.76	0.83	0.49	0.49
Il	1.82	1.88	1.84	1.96	1.80	1.82	1.63	3.17	2.09	1.99	1.90	1.73
Mt	8.48	4.97	6.81	4.39	5.19	5.73	5.18	4.29	4.29	3.61	5.80	4.93
Ab	23.19	24.29	24.54	28.77	22.42	24.45	35.20	25.22	33.93	37.99	17.77	31.31
Or	5.08	4.08	4.73	6.26	5.02	5.20	7.98	4.37	12.82	11.17	4.55	7.09
An	32.53	36.32	37.31	32.91	33.10	32.29	24.74	29.71	19.06	18.19	34.55	27.87
Qtz	2.10	0.00	1.73	1.22	0.27	0.00	9.33	0.00	7.73	7.06	0.00	9.90
Olv	0.00	4.37	0.00	0.00	0.00	0.00	9.33	6.70	0.00	0.00	9.73	0.00
Diop	13.47	11.33	9.18	9.61	13.72	13.62	5.58	16.69	5.92	8.37	16.35	5.51
Hyper	12.11	11.59	13.08	14.09	18.20	14.44	7.86	9.28	9.33	6.04	6.07	10.00
Total	99.24	99.29	99.73	99.77	100.21	99.00	97.98	99.89	95.93	95.25	97.21	98.83

Where Ap = apatite, Il = ilmenite, Mt = magnetite, Ab = albite, An = anorthite, Qtz = quartz, Olv = olivine, Diop = diopside, and Hyper = hypersthene. Water was not included in the oxide totals or the normative mineral calculations.

<u>AK-81-52</u>	<u>AK-81-61</u>	<u>AK-81-62</u>	<u>AK-81-102</u>	<u>AK-80-1A</u>	<u>AK-80-1B</u>	<u>AK-80-1D</u>	<u>AK-80-2A</u>	<u>AK-80-3A</u>	<u>AK-80-4A</u>	<u>AK-80-5</u>	<u>AK-80-6</u>	<u>AK-80-7A</u>
52.84	49.73	56.70	49.43	53.87	51.56	56.91	56.35	56.97	51.78	52.13	57.78	63.18
0.97	1.07	0.93	0.94	1.40	0.98	0.74	0.83	1.06	1.04	0.94	0.88	0.84
18.31	20.06	18.50	17.94	16.61	22.12	18.32	16.90	18.19	18.78	17.08	19.00	17.02
3.63	6.03	3.46	3.24	6.54	4.34	2.83	4.54	2.49	5.38	3.37	3.24	3.14
5.22	3.51	3.51	5.72	3.60	3.00	5.15	3.87	5.73	3.11	5.54	3.65	2.52
0.18	0.21	0.16	0.17	0.22	0.14	0.25	0.18	0.21	0.13	0.17	0.19	0.20
3.82	3.63	2.31	5.85	4.07	2.72	2.78	4.54	2.59	4.10	6.16	2.37	1.46
8.67	9.65	7.06	11.84	6.17	10.58	7.63	8.67	7.43	8.43	10.81	6.79	4.09
3.74	3.36	4.12	2.92	4.19	3.18	3.91	3.32	4.34	2.71	2.57	4.45	5.31
1.00	0.76	1.53	0.87	1.49	0.98	0.85	1.19	0.94	0.84	1.16	1.36	1.93
0.20	0.33	0.32	0.18	0.42	0.30	0.51	0.23	0.21	0.26	0.23	0.25	0.31
98.58	98.34	98.60	99.10	98.58	100.90	99.88	100.62	100.16	96.56	100.06	99.96	100.00
0.46	0.76	0.74	0.42	0.97	0.70	1.18	0.53	0.49	0.60	0.53	0.58	0.72
1.84	2.03	1.77	1.79	2.66	1.86	1.41	1.58	2.01	1.98	1.79	1.67	1.60
5.26	8.74	5.02	4.70	8.26	6.29	4.25	6.58	3.61	7.43	4.89	4.70	4.55
31.65	28.43	34.86	23.86	35.45	26.91	33.09	28.09	36.72	22.93	21.75	37.65	44.93
5.91	4.49	9.04	5.14	8.80	5.79	5.02	7.03	5.55	4.96	6.85	8.04	11.40
30.22	37.41	27.47	33.72	22.11	43.19	29.93	27.70	27.38	36.60	31.64	27.85	16.91
3.61	3.87	9.32	0.00	6.94	4.76	9.99	9.71	7.46	10.12	2.67	8.89	14.67
0.00	0.00	0.00	3.98	0.00	0.00	0.00	0.00	0.00	0.00	0.00	0.00	0.00
9.33	6.47	4.40	18.45	4.48	5.76	3.78	10.86	6.73	2.74	16.49	3.40	1.09
10.30	6.12	5.98	6.75	8.06	4.64	11.33	8.43	10.21	8.94	13.56	7.18	4.14
96.58	100.32	98.60	98.81	97.63	99.90	99.98	100.51	100.16	96.30	100.17	99.96	100.01

AK-80-8 AK-80-9B AK-80-12B AK-80-14 AK-80-15 AK-80-16

62.54	49.47	51.87	55.19	55.49	55.21
0.87	1.15	1.04	1.18	1.16	1.16
16.86	18.47	17.76	17.32	17.40	17.46
1.42	3.82	4.80	2.98	2.80	3.04
2.84	6.15	5.01	6.44	6.57	6.30
0.17	0.17	0.23	0.23	0.23	0.23
1.37	5.41	4.71	3.74	3.65	3.68
4.05	10.84	9.58	7.87	7.98	8.00
5.38	2.56	3.04	3.83	4.07	4.12
1.90	0.86	0.84	0.85	0.87	0.85
0.30	0.23	0.21	0.27	0.21	0.21
97.70	99.13	99.09	99.90	100.43	100.26

0.70	0.53	0.49	0.63	0.49	0.49
1.65	2.18	1.98	2.24	2.20	2.20
2.06	5.54	6.96	4.32	4.06	4.41
45.52	21.66	25.72	32.41	34.44	34.86
11.23	5.08	4.96	5.02	5.14	5.02
16.24	36.37	32.33	27.56	26.64	26.64
13.18	1.10	5.20	6.51	5.28	5.03
0.00	0.00	0.00	0.00	0.00	0.00
1.55	12.87	11.08	8.00	9.55	9.60
5.57	13.80	10.37	13.22	12.64	12.01
97.70	99.13	99.09	99.91	100.44	100.26

APPENDIX III - Microprobe data for Akutan lavas.

AK-81-1

	Olv Core	Olv Core	Olv Core	Olv Rim	Olv Rim	Olv Rim	Cpx Cpx	Cpx Core	Cpx Core	Cpx Core	Cpx Rim	Cpx Rim	Cpx Rim	Cpx Mid	Cpx Mid	Plag Core
<u>Oxides</u>																
SiO ₂	38.66	37.95	38.33	38.06	36.77	37.94	52.15	50.98	50.98	52.39	48.90	50.37	48.56	51.20	48.21	46.19
TiO ₂	0.04	0.04	0.03	0.04	0.05	0.03	0.27	0.37	0.41	0.18	0.74	0.53	0.84	0.42	0.80	0.02
Al ₂ O ₃	0.00	0.02	0.00	0.00	0.00	0.00	2.58	3.32	3.69	1.91	5.90	4.20	5.47	3.59	5.95	34.34
Cr ₂ O ₃	0.02	0.03	0.05	0.05	0.00	0.01	0.29	0.28	0.13	0.61	0.00	0.00	0.01	0.25	0.00	0.00
FeO	23.00	27.92	22.83	25.49	30.21	23.69	4.57	5.26	5.45	3.48	8.59	8.02	9.21	5.37	8.45	0.65
MnO	0.45	0.67	0.49	0.51	0.69	0.47	0.13	0.16	0.14	0.08	0.25	0.31	0.26	0.16	0.25	0.03
NiO	0.06	0.07	0.05	0.11	0.00	0.10	0.05	0.03	0.03	0.02	0.03	0.04	0.04	0.04	0.07	0.02
MgO	38.76	35.52	38.93	36.68	31.77	38.05	16.34	16.28	15.74	17.29	14.06	15.33	13.85	15.59	14.04	0.01
CaO	0.19	0.23	0.19	0.18	0.23	0.20	22.66	22.34	22.86	23.07	20.85	20.04	20.61	22.74	20.64	17.39
Na ₂ O	0.02	0.00	0.04	0.00	0.00	0.00	0.29	0.24	0.19	0.17	0.42	0.27	0.34	0.26	0.35	1.56
K ₂ O	0.00	0.00	0.00	0.01	0.00	0.01	0.00	0.01	0.01	0.02	0.01	0.00	0.01	0.01	0.02	0.04
P ₂ O ₅	0.06	0.08	0.06	0.03	0.05	0.06	0.00	0.01	0.02	0.01	0.00	0.01	0.01	0.01	0.05	0.01
Total	101.26	102.53	101.00	101.16	99.83	100.56	99.33	99.28	99.65	98.23	94.75	99.12	99.21	99.64	98.82	100.26
<u>Molecular Proportions</u>																
SiO ₂	1.028	0.955	1.016	1.024	0.955	1.004	1.895	1.860	1.870	1.897	1.817	1.845	1.798	1.877	1.770	2.136
TiO ₂	0.000	0.001	0.001	0.000	0.001	0.001	0.008	0.010	0.011	0.005	0.021	0.015	0.023	0.011	0.022	0.000
Al ₂ O ₃	0.000	0.000	0.000	0.000	0.000	0.000	1.911	0.142	0.155	0.257	0.258	0.000	1.872	0.181	0.239	1.825
Cr ₂ O ₃	0.000	0.001	0.001	0.001	0.000	0.000	0.008	0.008	0.004	0.018	0.000	0.000	0.000	0.007	0.000	0.000
FeO	0.512	0.649	0.506	0.574	0.683	0.525	0.139	0.160	0.168	0.105	0.267	0.245	0.285	0.165	0.259	0.025
MnO	0.010	0.016	0.011	0.011	0.016	0.011	0.004	0.005	0.004	0.003	0.008	0.010	0.008	0.005	0.008	0.001
NiO	0.001	0.001	0.001	0.002	0.000	0.002	0.001	0.000	0.001	0.001	0.001	0.001	0.001	0.001	0.002	0.000
MgO	1.536	0.472	1.538	1.472	1.281	1.500	0.885	0.885	0.861	0.933	0.779	0.837	0.764	0.852	0.768	0.000
CaO	0.006	0.007	0.006	0.005	0.008	0.006	0.883	0.873	0.898	0.895	0.830	0.786	0.818	0.894	0.812	0.862
Na ₂ O	0.001	0.000	0.002	0.000	0.000	0.000	0.003	0.017	0.013	0.012	0.031	0.019	0.025	0.018	0.025	0.139
K ₂ O	0.000	0.000	0.000	0.000	0.000	0.000	0.000	0.000	0.000	0.001	0.000	0.000	0.001	0.000	0.001	0.003
P ₂ O ₅	0.001	0.002	0.001	0.000	0.001	0.001	0.000	0.000	0.001	0.000	0.000	0.000	0.000	0.000	0.002	0.000
Total	3.095	3.204	3.083	3.089	2.986	3.049	3.821	3.960	3.991	3.952	4.012	3.938	3.962	3.985	3.924	5.038

Plag Core	Plag Mid	Plag Mid1	Plag Mid2	Plag Rim	Plag Rim
45.20	46.80	47.21	48.72	46.21	46.40
0.03	0.04	0.07	0.03	0.05	0.01
35.12	33.61	33.47	32.43	34.64	34.42
0.03	0.02	0.02	0.01	0.08	0.00
0.67	0.67	0.72	0.73	0.73	0.67
0.00	0.05	0.05	0.00	0.01	0.05
0.04	0.04	0.00	0.01	0.01	0.02
0.06	0.10	0.16	0.10	0.04	0.07
17.68	16.72	16.40	15.25	17.41	17.21
1.13	1.87	2.12	2.80	1.65	1.61
0.05	0.07	0.11	0.10	0.06	0.05
0.02	0.03	0.07	0.01	0.00	0.01
100.03	100.02	100.46	100.19	100.02	100.52
2.087	2.155	2.183	2.240	1.035	2.151
0.001	0.001	0.003	0.001	0.001	0.000
1.825	1.905	1.756	1.882	0.001	0.111
0.001	0.001	0.001	0.000	0.003	0.000
0.026	0.026	0.027	0.025	0.029	0.026
0.000	0.001	0.001	0.000	0.000	0.003
0.001	0.001	0.000	0.000	0.000	0.000
0.004	0.008	0.012	0.006	0.003	0.004
0.874	0.825	0.813	0.751	0.870	0.855
0.102	0.167	0.189	0.249	0.148	0.145
0.003	0.004	0.007	0.005	0.004	0.003
0.000	0.001	0.003	0.000	0.000	0.000
5.009	5.016	5.064	5.035	5.118	5.068

APPENDIX III

Ak-81-13

Oxides	Olv		Olv		Olv		Olv		Cpx		Cpx		Cpx		Plag		Plag		Plag		Flag		
	Core	Rim	Core	Rim	Core	Rim	Core	Rim	Core	Rim	Core	Rim	Core	Rim	Core	Rim	Core	Rim	Core	Rim	Core	Rim	
SiO ₂	37.87	37.60	38.06	37.69	38.12	37.42	48.88	49.59	48.88	51.30	50.96	45.29	47.40	45.92	50.08								
TiO ₂	0.06	0.01	0.05	0.05	0.02	0.06	0.73	0.69	0.78	0.30	0.49	0.00	0.03	0.01	0.06								
Al ₂ O ₃	0.05	0.01	0.00	0.00	0.01	0.03	5.17	4.09	4.80	2.88	2.36	33.46	32.66	33.66	30.78								
Cr ₂ O ₃	0.02	0.02	0.04	0.03	0.01	0.03	0.02	0.02	0.03	0.29	0.00	0.00	0.00	0.01	0.03								
FeO	23.82	23.20	23.62	24.32	23.58	24.13	7.08	8.61	8.18	4.98	8.22	0.64	0.67	0.69	0.85								
MnO	0.51	0.47	0.47	0.54	0.46	0.55	0.19	0.30	0.20	0.17	0.30	0.03	0.01	0.00	0.04								
NiO	0.09	0.03	0.00	0.07	0.08	0.01	0.01	0.05	0.04	0.01	0.01	0.01	0.07	0.00	0.02								
MgO	38.78	35.15	38.98	38.01	38.96	37.47	14.62	14.72	14.50	16.48	15.72	0.06	0.13	0.08	0.14								
CaO	0.20	0.19	0.20	0.02	0.18	0.21	21.79	20.58	21.10	22.24	20.42	17.00	15.72	17.73	13.49								
Na ₂ O	0.00	0.01	0.00	0.00	0.00	0.02	0.28	0.34	0.36	0.16	0.26	1.59	2.22	1.57	3.54								
K ₂ O	0.01	0.00	0.01	0.00	0.00	0.00	0.00	0.01	0.00	0.00	0.00	0.05	0.08	0.05	0.14								
P ₂ O ₅	0.02	0.05	0.01	0.03	0.00	0.00	0.00	0.03	0.01	0.04	0.02	0.06	0.06	0.05	0.00								
Total	101.43	96.74	101.44	100.76	101.42	99.93	98.72	99.03	98.88	98.85	98.76	98.19	99.05	98.71	99.17								

Molecular Proportions		Molecular Proportions		Molecular Proportions		Molecular Proportions		Molecular Proportions		Molecular Proportions		Molecular Proportions		Molecular Proportions		Molecular Proportions		Molecular Proportions		Molecular Proportions		Molecular Proportions		
Core	Rim	Core	Rim	Core	Rim	Core	Rim	Core	Rim	Core	Rim	Core	Rim	Core	Rim	Core	Rim	Core	Rim	Core	Rim	Core	Rim	
SiO ₂	1.016	0.940	1.019	1.007	1.020	0.984	1.785	1.826	1.796	1.858	1.863	2.045	2.153	2.084	2.266									
TiO ₂	0.001	0.000	0.001	0.001	0.000	0.001	0.020	0.019	0.022	0.008	0.014	0.000	0.001	0.000	0.003									
Al ₂ O ₃	0.001	0.000	0.000	0.000	0.000	0.001	0.223	0.178	0.208	0.123	0.102	1.788	1.749	1.801	1.642									
Cr ₂ O ₃	0.001	0.001	0.001	0.001	0.000	0.001	0.000	0.001	0.001	0.008	0.000	0.000	0.000	0.000	0.001									
FeO	0.534	0.485	0.529	0.563	0.528	0.531	0.214	0.266	0.251	0.151	0.251	0.024	0.026	0.026	0.032									
MnO	0.011	0.010	0.011	0.012	0.011	0.012	0.006	0.009	0.006	0.005	0.005	0.001	0.000	0.000	0.001									
NiO	0.002	0.001	0.000	0.001	0.001	0.000	0.000	0.001	0.001	0.000	0.000	0.000	0.000	0.000	0.000									
MgO	1.551	1.310	1.556	1.513	1.554	1.469	0.795	0.807	0.794	0.890	0.856	0.004	0.009	0.005	0.010									
CaO	0.006	0.005	0.006	0.006	0.005	0.006	0.853	0.811	0.831	0.863	0.799	0.822	0.765	0.814	0.654									
Na ₂ O	0.000	0.001	0.000	0.000	0.000	0.001	0.020	0.025	0.026	0.011	0.019	0.139	0.195	0.138	0.310									
K ₂ O	0.000	0.000	0.001	0.000	0.000	0.000	0.000	0.001	0.000	0.000	0.000	0.003	0.005	0.003	0.008									
P ₂ O ₅	0.000	0.001	0.000	0.001	0.000	0.000	0.000	0.000	0.000	0.000	0.001	0.001	0.003	0.001	0.003									
Total	3.124	2.754	3.123	3.085	3.119	3.006	3.916	3.945	3.935	3.917	3.913	4.821	4.908	4.872	4.928									

1
6
6

APPENDIX III

AK-81-71

	Hd Core	Hd Rim	Opx Opx	Opx Opx	Opx Core	Opx Rim	Plag Core	Plag Core	Plag Mid	Plag Rim
<u>Oxides</u>										
SiO ₂	41.86	42.14	52.59	53.04	52.76	51.81	53.64	53.13	53.61	53.51
TiO ₂	3.31	3.19	0.29	0.22	0.20	0.27	0.04	0.06	0.04	0.03
Al ₂ O ₃	11.23	11.26	1.30	0.97	0.68	1.29	29.34	29.37	29.32	29.35
Cr ₂ O ₃	0.01	0.00	0.00	0.07	0.03	0.02	0.03	0.05	0.02	0.00
FeO	13.98	14.21	19.37	18.69	20.64	21.99	0.39	0.45	0.46	0.42
MnO	0.44	0.54	1.08	1.05	1.23	1.33	0.00	0.04	0.03	0.02
NiO	0.02	0.05	0.05	0.07	0.08	0.07	0.00	0.02	0.00	0.00
MgO	12.64	12.45	24.16	24.20	22.95	21.23	0.05	0.06	0.04	0.00
CaO	10.47	10.56	1.50	1.51	1.42	1.43	11.30	11.41	11.21	11.11
Na ₂ O	2.80	3.04	0.00	0.06	0.00	0.05	5.06	4.89	5.13	5.29
K ₂ O	0.41	0.46	0.00	0.01	0.00	0.00	0.14	0.15	0.13	0.17
P ₂ O ₅	0.02	0.05	0.04	0.04	0.00	0.01	0.00	0.00	0.00	0.00
Total	97.19	97.95	100.38	99.93	99.99	99.80	99.98	99.63	99.49	99.91
SiO ₂	5.609	5.711	1.955	1.954	1.963	1.930	2.427	2.398	2.428	2.421
TiO ₂	0.333	0.324	0.008	0.006	0.006	0.007	0.001	0.003	0.001	0.001
Al ₂ O ₃	1.772	1.801	0.057	0.042	0.030	0.057	1.564	0.562	1.565	1.565
Cr ₂ O ₃	0.000	0.000	0.000	0.002	0.001	0.001	0.001	0.001	0.001	0.000
FeO	1.566	1.611	0.603	0.576	0.641	0.686	0.014	0.017	0.017	0.016
MnO	0.051	0.062	0.034	0.033	0.039	0.042	0.000	0.001	0.001	0.001
NiO	0.004	0.004	0.001	0.002	0.002	0.002	0.000	0.001	0.000	0.000
MgO	2.524	2.515	1.339	1.329	1.273	1.179	0.003	0.004	0.003	0.000
CaO	1.501	1.535	0.059	0.060	0.056	0.057	0.548	0.551	0.544	0.539
Na ₂ O	0.727	0.798	0.000	0.004	0.000	0.003	0.444	0.428	0.450	0.463
K ₂ O	0.072	0.080	0.000	0.000	0.000	0.000	0.008	0.009	0.008	0.010
P ₂ O ₅	0.000	0.004	0.001	0.001	0.000	0.000	0.000	0.000	0.000	0.000
Total	14.159	14.443	4.057	4.009	4.012	3.964	5.010	4.975	5.018	5.016

Appendix III

AK-81-23

	Opx	Opx	Opx Core	Opx Core	Opx Core	Opx Rim	Opx Rim	Opx Rim	Opx Rim	Cpx	Cpx	Cpx	Cpx	Cpx	Cpx	Plag	Plag	Plag	Plag	Plag Midl
Oxides																				
SiO ₂	52.82	52.37	52.75	52.60	52.55	52.76	52.53	52.69	50.64	50.38	51.44	51.18	51.33	51.30	54.27	53.82	54.50	54.31	55.46	
TiO ₂	0.19	0.29	0.24	0.21	0.20	0.24	0.29	0.24	0.50	0.58	0.44	0.46	0.42	0.43	0.06	0.03	0.04	0.01	0.06	
Al ₂ O ₃	0.61	1.40	0.95	0.75	0.53	0.79	0.90	0.86	2.18	2.55	1.66	1.81	0.42	1.76	28.23	28.63	28.22	28.26	27.52	
Cr ₂ O ₃	0.02	0.02	0.00	0.03	0.04	0.00	0.03	0.00	0.14	0.02	0.00	0.00	0.03	0.02	0.00	0.02	0.03	0.02	0.08	
FeO	21.00	20.18	20.24	20.62	21.62	20.39	20.09	20.32	9.96	10.15	9.96	10.72	10.45	9.68	0.53	0.48	0.47	0.49	0.51	
MnO	1.05	0.93	1.00	1.14	1.17	1.02	1.03	1.06	0.56	0.56	0.56	0.62	0.60	0.55	0.00	0.04	0.00	0.01	0.05	
NiO	0.03	0.00	0.04	0.00	0.04	0.02	0.00	0.00	0.05	0.03	0.03	0.00	0.04	0.00	0.05	0.00	0.00	0.00	0.05	
MgO	23.42	23.75	23.67	23.75	22.39	23.68	23.62	23.34	14.86	14.50	15.10	14.80	14.81	15.01	0.02	0.00	0.05	0.05	0.02	
CaO	1.55	1.48	1.50	1.52	1.52	1.53	1.52	1.50	19.96	19.90	19.78	19.49	19.80	19.89	10.54	10.65	10.13	1.021	9.51	
Na ₂ O	0.08	0.00	0.00	0.00	0.00	0.04	0.00	0.04	0.39	0.21	0.31	0.38	0.32	0.28	5.43	5.08	5.33	5.27	5.80	
K ₂ O	0.00	0.01	0.00	0.00	0.01	0.02	0.00	0.01	0.00	0.02	0.00	0.01	0.01	0.00	0.25	0.19	0.19	0.22	0.25	
P ₂ O ₅	0.02	0.01	0.00	0.00	0.04	0.00	0.01	0.04	0.00	0.00	0.04	0.05	0.05	0.02	0.00	0.00	0.02	0.00	0.03	
Total	100.78	100.44	100.39	100.62	100.10	100.49	100.02	99.52	99.23	98.90	99.30	99.52	98.97	98.94	99.38	98.94	98.98	98.83	99.34	
Molecular Proportions																				
SiO ₂	1.990	1.956	1.969	1.975	1.968	1.975	1.951	1.960	1.878	1.860	1.905	1.908	1.192	1.890	2.437	2.403	2.430	2.419	2.481	
TiO ₂	0.005	0.008	0.007	0.006	0.006	0.007	0.008	0.007	0.014	0.016	0.012	0.013	0.012	0.012	0.003	0.001	0.001	0.000	0.001	
Al ₂ O ₃	0.027	0.061	0.042	0.033	0.023	0.035	0.039	0.038	0.096	0.111	0.073	0.080	0.072	0.076	1.495	1.507	1.483	1.484	1.451	
Cr ₂ O ₃	0.001	0.001	0.000	0.001	0.001	0.000	0.001	0.000	0.001	0.001	0.000	0.001	0.000	0.001	0.000	0.001	0.001	0.001	0.003	
FeO	0.662	0.630	0.632	0.648	0.677	0.639	0.624	0.632	0.309	0.314	0.309	0.335	0.325	0.299	0.019	0.018	0.018	0.018	0.019	
MnO	0.033	0.003	0.031	0.036	0.037	0.032	0.032	0.033	0.018	0.018	0.017	0.020	0.019	0.017	0.000	0.001	0.000	0.000	0.001	
NiO	0.001	0.000	0.001	0.000	0.001	0.001	0.000	0.000	0.001	0.000	0.001	0.000	0.001	0.000	0.001	0.000	0.000	0.000	0.001	
MgO	1.315	1.322	1.317	1.330	1.250	1.321	1.307	1.294	0.822	0.798	0.834	0.822	0.822	0.824	0.001	0.000	0.004	0.003	0.001	
CaO	0.063	0.059	0.060	0.061	0.061	0.061	0.061	0.059	0.490	0.788	0.779	0.790	0.785	0.431	0.492	0.509	0.484	0.487	0.455	
Na ₂ O	0.006	0.000	0.000	0.000	0.000	0.003	0.000	0.003	0.028	0.015	0.019	0.027	0.023	0.020	0.473	0.440	0.462	0.455	0.503	
K ₂ O	0.000	0.001	0.000	0.000	0.001	0.001	0.000	0.000	0.012	0.001	0.001	0.001	0.000	0.014	0.020	0.010	0.010	0.013	0.014	
P ₂ O ₅	0.001	0.000	0.000	0.000	0.001	0.000	0.000	0.001	0.000	0.000	0.001	0.002	0.002	0.001	0.000	0.000	0.001	0.000	0.001	
Total	4.104	4.041	4.059	4.090	4.027	4.075	4.023	4.027	3.964	3.922	4.156	3.973	3.990	3.924	4.951	4.891	4.894	4.880	4.931	

Plag Mid	Plag Rim	Plag Rim	Plag Rim	Plag Core						
53.96	53.73	54.74	54.54	56.24	54.53	51.35	54.87	55.69	54.98	
0.28	0.09	0.05	0.03	0.05	0.05	0.05	0.06	0.08	0.00	
27.53	28.44	27.67	27.69	26.64	28.37	30.40	27.99	27.45	27.57	
0.03	0.00	0.00	0.01	0.02	0.04	0.04	0.01	0.01	0.05	
1.19	0.47	0.53	0.50	0.43	0.48	0.62	0.51	0.46	0.45	
0.07	0.01	0.04	0.00	0.01	0.02	0.01	0.04	0.04	0.00	
0.05	0.01	0.01	0.01	0.04	0.01	0.00	0.01	0.03	0.02	
0.15	0.05	0.01	0.03	0.04	0.03	0.01	0.00	0.05	0.08	
10.15	11.05	10.21	10.19	9.04	10.18	12.72	10.02	9.28	9.63	
5.41	5.29	5.87	5.48	6.25	5.51	4.08	5.41	5.89	5.26	
0.49	0.19	0.33	0.32	0.26	0.20	0.02	0.23	0.26	0.25	
0.06	0.03	0.04	0.00	0.00	0.03	0.00	0.00	0.01	0.05	
100.11	99.36	99.50	99.37	99.02	99.45	98.80	99.15	99.25	98.34	
2.435	2.415	2.463	2.431	2.503	2.447	2.324	2.449	2.485	2.430	
0.009	0.003	0.001	0.001	0.001	0.001	0.001	0.003	0.003	0.001	
1.465	1.506	1.468	1.455	1.400	1.500	1.621	1.474	1.449	1.437	
0.001	0.000	0.001	0.000	0.004	0.000	0.000	0.000	0.000	0.001	
0.045	0.018	0.020	0.018	0.016	0.018	0.023	0.019	0.017	0.017	
0.003	0.000	0.001	0.000	0.000	0.001	0.000	0.001	0.001	0.000	
0.001	0.000	0.000	0.000	0.001	0.000	0.000	0.000	0.001	0.000	
0.010	0.003	0.000	0.003	0.003	0.003	0.001	0.000	0.004	0.005	
0.491	0.532	0.617	0.487	0.794	0.508	0.785	0.480	0.443	0.456	
0.473	0.461	0.513	0.474	0.540	0.479	0.358	0.469	0.509	0.451	
0.029	0.010	0.012	0.013	0.000	0.014	0.000	0.013	0.014	0.014	
0.003	0.001	0.001	0.001	0.000	0.001	0.000	0.000	0.000	0.001	
4.965	4.949	4.977	4.883	4.906	4.953	4.958	4.908	4.921	4.813	

APPENDIX III

AK-81-73

	Cpx	Cpx	Cpx Core	Cpx Core	Cpx Rim	Cpx Rim	Plag Core	Plag Core	Plag Core	Plag Mid	Plag Mid	Plag Rim	Plag Rim	Plag Rim	Plag Rim
Oxides															
SiO ₂	50.93	50.01	50.68	49.86	51.08	49.21	44.31	45.18	45.69	45.50	45.88	51.70	65.17	65.07	56.21
TiO ₂	0.72	0.99	0.68	1.15	0.73	0.69	0.04	0.04	0.04	0.05	0.07	0.05	0.07	0.04	0.06
Al ₂ O ₃	2.06	3.15	2.07	3.28	1.75	4.39	35.77	35.27	34.63	34.94	34.71	30.53	18.86	18.98	27.14
Cr ₂ O ₃	0.03	0.02	0.01	0.00	0.00	0.00	0.00	0.00	0.02	0.04	0.02	0.00	0.00	0.01	0.02
FeO	10.16	9.95	10.03	10.50	11.38	11.01	0.49	0.50	0.52	0.58	0.57	0.71	0.32	0.28	0.46
MnO	0.33	0.27	0.32	0.30	0.40	0.39	0.03	0.03	0.03	0.00	0.02	0.00	0.03	0.00	0.02
NiO	0.00	0.01	0.03	0.04	0.00	0.00	0.01	0.03	0.00	0.02	0.01	0.00	0.05	0.02	0.00
MgO	14.54	13.64	14.63	13.83	13.58	12.48	0.02	0.04	0.02	0.04	0.06	0.09	0.01	0.00	0.04
CaO	19.90	20.40	20.14	20.02	19.95	18.80	18.78	17.99	17.31	17.59	17.29	12.76	0.22	0.26	9.07
Na ₂ O	0.22	0.25	1.39	0.34	0.25	0.90	0.80	1.24	1.48	1.49	1.50	4.25	4.32	4.82	6.19
K ₂ O	0.00	0.00	0.00	0.02	0.01	0.01	0.03	0.03	0.04	0.02	0.04	0.19	10.40	9.71	0.37
P ₂ O ₅	0.02	0.03	0.00	0.03	0.02	0.06	0.00	0.04	0.03	0.05	0.01	0.03	0.01	0.04	0.03
Total	98.91	98.72	94.98	99.37	99.15	97.94	100.27	100.39	99.87	100.32	100.18	100.31	99.46	99.23	99.61
Molecular Proportions															
SiO ₂	1.878	1.841	1.874	1.856	1.900	1.798	2.057	2.096	2.101	2.108	2.119	2.363	2.941	2.923	2.519
TiO ₂	0.020	0.028	0.019	0.014	0.020	0.090	0.001	0.001	0.001	0.001	0.003	0.001	0.003	0.001	0.003
Al ₂ O ₃	0.089	0.137	0.090	0.144	0.077	0.189	1.958	1.929	1.877	1.907	1.890	1.645	1.004	1.005	1.433
Cr ₂ O ₃	0.001	0.001	0.000	0.000	0.000	0.000	0.000	0.001	0.000	0.000	0.000	0.000	0.000	0.000	0.001
FeO	0.313	0.307	0.310	0.237	0.354	0.336	0.020	0.020	0.020	0.022	0.022	0.022	0.012	0.010	0.017
MnO	0.010	0.008	0.010	0.010	0.013	0.012	0.001	0.001	0.001	0.000	0.001	0.000	0.001	0.000	0.001
NiO	0.000	0.000	0.001	0.001	0.000	0.000	0.000	0.001	0.000	0.001	0.000	0.000	0.001	0.001	0.000
MgO	0.799	0.749	0.806	0.767	0.753	0.680	0.001	0.003	0.001	0.003	0.004	0.007	0.000	0.000	0.003
CaO	0.786	0.804	0.798	0.798	0.794	0.736	0.934	0.895	0.852	0.873	0.856	0.624	0.010	0.013	0.436
Na ₂ O	0.016	0.018	0.028	0.025	0.018	0.064	0.072	0.111	0.131	0.135	0.134	0.376	0.378	0.420	0.538
K ₂ O	0.000	0.000	0.000	0.001	0.001	0.000	0.001	0.003	0.003	0.001	0.003	0.012	0.598	0.556	0.021
P ₂ O ₅	0.001	0.001	0.000	0.001	0.001	0.002	0.000	0.001	0.001	0.001	0.000	0.001	0.000	0.001	0.001
Total	3.912	2.894	3.936	3.944	3.931	3.907	5.045	5.061	4.989	5.053	5.033	5.056	4.946	4.930	4.973

Where Plag = plagioclase, Opx = orthopyroxene, Cpx = clinopyroxene, and Oliv = olivine. Oxide values are in weight percent.

Appendix IV - Rb and Sr analyses

<u>Sample</u>	<u>Rb (ppm)</u>	<u>Sr (ppm)</u>	<u>Rb/Sr</u>
AK-81-1	21	442	0.050
AK-81-2	ND	455	ND
AK-81-3	16	465	0.034
AK-81-5	10	480	0.021
AK-81-8A	22	440	0.050
AK-81-8B	13	440	0.029
AK-81-11	11	440	0.025
AK-81-14	19	430	0.044
AK-81-17	29	310	0.094
AK-81-22	71	205	0.346
AK-81-23	31	305	0.102
AK-81-24	33	335	0.098
AK-81-26	27	365	0.074
AK-81-30	12	405	0.030
AK-81-31	12	460	0.026
AK-81-33	49	325	0.151
AK-81-51	31	355	0.087
AK-81-52A	31	290	0.107
AK-81-52B	25	290	0.086
AK-81-102	20	350	0.057
AK-80-9A	25	355	0.070
AK-80-11	26	330	0.079

Samples AK-81-8A and 8B, and AK-52A and 52B were duplicates submitted to test the reproducibility of the analyses.

Appendix V
Petrographic Descriptions of Akutan Lavas

- AK-81-1: Porphyritic basalt dike containing plagioclase, clinopyroxene, and olivine phenocrysts in a holocrystalline groundmass.
- AK-81-2: Porphyritic basalt lava flow containing olivine, clinopyroxene, and plagioclase phenocrysts in a holocrystalline groundmass.
- AK-81-3: Porphyritic basalt lava flow containing the same mineralogy as AK-81-2.
- AK-81-4: Similar mineralogy and texture to AK-81-3.
- AK-81-5: Similar to AK-81-4.
- AK-81-6: Similar to AK-81-5.
- AK-81-7: Similar to AK-81-6.
- AK-81-8: Similar to AK-81-7.
- AK-81-9: Similar to AK-81-8.
- AK-81-10: Similar to AK-81-9.
- AK-81-11: Similar to AK-81-11.
- AK-81-12: Similar to AK-81-12.
- AK-81-13: Similar to AK-81-13.
- AK-81-14: Similar to AK-81-14.
- AK-81-16: Porphyritic andesite lava flow containing plagioclase, olivine, and clinopyroxene phenocrysts in a very fine-grained, vesicular groundmass.
- AK-81-17: Porphyritic andesite lava flow containing plagioclase, clinopyroxene, orthopyroxene, and trace olivine phenocrysts in a very fine-grained groundmass.
- AK-81-18: Porphyritic andesite lava flow containing plagioclase, olivine, clinopyroxene, and orthopyroxene phenocrysts in a fine-grained groundmass.
- AK-81-19: Float from the northern flank of Akutan Volcano. Porphyritic rock containing plagioclase, olivine, orthopyroxene, and clinopyroxene phenocrysts in a vesicular glassy groundmass.
- AK-81-20: Andesite from Pickup Valley. Porphyritic rock containing plagioclase, orthopyroxene, and clinopyroxene phenocrysts in a trachytic groundmass.

- AK-81-21: Andesite plug containing clinopyroxene and plagioclase phenocrysts. The groundmass is partially altered to chlorite and carbonate. Quartz veinlets intrude the rock.
- AK-81-22: Porphyritic andesite containing about 8 percent phenocrysts (plagioclase, orthopyroxene, and clinopyroxene).
- AK-81-23: Porphyritic, partially altered andesite lava flow. The rock contains clinopyroxene, orthopyroxene, and plagioclase phenocrysts in a trachytic groundmass which is partially altered to carbonate.
- AK-81-24: Porphyritic andesite lava flow containing phenocrysts of plagioclase, clinopyroxene, and olivine in a trachytic groundmass. The olivine is largely altered to serpentine minerals, while the clinopyroxene and groundmass are partially altered to carbonate and chlorite.
- AK-81-26: Aphanitic basalt flow. Trace plagioclase phenocrysts in a very fine-grained trachytic groundmass consisting of olivine, clinopyroxene, opaques, and plagioclase.
- AK-81-27: Porphyritic andesite lava flow containing clinopyroxene, orthopyroxene, plagioclase, and trace olivine phenocrysts in a brown, vesicular, glassy groundmass.
- AK-81-28: Similar mineralogy and texture to AK-81-27.
- AK-81-29: Same as AK-81-28.
- AK-81-30: Aphanitic basaltic dike consisting of an equigranular mass of olivine, clinopyroxene, plagioclase, and opaque minerals.
- AK-81-31: Porphyritic andesite dike containing plagioclase phenocrysts in a fine-grained vesicular groundmass consisting of olivine, plagioclase, clinopyroxene, and opaque minerals.
- AK-81-32: Aphanitic dike. Contains rare plagioclase phenocrysts in a very fine-grained vesicular groundmass.
- AK-81-33: Similar to AK-81-32. The groundmass has a trachytic texture and contains brown glass.
- AK-81-34: Slightly porphyritic dike containing large plagioclase and clinopyroxene phenocrysts in a fine-grained groundmass.
- AK-81-35: Porphyritic andesite lava flow containing plagioclase, clinopyroxene, and rare olivine phenocrysts in a glassy trachytic groundmass.
- AK-81-36: Altered andesite dike. Plagioclase phenocrysts in a partially altered, fine-grained, groundmass. The mafic phenocrysts have been altered to chlorite and carbonate.

- AK-81-37: Altered andesite dike. Two percent plagioclase phenocrysts in an altered groundmass.
- AK-81-38: Partially altered porphyritic andesite dike. The rock contains plagioclase, clinopyroxene, and opaque phenocrysts in a fine-grained trachytic groundmass. The phenocrysts are usually in the form of crystal clots.
- AK-81-40: Partially altered porphyritic andesite dike. The rock contains plagioclase phenocrysts in a dark brown groundmass. The mafic phenocrysts have been altered to chlorite as has part of the groundmass.
- AK-81-41: Aphanitic dike. The rock consists of an equigranular mixture of plagioclase and opaque minerals, and is partially altered to carbonate.
- AK-81-42: Similar to AK-81-41, but vesicular and has a well developed trachytic texture.
- AK-81-43: Hornblende andesite dike. The rock is porphyritic and contains plagioclase, hornblende, and clinopyroxene phenocrysts in a holocrystalline groundmass. The hornblende has reaction rims of plagioclase and opaque minerals.
- AK-81-44: Slightly porphyritic andesite dike. The rock contains about 10 percent plagioclase phenocrysts in a fine-grained groundmass consisting of plagioclase and opaques. Both the plagioclase and the groundmass are partially altered to chlorite.
- AK-81-45: Similar to AK-81-44, but is slightly coarser grained. The rock also contains xenoliths which have a similar mineralogy as the host rock, but are more highly altered. The amygdules are filled with carbonate.
- AK-81-46: Partially altered porphyritic andesite dike. The rock contains plagioclase and clinopyroxene phenocrysts in a trachytic groundmass. The amygdules are filled with carbonate, while the groundmass contains both carbonate and chlorite.
- AK-81-47: Similar to AK-81-46.
- AK-81-48: Similar to AK-81-47, except that carbonate alteration is more pervasive.
- AK-81-50: Slightly altered porphyritic basaltic dike. Plagioclase and clinopyroxene phenocrysts in a holocrystalline groundmass. The clinopyroxene exhibits two periods of growth: an early state as independent phenocrysts and a late stage where it optically encloses groundmass plagioclase laths. The two stages are optically continuous.

- AK-81-51: Porphyritic andesite lava flow. The rock contains clinopyroxene, orthopyroxene, plagioclase, and opaque phenocrysts in a trachytic groundmass. Minor amounts of carbonate and chlorite are present.
- AK-81-52: Slightly altered porphyritic andesite lava flow. The flow contains plagioclase, orthopyroxene, clinopyroxene, and opaque phenocrysts in a holocrystalline groundmass. The orthopyroxene occurs in trace amounts.
- AK-81-53: Altered porphyritic andesite dike. The rock contains plagioclase, clinopyroxene, and altered olivine phenocrysts in a holocrystalline groundmass. The olivine is altered to chlorite. Chlorite-filled amygdules and carbonate-filled amygdules, rimmed by chlorite, are also present.
- AK-81-54: Altered andesite dike. A few plagioclase phenocrysts in a very fine-grained groundmass. Carbonate and chlorite alteration is pervasive.
- AK-81-55: Aphanitic dike. Less than 1 percent plagioclase phenocrysts in a fine-grained trachytic groundmass containing plagioclase and opaque minerals, and some chlorite alteration.
- AK-81-56: Altered dike. Holocrystalline rock containing less than 1 percent plagioclase phenocrysts in a groundmass composed of plagioclase laths, opaque minerals and clinopyroxene. Chlorite and carbonate occur as amygdule fillings and in the groundmass.
- AK-81-57: Partially altered andesite dike. The dike contains large plagioclase phenocrysts in a very fine-grained groundmass. Chlorite alteration is common.
- AK-81-57a: Partially altered andesite dike. Similar to AK-81-56.
- AK-81-57b: Similar to AK-81-57a.
- AK-81-58: Similar to AK-81-57b.
- AK-81-59: Altered andesite dike. The dike contains large plagioclase phenocrysts in a groundmass altering to chlorite.
- AK-81-60: Similar to AK-81-59.
- AK-81-61: Coarsely porphyritic basaltic dike. The dike contains large plagioclase, and minor olivine, phenocrysts in a holocrystalline groundmass. There is a great deal of brown alteration material present.
- AK-81-62: Partially altered andesite lava flow. The flow contains crystal clots of plagioclase, opaque minerals, and clinopyroxene in a fine-grained trachytic groundmass.

- AK-81-63: Andesite lava flow. The flow contains plagioclase phenocrysts in a trachytic groundmass composed of opaque minerals, plagioclase, and clinopyroxene. Olivine was present, but has altered to chlorite. Chlorite, and carbonate are present in the groundmass.
- AK-81-64: Similar to AK-81-63.
- AK-81-65: Porphyritic andesite lava flow. The flow contains olivine, plagioclase, and clinopyroxene phenocrysts in a holocrystalline groundmass. Olivine has oxidized rims, but is otherwise unaltered.
- AK-81-66: Porphyritic andesite lava flow. The flow contains plagioclase and clinopyroxene phenocrysts in a trachytic groundmass.
- AK-81-69: Similar to AK-81-66 but originally contained olivine phenocrysts which have been altered to chlorite.
- AK-81-70: Altered andesite dike. The dike contains plagioclase phenocrysts in a groundmass composed of plagioclase, clinopyroxene, and opaque minerals. The groundmass has been partially altered to chlorite and carbonate. Amygdules are filled with chlorite and carbonate.
- AK-81-71: Coarsely crystalline andesite dike. the dike contains hornblende, orthopyroxene, and plagioclase phenocrysts. There is very little groundmass present. Carbonate is present as an interstitial filling between grains.
- AK-81-72: Porphyritic andesite dike. The dike contains aligned phenocrysts of plagioclase, clinopyroxene, olivine, and opaque minerals in a microcrystalline groundmass.
- AK-81-73: Plagioclase, clinopyroxene gabbro. Intrusive rock containing large plagioclase grains ophitically enclosed by clinopyroxene.
- AK-81-100: Plagioclase, clinopyroxene gabbro. Intrusive rock containing large plagioclase grains ophitically enclosed by clinopyroxene.
- AK-81-101: Porphyritic andesite. Plagioclase and orthopyroxene phenocrysts in a brown glassy groundmass.
- AK-81-102: Porphyritic basaltic plug. The intrusive contains clinopyroxene and plagioclase phenocrysts in a groundmass consisting of plagioclase, clinopyroxene, and opaque minerals. The plagioclase phenocrysts commonly contain inclusions of clinopyroxene and opaque minerals.
- AK-81-102A: Porphyritic andesite dike. The dike contains plagioclase and phenocrysts in a holocrystalline groundmass.

- AK-81-102B: Partially altered andesite dike. The dike contains phenocrysts of olivine, clinopyroxene, and plagioclase in a holocrystalline groundmass.
- AK-81-106- 1.5 through
10: Altered andesite dike. The dike contains clinopyroxene and plagioclase phenocrysts in a holocrystalline groundmass. The amount of alteration of the clinopyroxene, phenocrysts as well as groundmass, increases across the dike. At the top of the dike the mafic minerals are completely altered to chlorite and carbonate.
- AK-80-7a: Porphyritic andesite/dacite lava flow. The flow contains plagioclase, orthopyroxene, and clinopyroxene phenocrysts in a very fine-grained, unaltered groundmass.
- AK-80-8: Similar to AK-80-7a.

APPENDIX VI
Application of discriminant functions

The following Discriminant functions were produced by the stepwise multiple discriminant analysis (Jennrich and Sampson, 1981) and are listed in the text. P_2O_5 and TiO_2 are in weight percent.

WestF	$X=100.33TiO_2+264.09P_2O_5-83.22$
EastF	$X=93.55TiO_2+245.03P_2O_5-72.26$
WestD	$X=151.90TiO_2+414.89P_2O_5-194.84$
EastD	$X=125.68TiO_2+343.05P_2O_5-133.74$

A particular case is classified into the group where the value of the discriminant function is the largest. For example, AK-81-61, a dike from Hot Springs Bay, containing 0.33 percent P_2O_5 and 1.07 percent TiO_2 . Putting these values into the four discriminant functions produces the values listed below:

WestF	$107.35+87.15-83.22=111.28$
EastF	$100.10+80.86-72.26=108.69$
WestD	$162.53+136.91-194.84=104.60$
EastD	$134.48+113.21-133.74=113.95$

The value for EastD is the largest and AK-81-61 would be classified with that group. Table 8 shows that AK-81-61 has been technique, see Jennrich (1977).

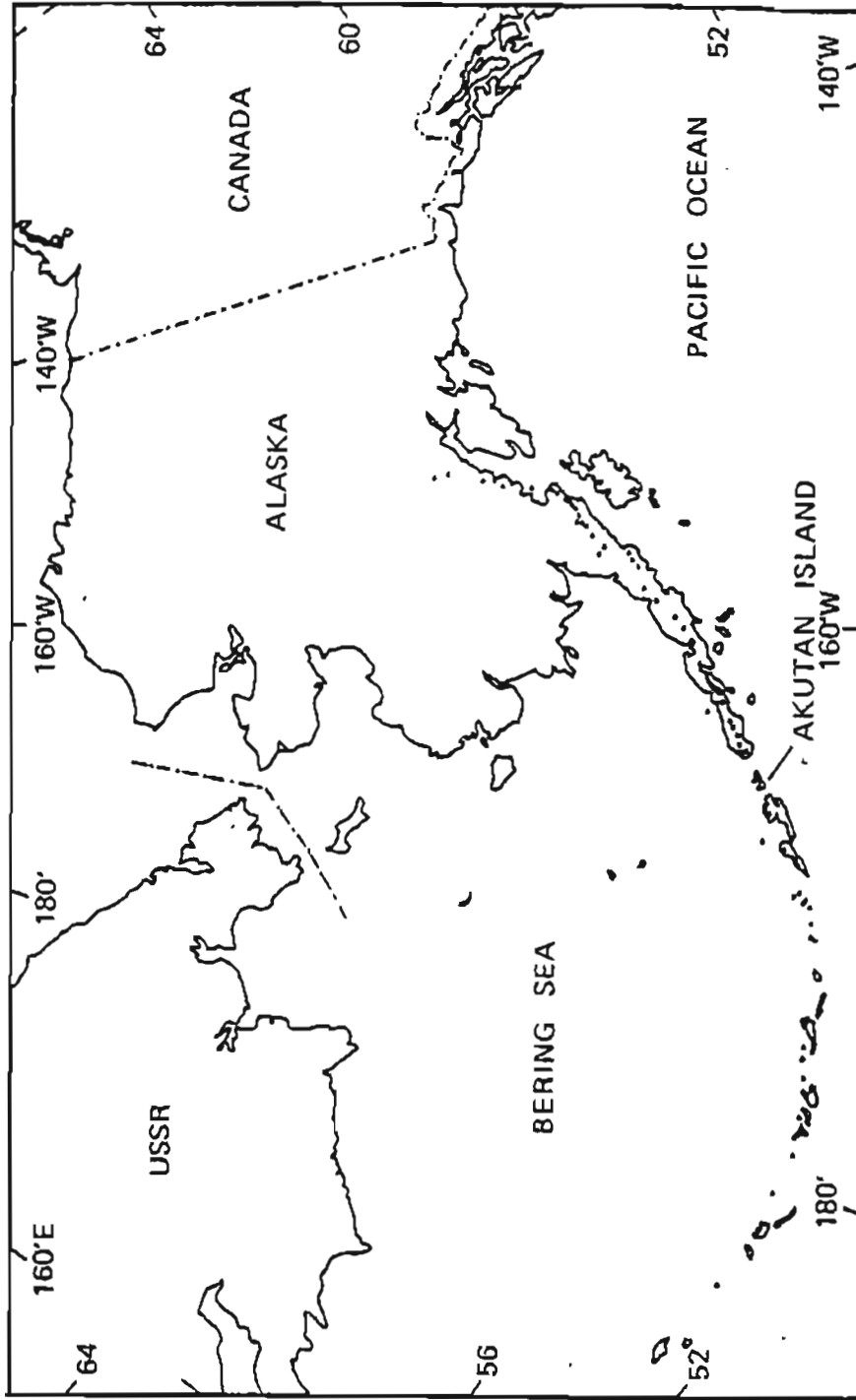


Figure 1. Position of Akutan Island within the Aleutian Arc. Dots represent volcano locations along the arc.

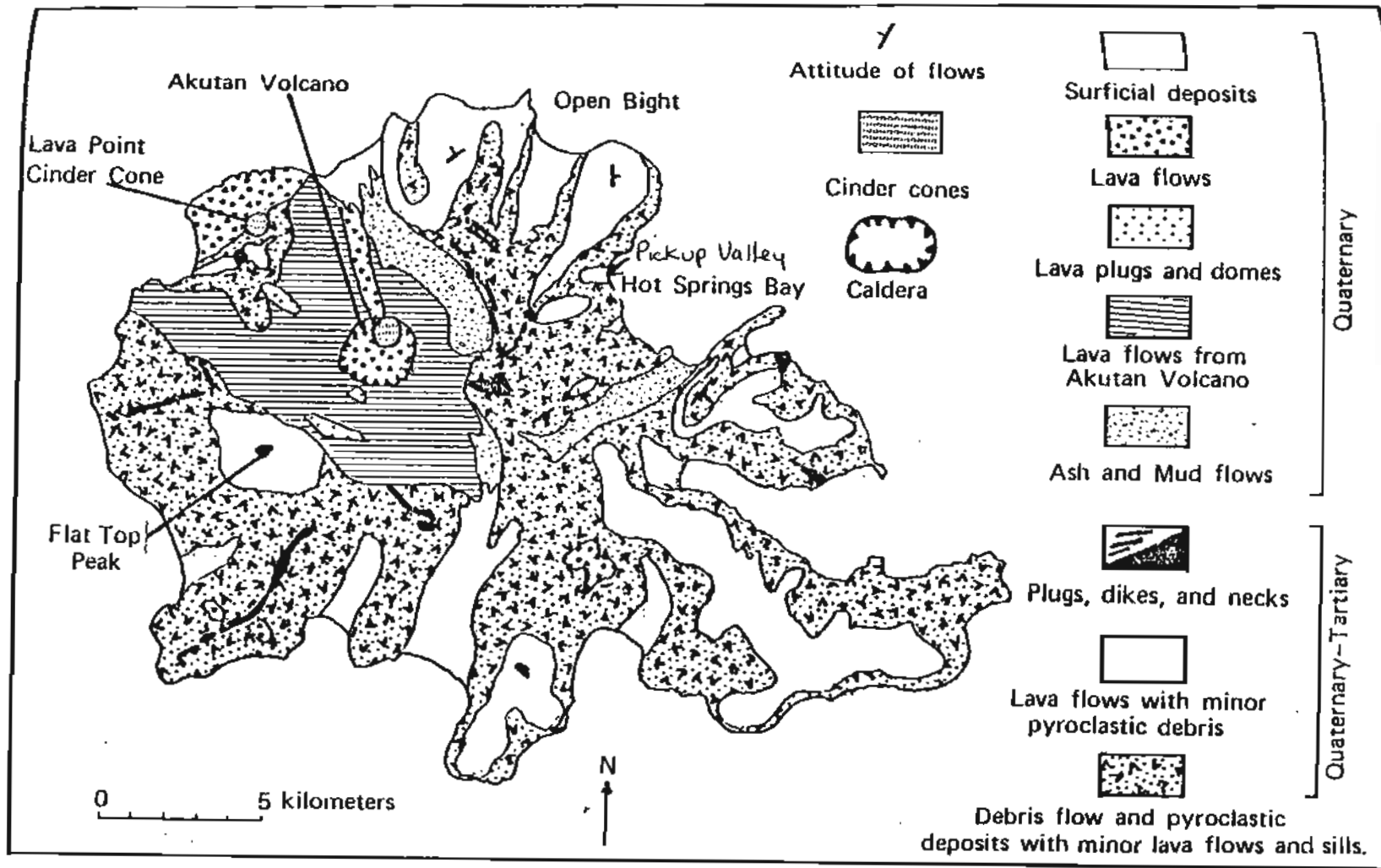


Figure 2. Generalized geology of Akutan Island adapted from Byers and Barth (unpublished) Swanson (in reparation). Sample locations are indicated by .

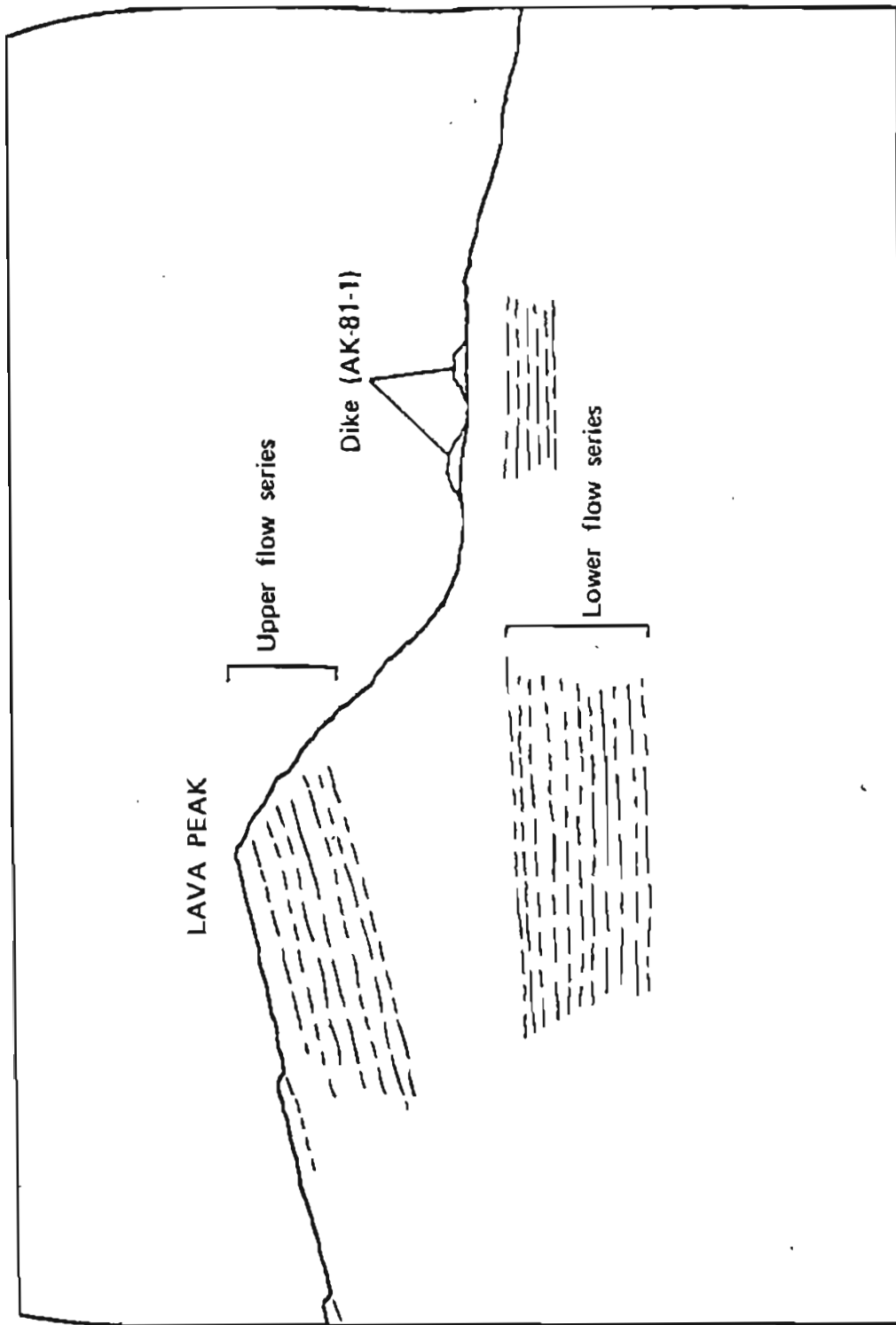


Figure 3. Sketch of Lava Peak showing the relationship between the upper and lower flow series.

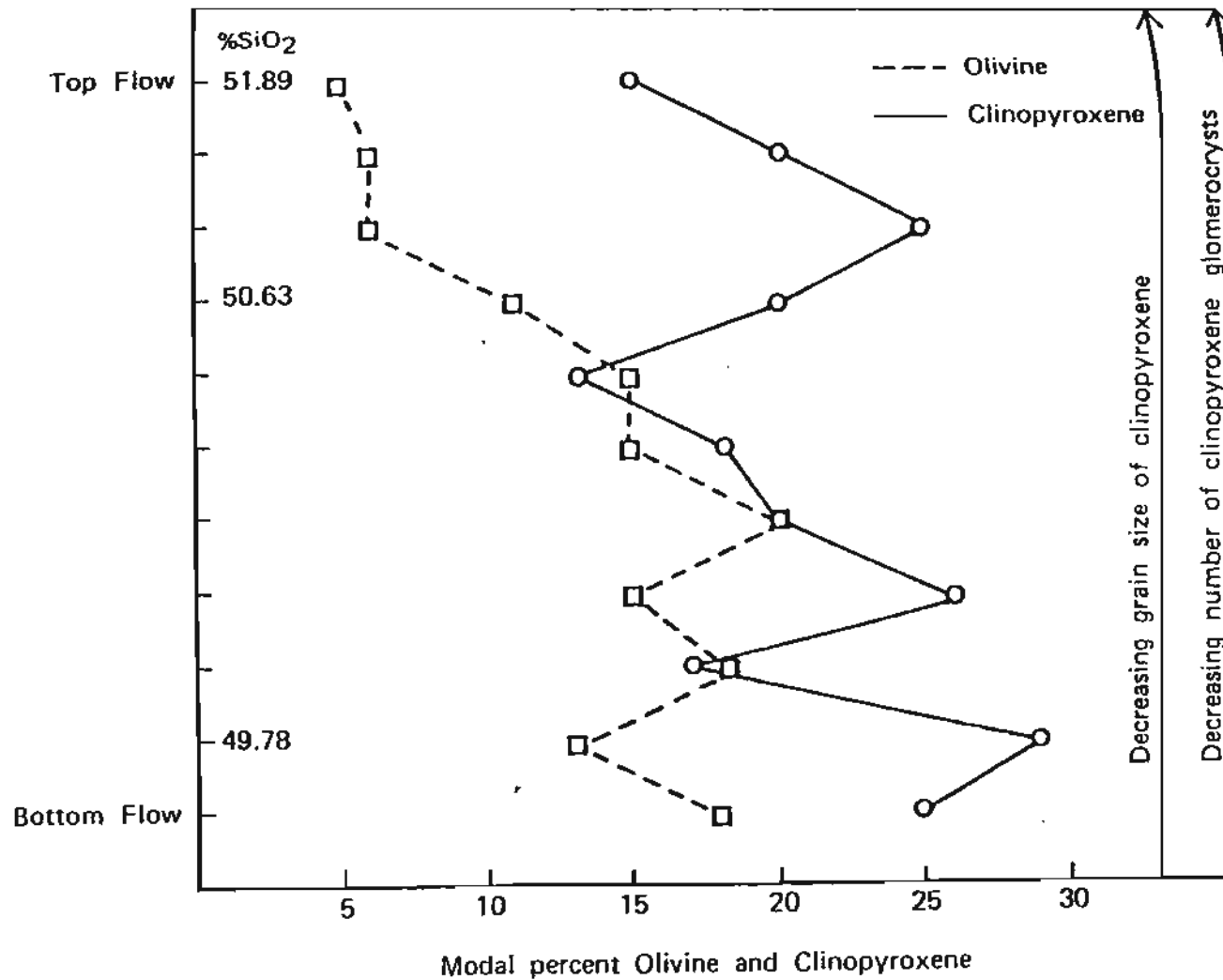


Figure 4. Change in percentage of olivine and clinopyroxene in the lower flow series exposed on Lava Peak. Percentages were recalculated using olivine, clinopyroxene, and plagioclase phenocrysts only.



Figure 5. Mineral banding in a Cow Point dike. The dike is about 1 m across.



Figure 6. Intrusive rocks. A) Coarse grained intrusive from western Akutan Island. B) Plagioclase-clinopyroxene gabbro from Hot Springs Bay. Scale = 1 mm.

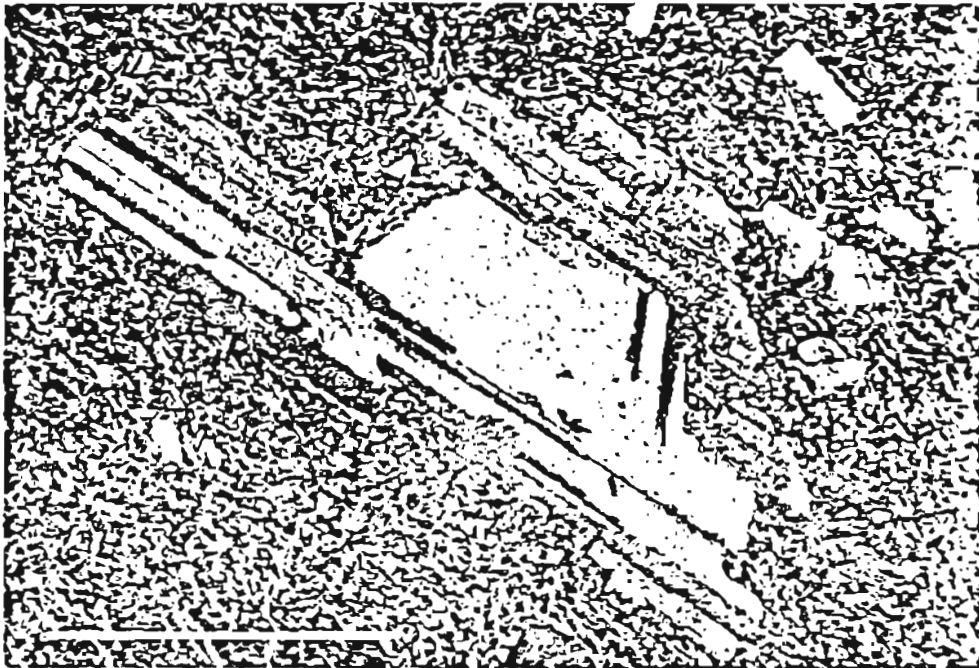


Figure 7. Porphyritic intrusive from Sandy Cove. Scale = 1 mm.

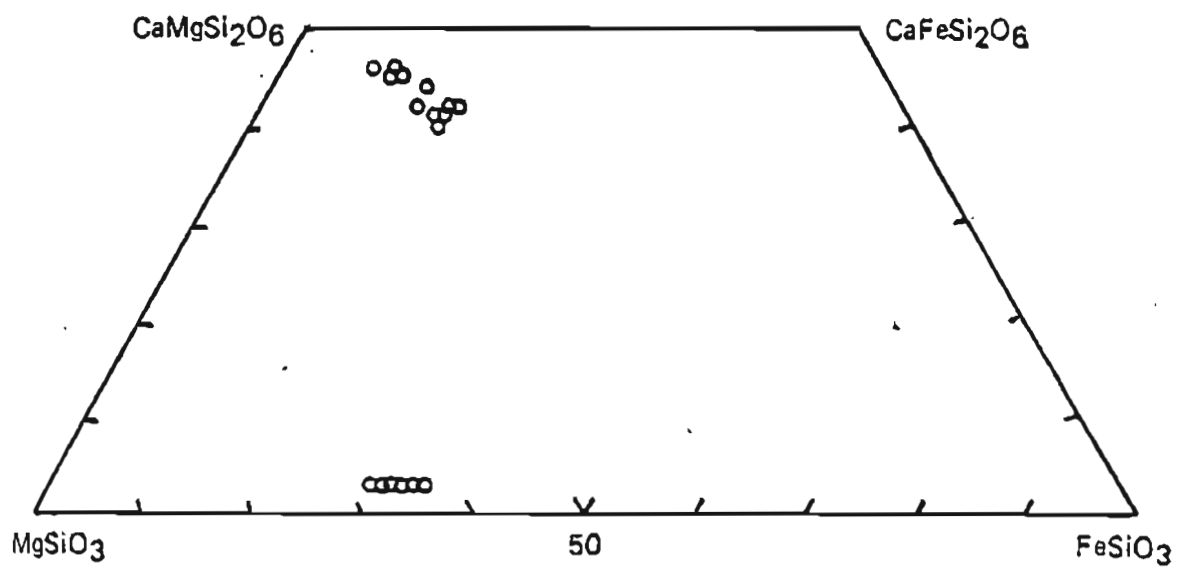


Figure 8. Microprobe analyses for Akutan clinopyroxenes and orthopyroxenes.



Figure 9. Clinopyroxene zoning types. A) Hourglass zoning. B) Concentric zoning. Scale = 1 mm.



Figure 10. Common clinopyroxene twinning types. A) Simple growth twins. B) Polysynthetic twinning (bottom center). Scale = 1 mm.

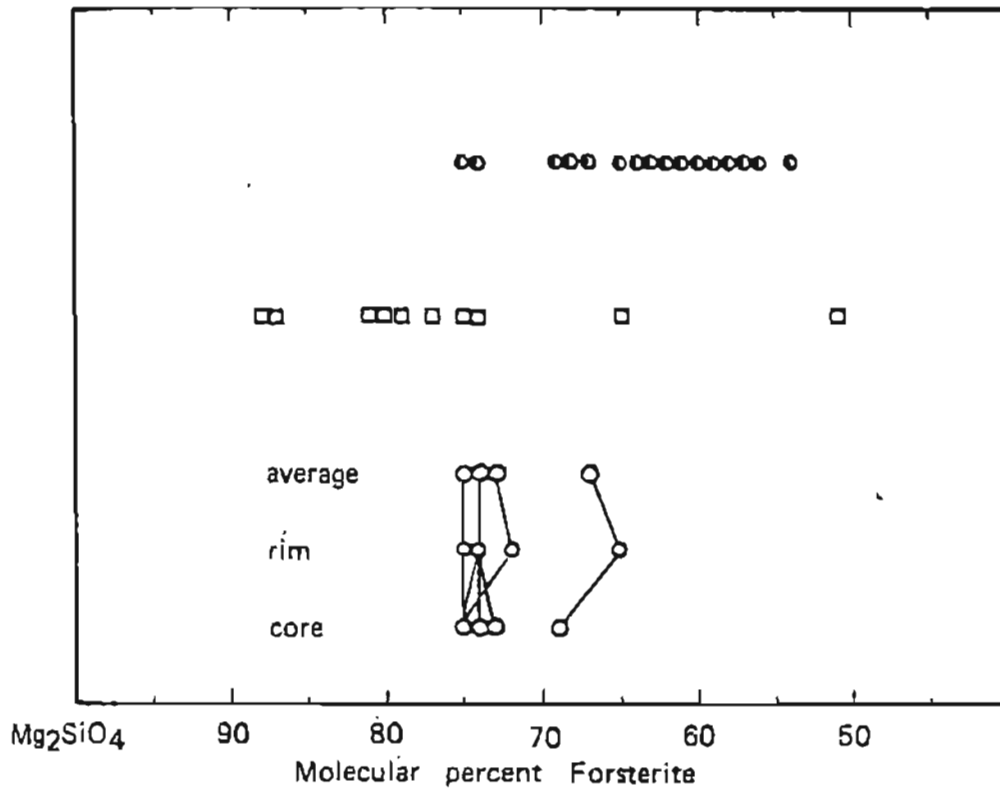


Figure 11. Microprobe analyses of olivine phenocrysts. Also included are analyses from Perfit and Gust (1981). o represent analyses from this study, ● represent analyses from Perfit and Gust (1981) where olivine exists in orthopyroxene and clinopyroxene, and □ represents Perfit and Gust's (1981) analyses where olivine exists only with clinopyroxene.

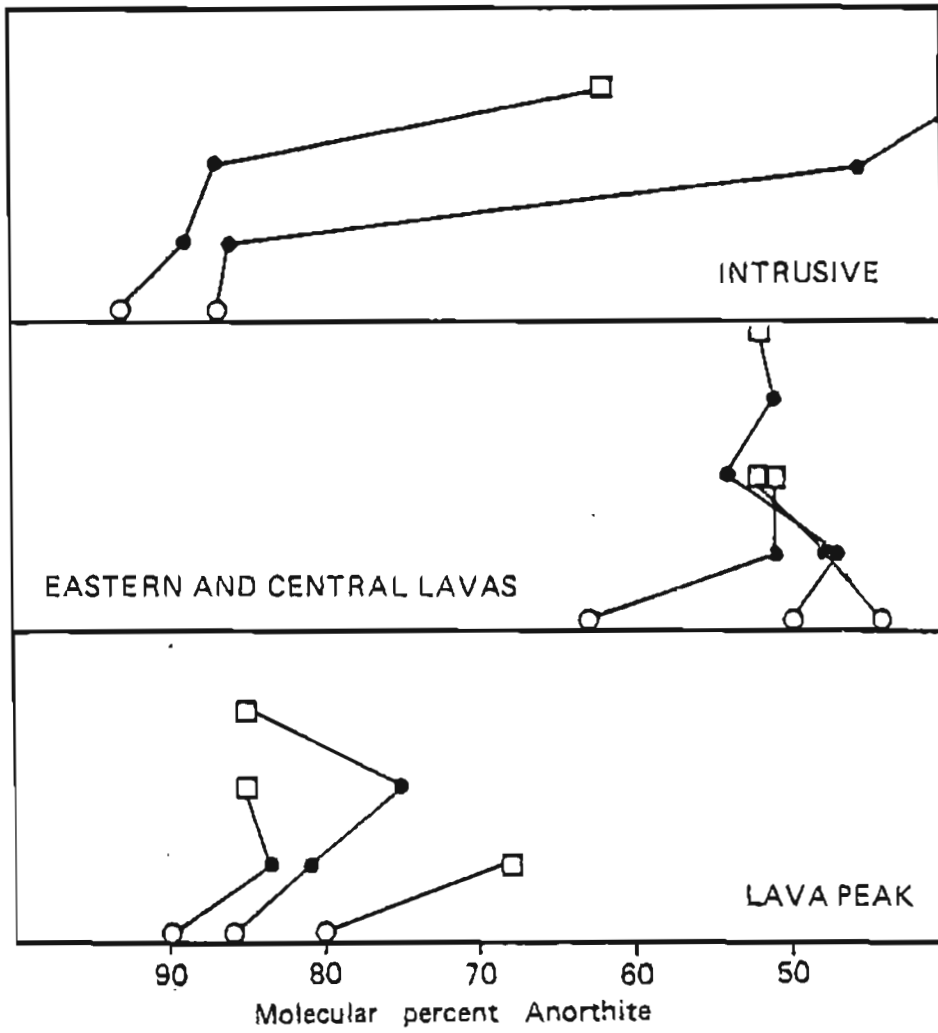


Figure 12. Microprobe analyses of plagioclase phenocrysts. core O; rim □; intermediate values ●.

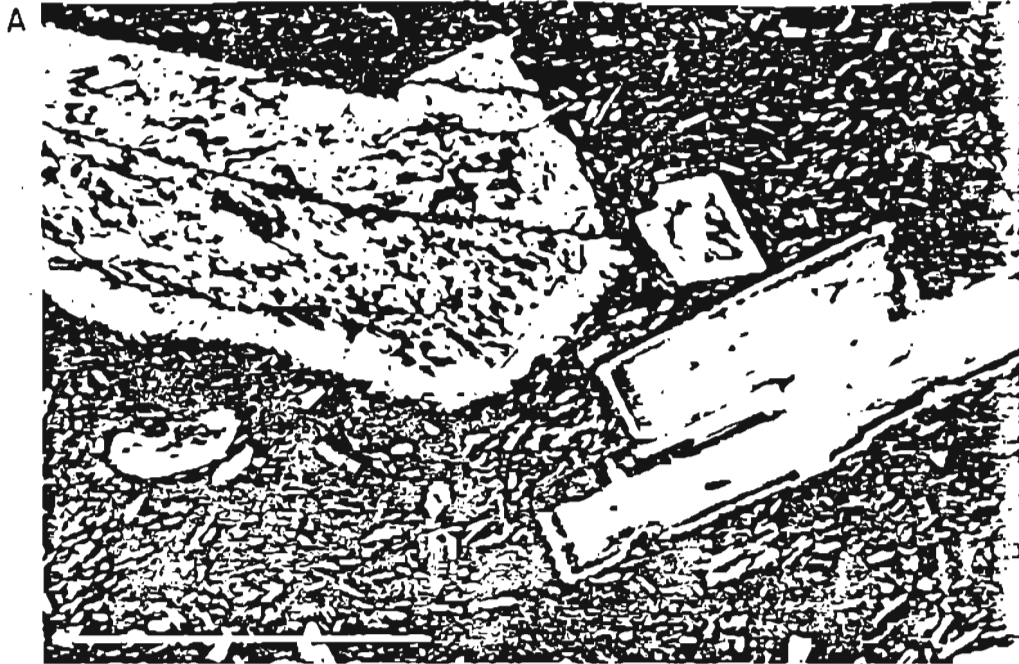


Figure 13. Inclusions in plagioclase phenocrysts. A) Glass inclusions parallel to the margins of the crystal and brown glass in the interior of the crystal. B) Opaque minerals and clinopyroxene within the crystal. Scale = 1 mm.

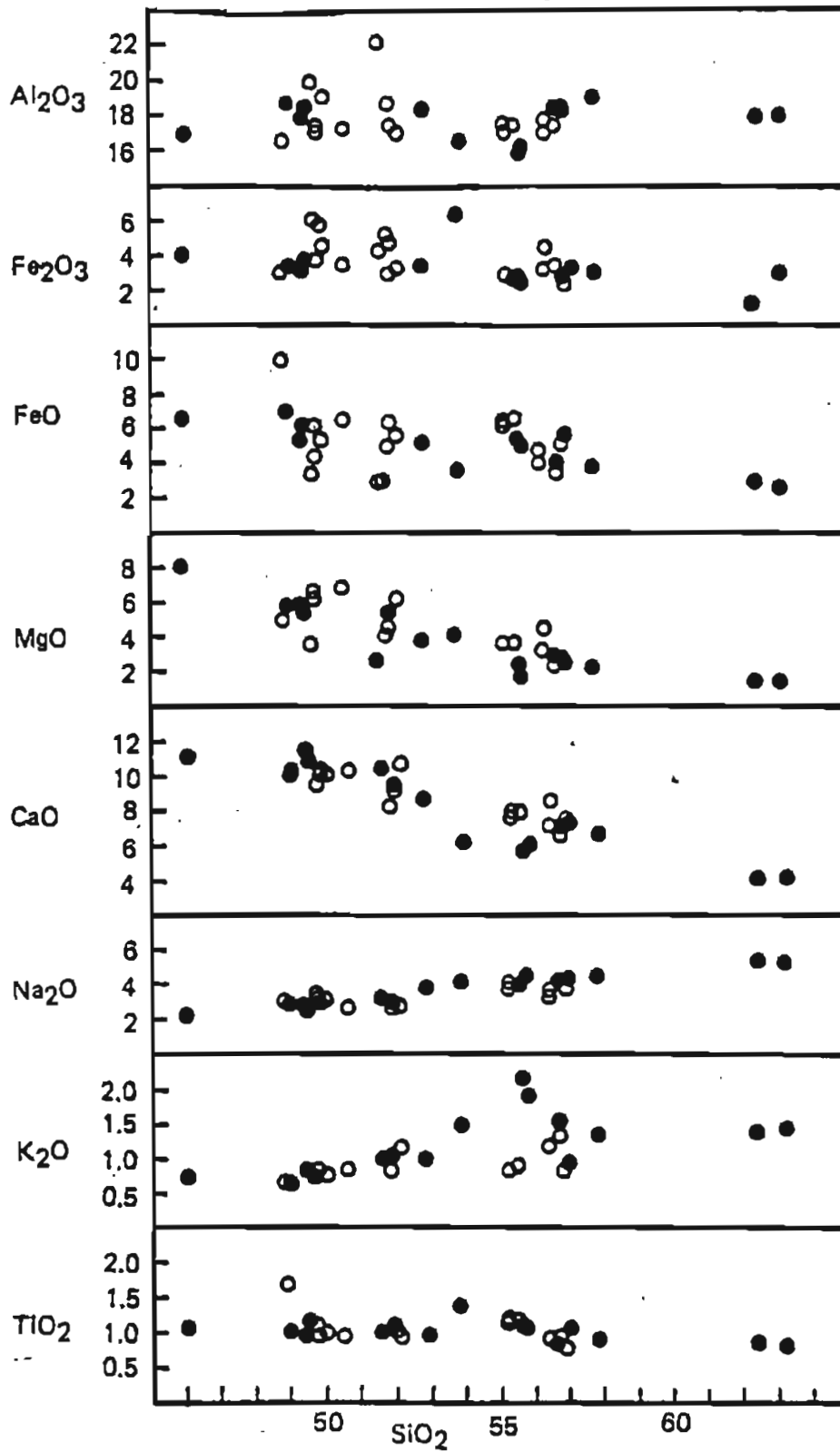


Figure 14. Harker variation diagram. ● are eastern lavas; ○ are western lavas. Amounts are in weight percent.

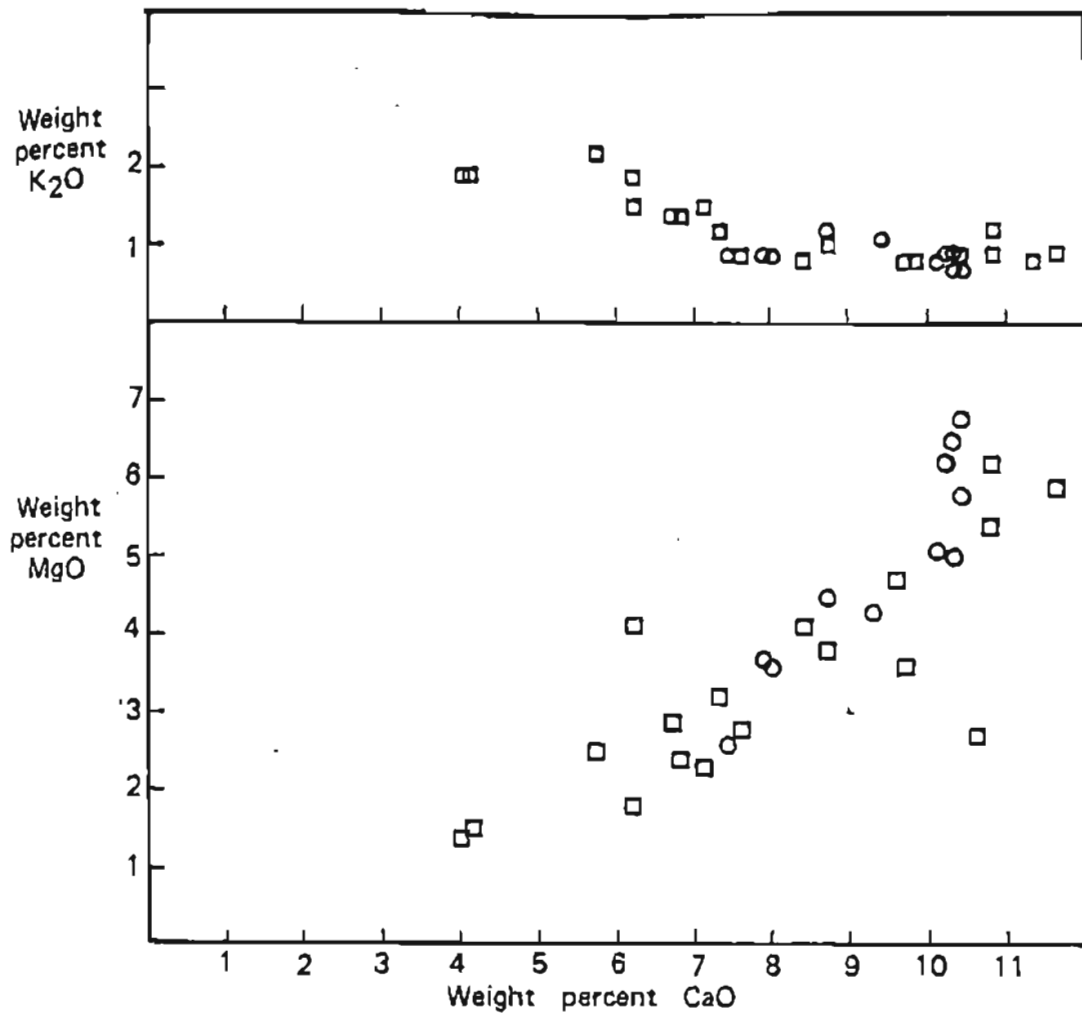


Figure 15. MgO-CaO and K₂O-CaO plots of Akutan samples. O represents western lavas and □ represents eastern lavas.

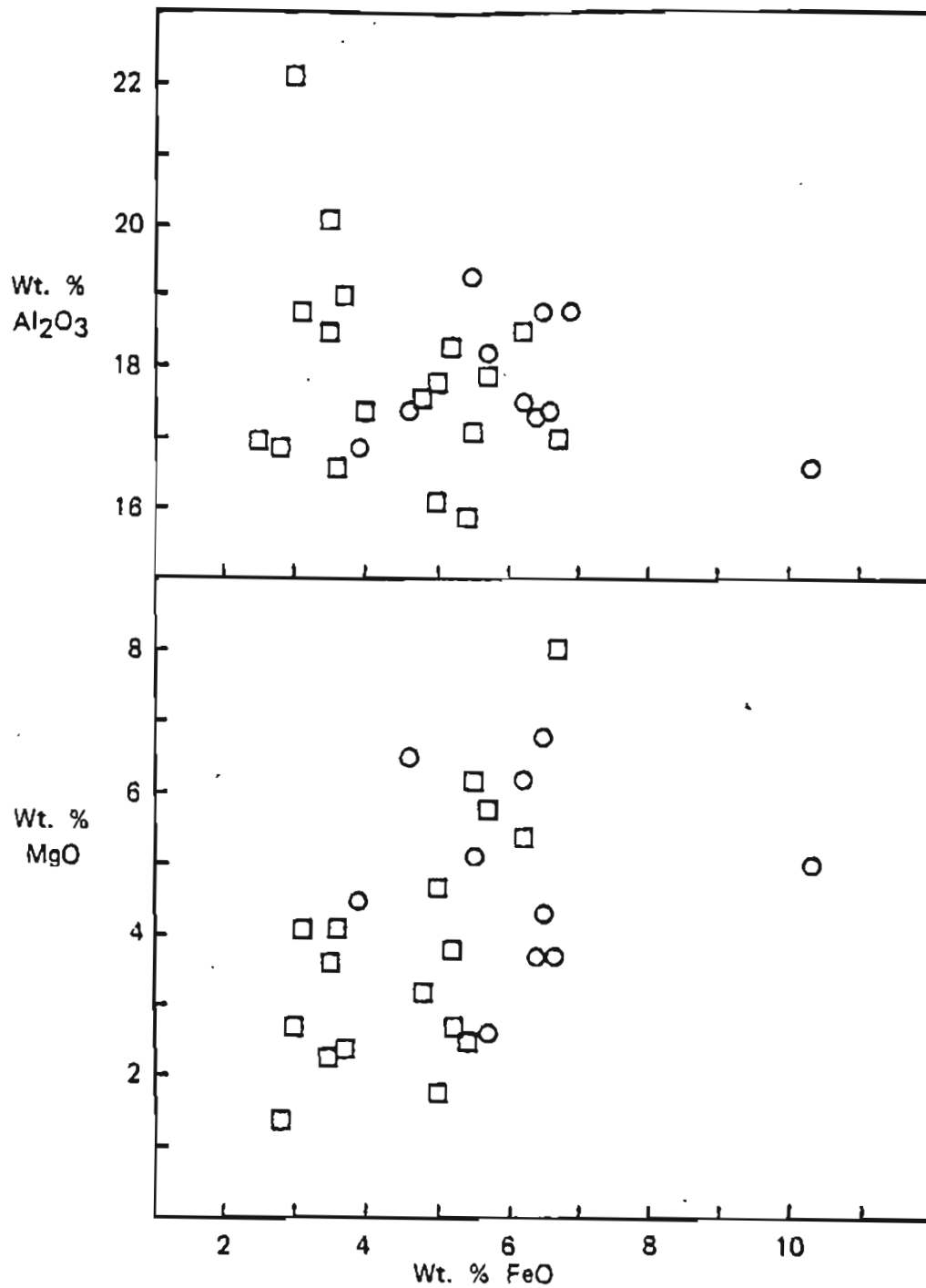


Figure 16. MgO-FeO and Al₂O₃-FeO plots of Akutan samples. ○ are western lavas and □ are eastern lavas.

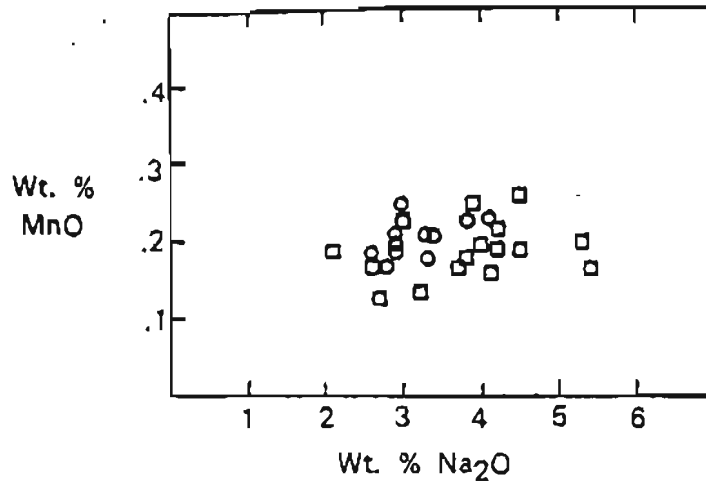


Figure 17. Na₂O-MnO plots of Akutan samples. ○ are western lavas and □ are eastern lavas.

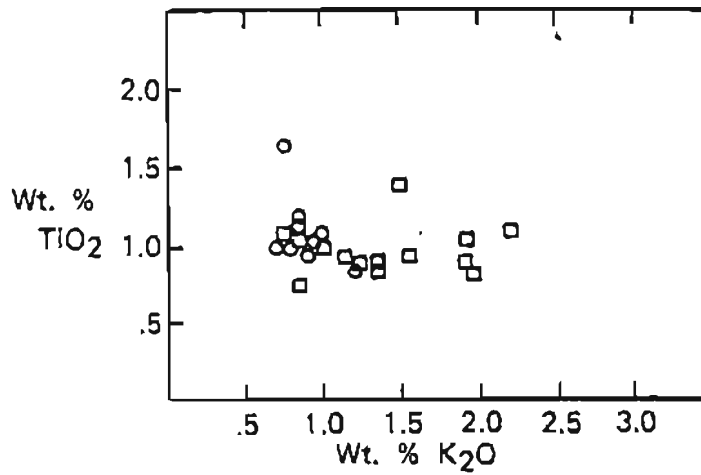


Figure 18. TiO₂-K₂O plots of Akutan samples. ○ are western lavas and □ are eastern lavas.

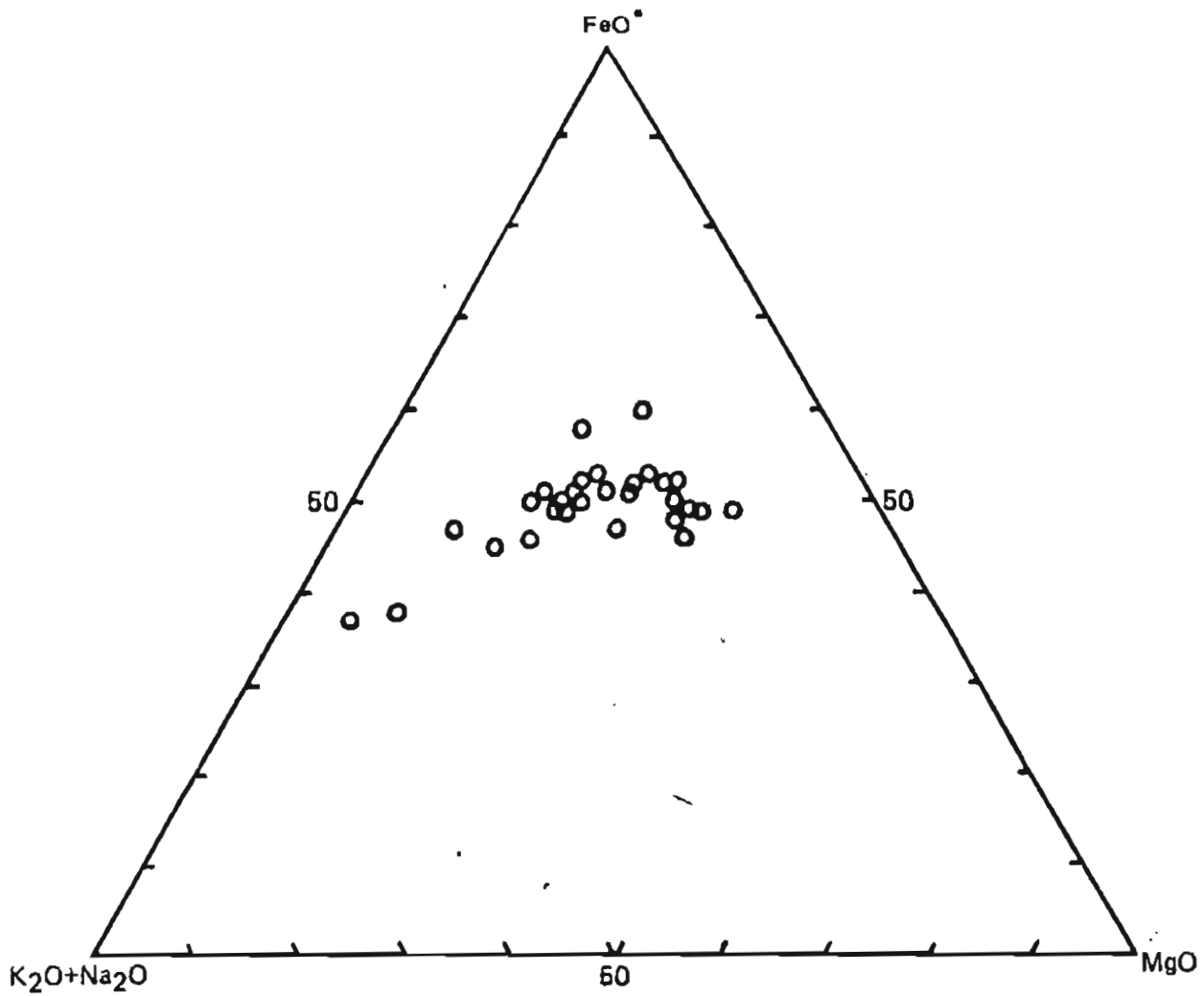


Figure 19. AFM diagram for Akutan samples.

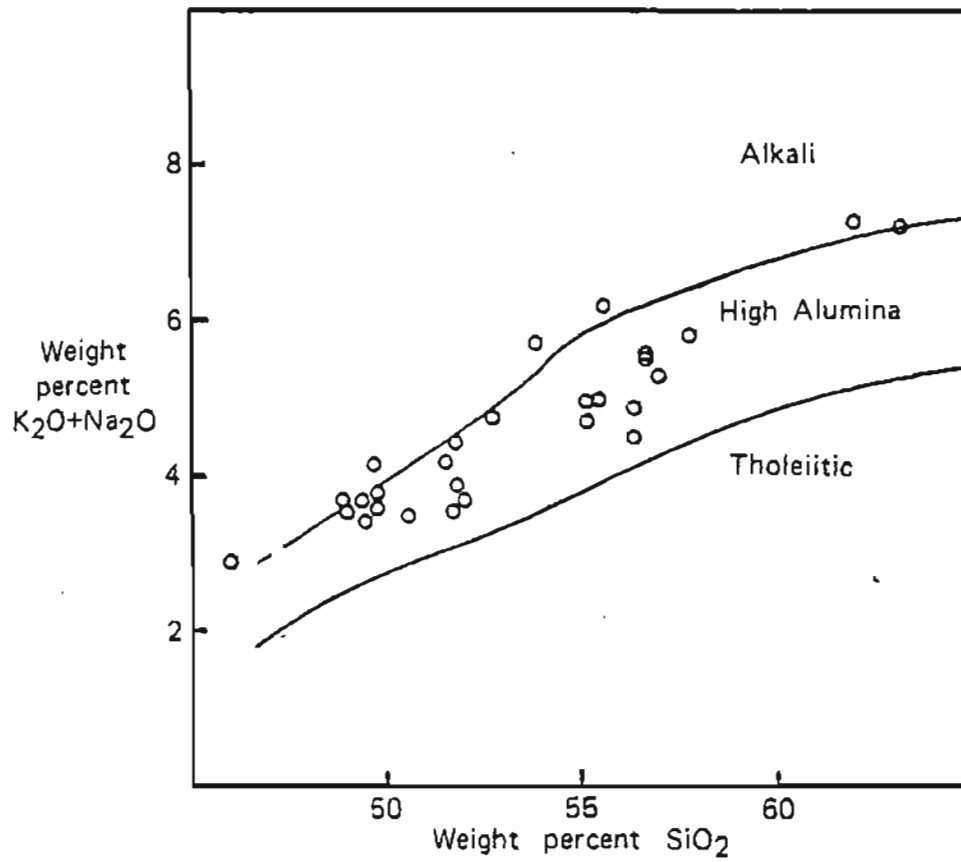


Figure 20. Total alkalis vs. silica diagram from Kuno (1966). Akutan lavas fall in the high alumina field.

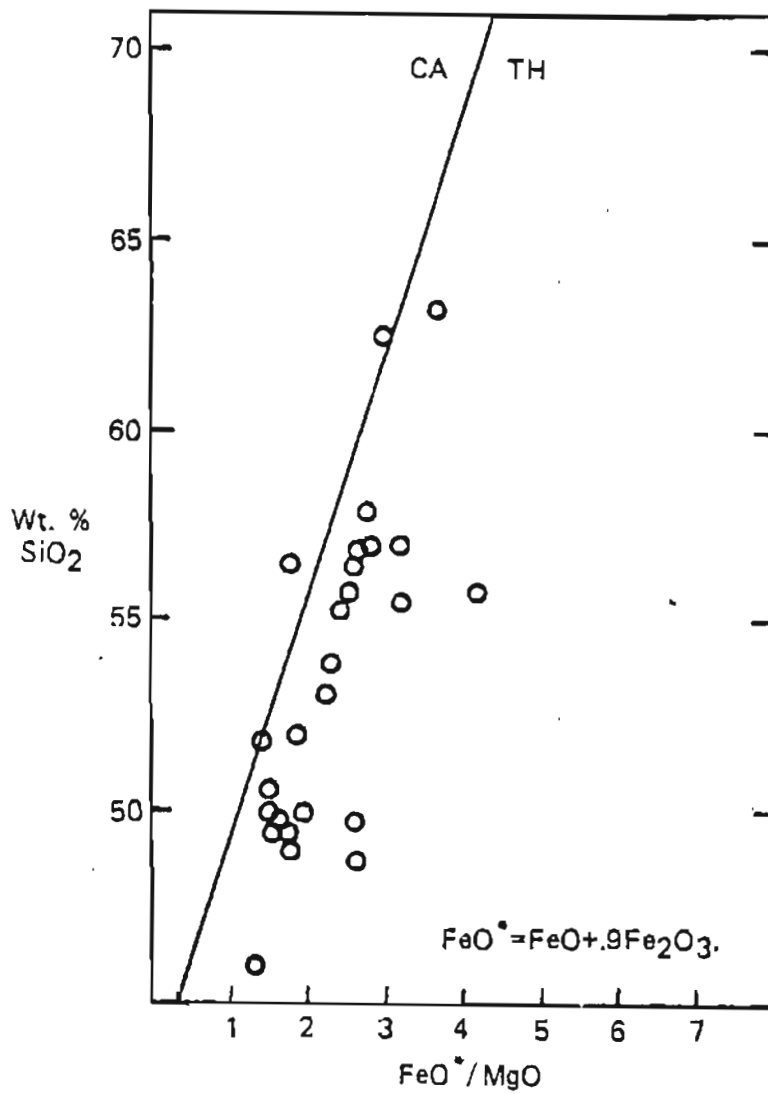


Figure 21. FeO^{*}/MgO vs. SiO₂ diagram for Akutan samples. Diagram is from Miyashiro (1974).

figure missing

Figure 22. $\text{CaO}/\text{Al}_2\text{O}_3$ vs. FeO/MgO diagram showing CaO and MgO fractionation in Akutan lavas.

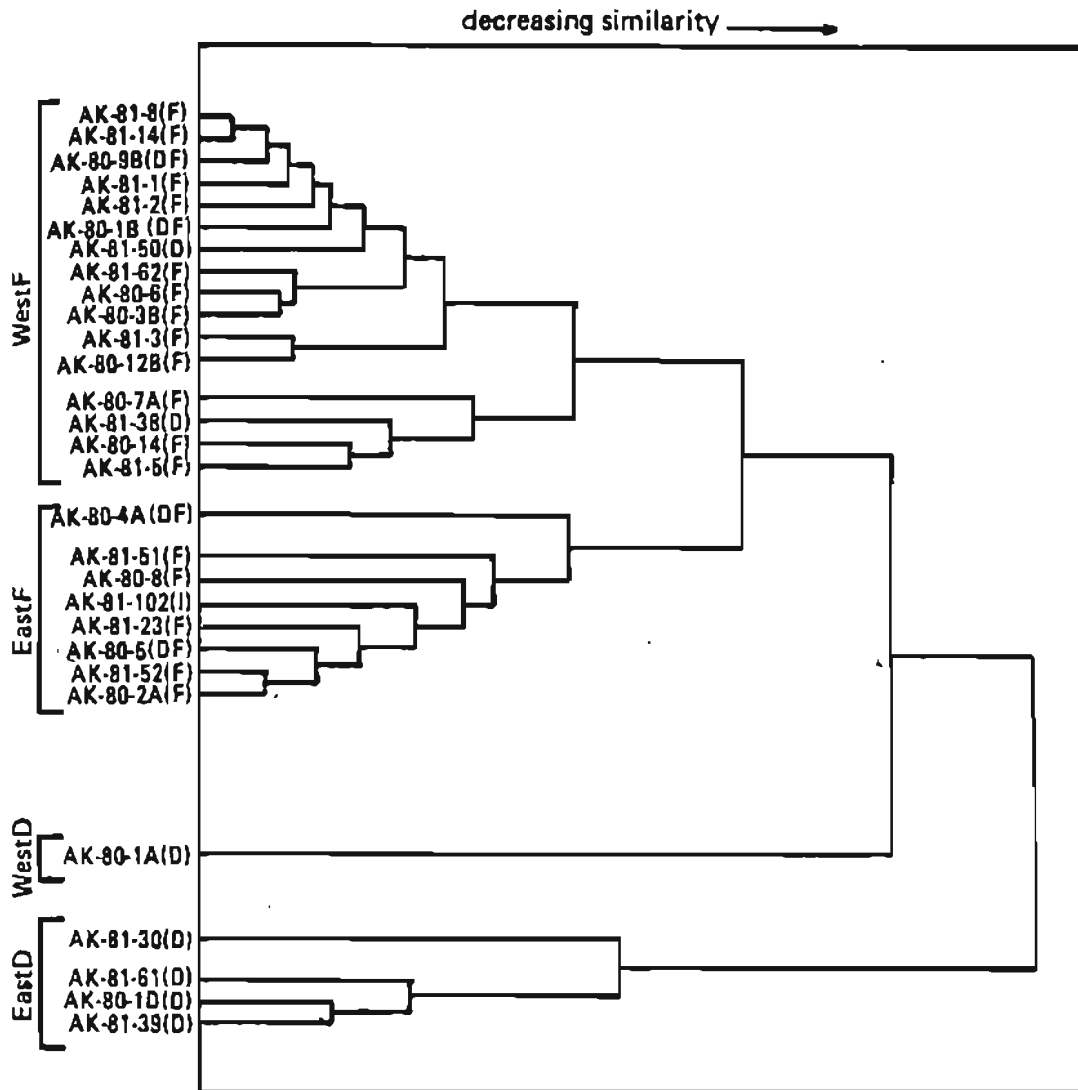


Figure 23. Dendrograph plot of Akutan lava flows and dikes. D = dikes, F = lava flows, I = intrusives, and DF = debris flows deposits.

figure missing

Figure 24. Canonical plot of groups, group means, and samples. Solid symbols represent the group means.

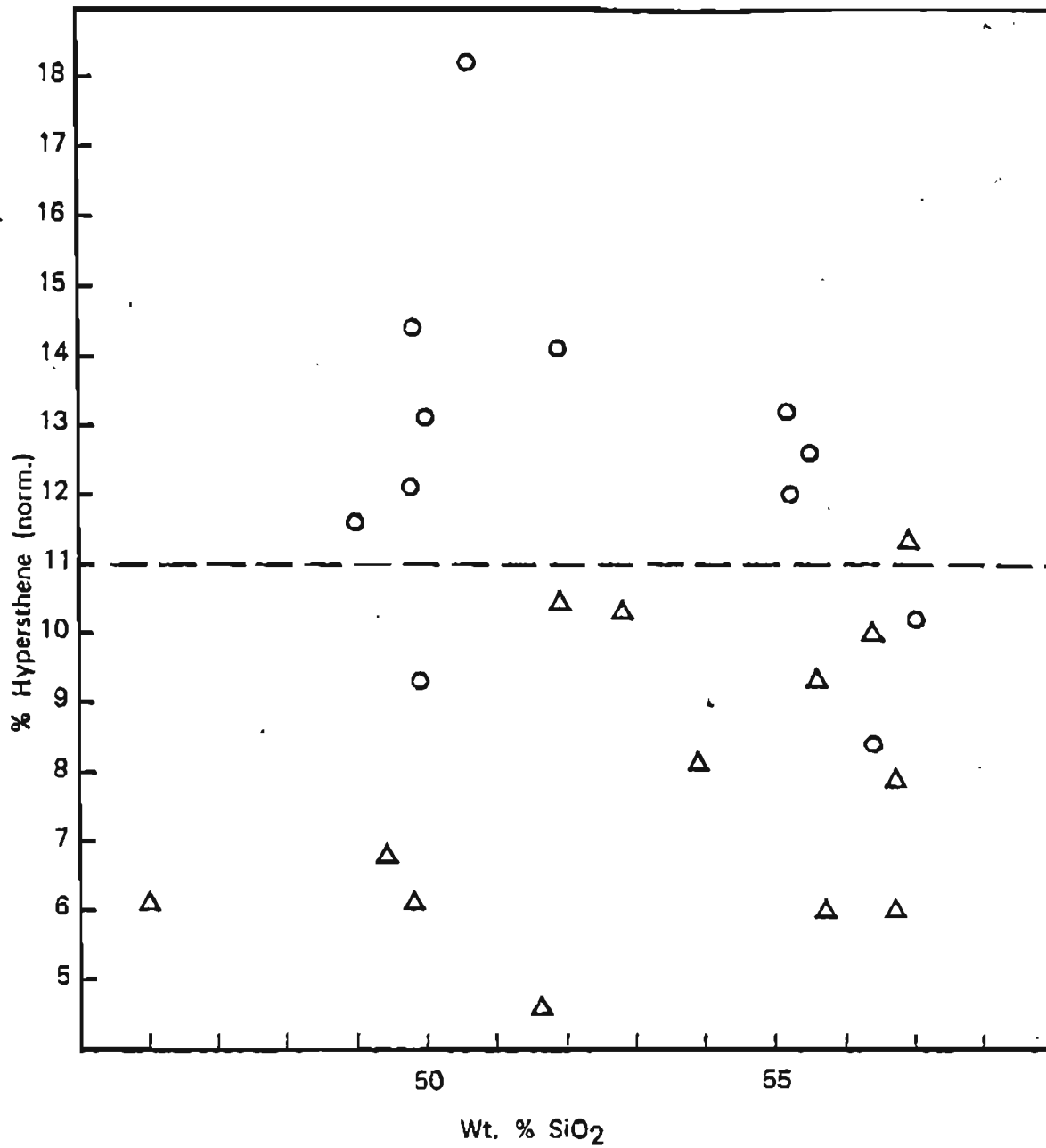


Figure 25. Normative hypersthene vs. wt percent SiO₂. Δ are eastern lavas, \circ are western lavas.

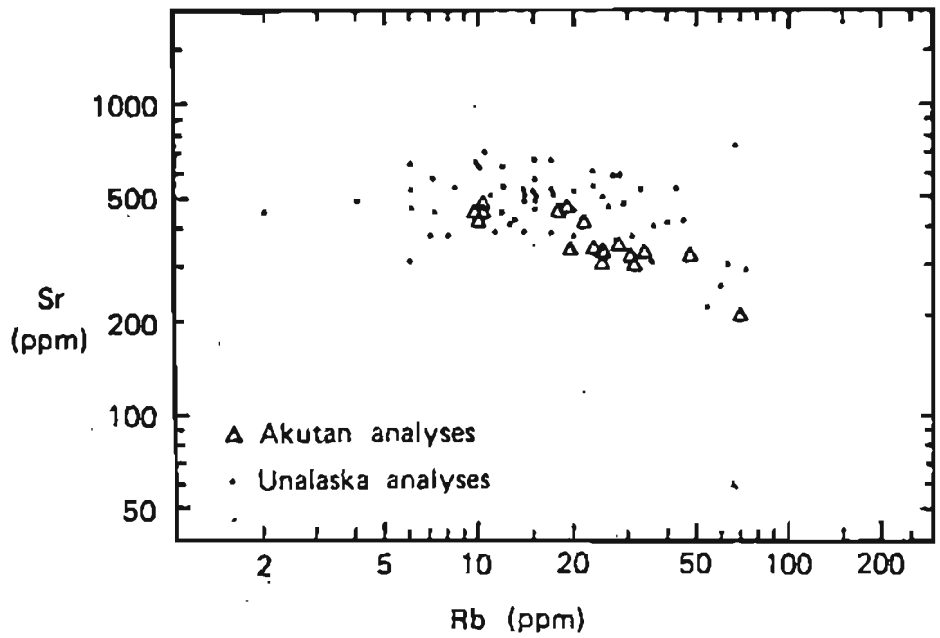


Figure 26. Sr vs. Rb diagram. Unalaska analyses taken from Perfit and others (1980).

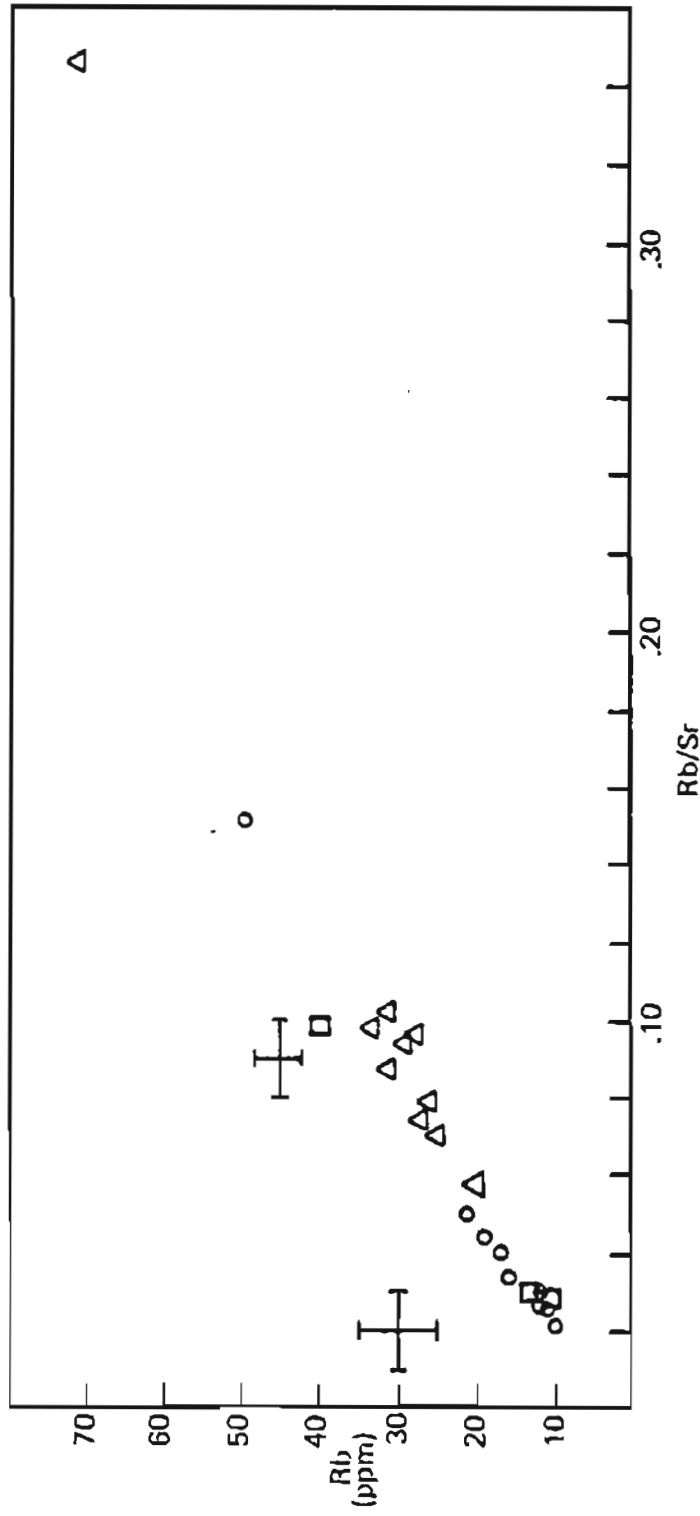


Figure 27. Rb vs. Rb/Sr diagram. Typical precision shown. ○ are Lava Peak rocks and △ are lavas from elsewhere on the island.

figure missing

Figure 28. Sr vs. Rb/Sr diagram. Typical precision shown.

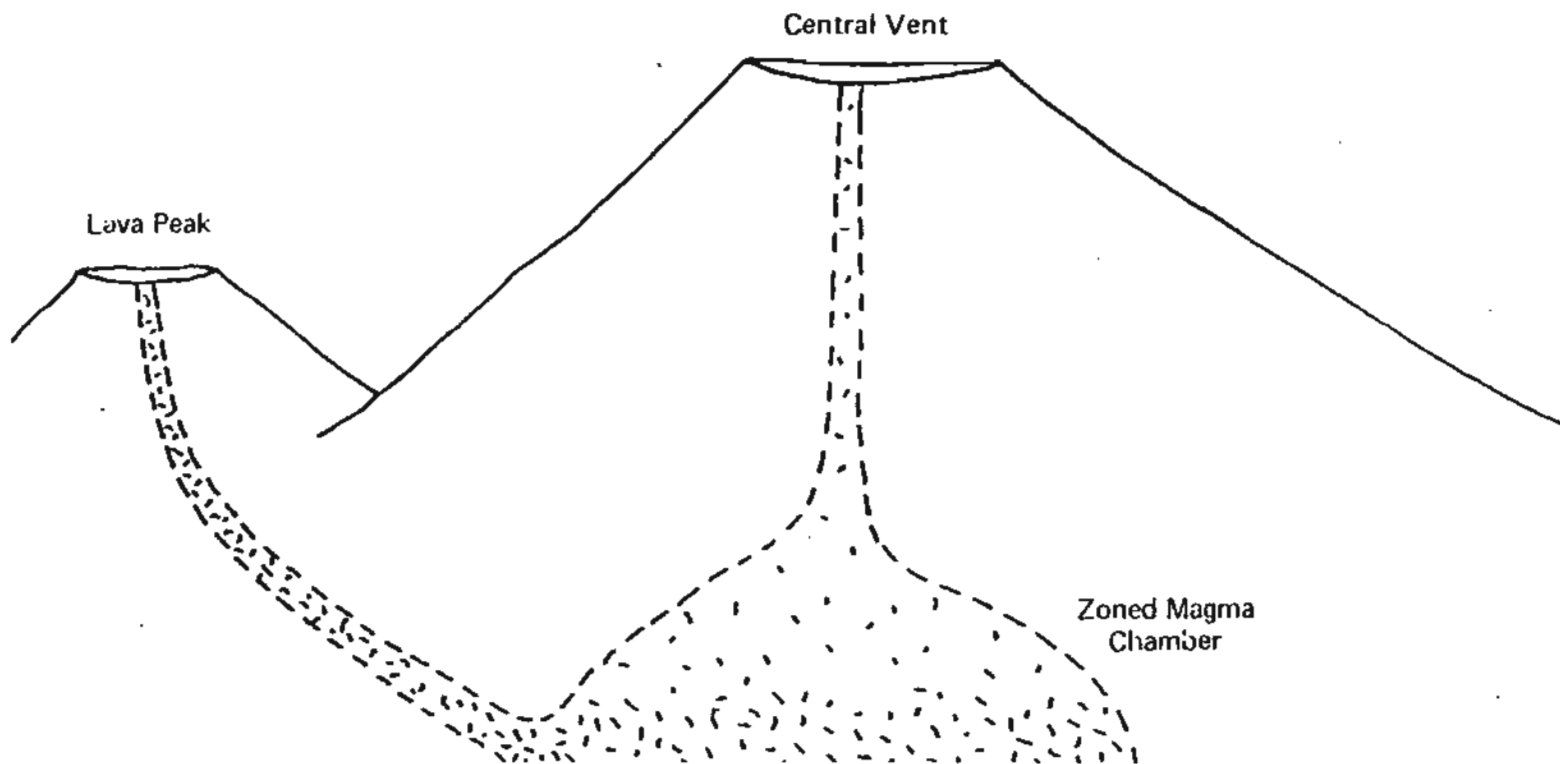


Figure 29. ⁰Carton for Akutan Island showing the central vent, Lava Peak, and the zoned magma chamber.

Table 1. Volcanic activity on Akutan Island since 1790.

<u>Date</u>	<u>Type of eruption</u>	<u>Location</u>
1790	Smoking	
1828	Smoking	
1838	Smoking	
1845	Smoking	
March 1848	Small explosive eruption	
1852	Parasitic cone eruption	NW of Summit
1862	Smoking	
1865	Glow seen from Unimak Pass	
1867	?	
1883	Small steam and ash eruption	
1887	Lava flow	
1892	?	
1896	Glowing	
1907	Continuously active	
Feb. 22, 1908	Lava flow	
1911	Ash fell on Akutan Village	
1912	Smoking	
1928	Smoke and "flaming"	
May 1929	Explosive eruption and lava flow	
1931	Explosive eruption	
1946-47	Lava flow and explosive eruption	
1948	Explosive eruption	
Oct. 1951	Explosive eruption	
1953	?	
1972	Explosive eruption	
1974	Parasitic cone, ash eruption, and lava flow	West flank?
1976-77	Explosive eruptions	
Sept. 25, 1978	Lava flow and ash eruption	
1980	Explosive eruption	

Sources: Finch (1935), Byers and Barth (1953), and Simkin and others (1981).

Table 2. Modal analyses for western Akutan lavas.

<u>Location</u>	<u>Sample #</u>	<u>plag</u>	<u>Olv</u>	<u>Cpx</u>	<u>Opx</u>	<u>Opq</u>	<u>GM</u>
Lava Peak(D)	AK-81-1	18.4	4.2	11.4		1.0	65.0
Lava Peak(U)	AK-81-2	41.8	8.6	3.4		0.2	46.0
Lava Peak(U)	AK-81-3	36.8	3.2	8.0		0.4	51.2
Lava Peak(U)	AK-81-4	39.2	1.6	4.2		1.6	53.4
Lava Peak(L)	AK-81-5	41.0	2.4	7.6		1.0	48.0
Lava Peak(L)	AK-81-6	25.6	2.4	6.8		1.4	63.0
Lava Peak(L)	AK-81-7	24.4	4.4	6.6		1.0	63.0
Lava Peak(L)	AK-81-8	24.2	4.0	7.2		1.0	64.4
Lava Peak(L)	AK-81-9	27.2	5.4	4.8		2.0	60.6
Lava Peak(L)	AK-81-10	23.0	5.2	6.0		1.2	64.6
Lava Peak(L)	AK-81-11	20.4	7.0	6.8		1.2	64.6
Lava Peak(L)	AK-81-12	21.8	5.6	9.6		1.2	61.8
Lava Peak(L)	AK-81-13	18.4	5.2	4.6		2.0	69.4
Lava Peak(L)	AK-81-14	23.0	5.0	11.2		1.6	59.0
Lava Peak(L)	AK-81-15	15.4	4.8	6.8		2.0	70.0
Old Flow	AK-81-16	17.0	1.0	3.0		0.75	79.0
Old Flow	AK-81-17	14.0	0.75	8.0	3.0	1.0	74.0
Old Flow	AK-81-18	35.0	1.8	7.6	0.4	2.0	53.2
Old Flow	AK-81-31	30.0	tr.				70.0
1978 Flow	AK-81-27	32.2	tr.	5.0	0.8	0.4	61.6
Pre-1870 Flow	AK-81-35	26.0	0.2	1.2		0.2	72.4

(D) = dike, (U) = upper series, (L) = lower series, Plag = plagioclase, Olv = olivine, Cpx = clinopyroxene, Opx = orthopyroxene, Opq = opaques, and GM = groundmass.

Table 3. Modal analyses for eastern and central Akutan lavas.

H.S.V. (D)	AK-81-37	1.8			tr.		10.2	88.0
H.S.V. (D)	AK-81-38	7.8	tr.	2.4		1.2	1.6	87.0
H.S.V. (D)	AK-81-39			tr.		tr.	12.0	88.0
H.S.V. (D)	AK-81-40	20.4		0.2				79.4
H.S.V. (D)	AK-81-44	10.0					8.0	82.0
H.S.V. (D)	AK-81-46	23.6		5.4			8.2	62.8
H.S.V. (D)	AK-81-47	17.4					9.4	72.8
Op.Bt. (F)	AK-81-51	31.8		5.0	0.8	2.2		60.2
Op.Bt. (F)	AK-81-52	32.6		7.2	0.6	1.4	1.8	56.2
H.S.V. (F)	AK-81-63	28.8				0.4		70.8
H.S.V. (F)	AK-RM-7a	10.6		1.2	0.6	1.4		86.2
H.S.V. (F)	AK-RM-8	12.8		1.6	0.6	1.6		83.4
P.V. (F)	AK-81-21	20.0		7.0		1.0	7.0	65.0
P.V. (F)	AK-81-22	6.4		0.6	0.6			91.8
P.V. (F)	AK-81-24	20.6	5.4	5.2		tr.	tr.	68.8
H.S.B. (I)	AK-81-102	19.6	0.4	3.4				76.6
P.V. (I)	AK-81-20	17.4	0.4	3.6	tr.	1.0		77.6

H.S.V. = Hot Springs Bay Valley, Op.Bt. = Open Bight, P.V. = Pickup Valley, I = intrusive, F = lava flow, D = dike, Plag = plagioclase, Oliv-olivine, Cpx = clinopyroxene, Opx = orthopyroxene, Opq = opaques, Alt = alternation minerals, and GM = groundmass.

Table 4. Crystallization sequence for Akutan lavas.

<u>Sample</u>	<u>Location</u>	<u>Crystallization sequence from left to right</u>
AK-81-1	Lava Peak(D)	Plag-Opq-Olv-Cpx-GM
AK-81-2	Lava Peak(U)	Plag-Opq-Olv-Cpx-GM
AK-81-3	Lava Peak(U)	Plag-Opq-Olv-Cpx-GM
AK-81-4	Lava Peak(U)	Plag-Opq-Olv-Cpx-GM
AK-81-5	Lava Peak(L)	Plag-Opq-Olv-Cpx-GM
AK-81-6	Lava Peak(L)	Plag-Opq-Olv-Cpx-GM
AK-81-7	Lava Peak(L)	Plag-Opq-Olv-Cpx-GM
AK-81-8	Lava Peak(L)	Plag-Opq-Olv-Cpx-GM
AK-81-9	Lava Peak(L)	Plag-Opq-Olv-Cpx-GM
AK-81-10	Lava Peak(L)	Plag-Opq-Olv-Cpx-GM
AK-81-11	Lava Peak(L)	Plag-Opq-Olv-Cpx-GM
AK-81-12	Lava Peak(L)	Plag-Opq-Olv-Cpx-GM
AK-81-13	Lava Peak(L)	Plag-Opq-Olv-Cpx-GM
AK-81-14	Lava Peak(L)	Plag-Opq-Olv-Cpx-GM
AK-81-15	Lava Peak(L)	Plag-Opq-Olv-Cpx-GM
AK-81-16	Old Flow	Plag-Opq-Olv-Cpx-GM
AK-81-17	Old Flow	Plag-Opq-Olv/Opx-Cpx-GM
AK-81-18	Old Flow	Plag-Opq-Olv-Opx-Cpx-GM
AK-81-31	Old Flow	Plag-Olv-GM
AK-81-32	Old Flow(D)	Plag-GM
AK-81-27	1978 Flow	Plag-Opx-Cpx-GM
AK-81-35	Pre-1870 Flow	Plag-Opq-Cpx-GM
AK-81-100	Float	Plag-Cpx
AK-81-51	Open Bight	Opq-Cpx/Plag-GM
AK-81-52	Open Bight	Plag-Opq-Cpx-GM
AK-81-21	Pickup Valley	Opq-Plag-Cpx-GM
AK-81-22	Pickup Valley	Plag-Opq-Cpx-GM
AK-81-23	Pickup Valley	Plag-Opq-Opx-Cpx-GM
AK-81-24	Pickup Valley	Olv/Plag-Cpx-GM
AK-81-54A	Cow Point(D)	Plag-Opq-Cpx-GM
AK-81-57A	Cow Point(D)	Opq-Plag-GM
AK-81-57B	Cow Point(D)	Plag-Opq-Cpx-GM
AK-81-38	H.S. Valley(D)	Plag-Cpx-GM
AK-81-43	H.S. Valley(D)	Plag-Cpx-Hb-GM
AK-81-50	H.S. Valley(D)	Plag-Cpx-Cpx/GM
AK-81-61	H.S. Valley(D)	Plag-Opq-Olv-GM
AK-81-70	H.S. Valley(D)	Ol-Plag-Cpx-GM
AK-81-71	H.S. Valley(D)	Plag-Opx-Hb-GM
AK-81-62	H.S. Valley(F)	Plag-Opq-Cpx-GM
AK-81-65	H.S. Valley(F)	Olv-Cpx-Plag-GM
AK-81-69	H.S. Valley(F)	Plag-Opq-Ol-GM
AK-81-73	West H.S.B.(I)	Opq-Plag-Cpx
AK-81-102	Sandy Cove(I)	Opq-Cpx-Plag

(D) = dike, (U) = upper series, (L) = lower series, Plag = plagioclase, Opq = opaque, Olv = olivine, Opx = orthopyroxene, Cpx = clinopyroxene, and GM = groundmass, H.S. Valley = Hot Springs Bay Valley, (F) = flow, (H) = hornblende.

Table 5. Posterior probabilities for the four groups of lavas distinguished by the cluster analysis.

<u>Sample</u>	<u>Class.</u>	<u>EastF</u>	<u>WestF</u>	<u>WestD</u>	<u>EastD</u>
AK-81-5	WestF	0.651	0.347		
AK-81-50	WestF	0.532	0.468		
AK-80-4a	WestF	0.735	0.249		
AK-81-62	WestF	0.704	0.165		0.131
AK-80-1b	WestF	0.731	0.175		
AK-80-9b	WestF	0.762	0.221		
AK-80-12b	WestF	0.532	0.468		
AK-80-3b	WestF	0.566	0.433		
AK-80-7a	WestF	0.651	0.345		
AK-80-8	WestF	0.655	0.341		
AK-81-1	EastF	0.348	0.652		
AK-81-2	EastF	0.397	0.602		
AK-81-3	EastF	0.457	0.603		
AK-81-8	EastF	0.376	0.624		
AK-81-14	EastF	0.439	0.561		
AK-80-5	EastF	0.442	0.558		
AK-81-23	EastF	0.320	0.680		
AK-81-51	EastF	0.313	0.687		
AK-81-52	EastF	0.364	0.636		
AK-81-102	EastF	0.240	0.760		
AK-80-5	EastF	0.452	0.548		
AK-8-2a	EastF	0.276	0.724		
AK-80-1a	WestD			0.998	0.002
AK-80-14	EastD	0.301	0.031		0.668
AK-81-30	EastD			0.046	0.954
AK-81-61	EastD	0.054	0.004		0.942
AK-80-1d	EastD			0.005	0.995
AK-81-38	EastD	0.025	0.001		0.973
AK-81-39	EastD	0.008			0.991

EastF = east flows, WestF = west flows, EastD = east dikes, and WestD = west dikes. The classifications are those assigned by the multiple discriminant analysis. The original classification was taken from the groups identified by the cluster analysis (see figure 26). Seven samples were run as unknowns to see if the multiple discriminant analysis would place them in more appropriate groups than the ones they were originally in.

Table 6. Neodymium and strontium data for Akutan Island.

<u>Sample</u>	<u>Location</u>	$\frac{87}{86}\text{Sr}$	$\frac{143}{144}\text{Nd}$
AK4-EJ	SE of Akutan Harbor	0.70342±44	0.51219±3
AK4-3	Akutan Harbor	0.70315±5	
AK4-15	Hot Springs Bay	0.70317±4	0.51225±2
AK4-22	Akutan Harbor	0.70302±6	
AK4-33	Sarana Bay	0.70308±5	0.51220±2
AK4-47	Sarana Bay	0.70324±3	

Data from McCulloch and Perfit (1981) and Perfit (unpublished data). Errors are in the last figures given and represent ± 2 mean.

Table 7. Whole rock K-Ar dates for Akutan lavas.

<u>Sample</u>	<u>Location</u>	<u>% K Wt %</u>	<u>10^{-10} $\frac{rAr^{40}}{mole/g}$</u>	<u>% rAr⁴⁰</u>	<u>Date ($\times 10^6$ yrs)</u>
AK-81-14	L.P.(L)	0.691	0.0133	8.5	1.1 \pm 0.2
AK-81-30	L.P.(L)	0.648	0.0175	23.8	1.5 \pm 0.1
AK-81-23	P.V.(F)	1.23	0.0305	10.0	1.4 \pm 0.2
AK-80-9a	H.S.B.V.	0.806	0.0159	13.6	1.1 \pm 0.1

(D) = dike, (L) = lower series, rAr⁴⁰ = radiogenic argon, L.P. = Lava Peak, P.V. = Pickup Valley, H.S.B.V. = Hot Springs Bay Valley, (F) = flows.

Table 8. Geothermometry for Akutan mineral pairs.

<u>Sample</u>	<u>Mineral Pair</u>	<u>Temp.</u>	<u>at 5 kb</u>	<u>at 10 kb</u>	<u>at 15 kb</u>
AK-81-23	Opx-Cpx	1180°C* 1185°C* 1317°C** 1329°C**			
AK-81-1	Olv-Cpx	992°C# 1009°C#	1020°C 1037°C	1044°C 1063°C	1075°C 1090°C
AK-81-10	Olv-Cpx	1015°C# 1012°C#	1042°C 1039°C	1068°C 1066°C	1095°C 1092°C

Opx = orthopyroxene, Cpx = clinopyroxene, and Olv= olivine. *Wood and Banno (1973) geothermometer, **Wells (1977) geothermometer, #at one bar pressure.